ABSTRACT

DEVELOPMENT OF ADSORPTION FILTRATION PROCESS FOR VIRUS REMOVAL FOR DRINKING WATER TREATMENT

by

Vishal Vijay Gawarikar

Recent monitoring studies have indicated that many ground water (GW) sources would benefit from the development of effective technologies for removing viruses. Although reverse osmosis can achieve high log removal it is not economical. The main objective of this study is to test and validate a novel adsorption filtration (AF) technology for removing viruses from GW sources for drinking water production in New Jersey.

The convective diffusion of viruses to adsorbent particle surfaces in flow packed beds (FPB) enhances their removal efficiency if the adsorbent particle size can be decreased to about 100 microns. The development of effective virus removal technologies has not been successful because of two fundamental difficulties. First, the pressure drop in FPBs increases very rapidly with decreasing adsorbent particle size, and becomes unacceptably high at about 100 microns. Second, additional difficulties in achieving high log virus removal can arise due to competition for adsorption sites between negatively-charged viruses and humic acid anions which are fractions of Natural Organic Matter (NOM).

The two main challenges to be overcome for developing an effective adsorption filtration technology for virus removal are: i) the selection of an appropriate adsorption medium, and ii) the development of means to minimize the effect of NOM on virus removal efficiency. Based on systematic experimental studies, calcite was selected as the

adsorbent for virus removal. In order to overcome the adverse effects of NOM, a special prefilter, to be placed upstream of the virus filter, was developed using large calcite particle size, about 600 microns. This was possible because NOM molecules are approximately 15 times smaller than viruses, and accordingly, their diffusivity is about 15 times larger. Consequently, NOM diffusional transport is sufficiently rapid in spite of the larger calcite particles used in the prefilter. This ability to utilize such larger particles in the NOM prefilter made it possible to use a small prefilter pressure head during filtration.

In order to decrease the head loss arising from the use of small particle size dimension in the virus filter, two sets of channel arrays were introduced in the flow packed bed design similar to the concepts used in membrane technology, namely: decreasing the filtration depth and expanding the filtration surface area. In the design, the filtration surface area was increased and the filtration depth was decreased so that the same footprint and volumetric filtration velocity of the conventional FPB could be accomplished. In the AF filter, virus-contaminated water enters the feeding channels, crosses the adsorbent layer and then exits along the receiving channels. Therefore, this design allows efficient virus removal (> 6 logs) using 100-micron particles without the need to use high pressures to drive the filtration process.

The experimental studies confirmed that a model composite NOM/virus filter can remove more that 6 logs of viruses in the presence of NOM. The composite filter run was about 100 hours, compared to only 10 hours without the NOM prefilter. The design of the composite NOM/virus filter with a linear velocity of 0.1 cm/sec, P ~ 0.1 bar, was elaborated for scaling up to an industrial scale.

DEVELOPMENT OF ADSORPTION FILTRATION PROCESS FOR VIRUS REMOVAL FOR DRINKING WATER TREATMENT

by
Vishal Vijay Gawarikar

A Dissertation
Submitted to the Faculty of
New Jersey Institute of Technology
in Partial Fulfillment of the Requirements for the Degree of
Doctor of Philosophy in Environmental Engineering

Department of Civil and Environmental Engineering

May 2005

APPROVAL PAGE

DEVELOPMENT OF ADSORPTION FILTRATION PROCESS FOR VIRUS REMOVAL FOR DRINKING WATER TREATMENT

Vishal Vijay Gawarikar

Dr. Mohamed E. Labib, Dissertation Co-advisor — Date
President, Novaflux Technologies, Princeton, NJ

Dr. Taha F. Marhaba, Dissertation Co-advisor — Date
Associate Professor of Civil and Environmental Engineering, NJIT

Dr. Stanislav S. Dukhin, Committee Member — Date
Senior Research Associate, NJIT

Dr. Thomas Atherholt, Committee Member — Date
Research Scientist, DSRT, NJDEP

Dr. Robert Dresnack, Committee Member — Date
Professor of Civil and Environmental Engineering, NJIT

Dr. Jay N. Meegoda, Committee Member — Date
Professor of Civil and Environmental Engineering, NJIT

BIOGRAPHICAL SKETCH

Author: Vishal Vijay Gawarikar

Degree: Doctor of Philosophy

Date: May 2005

Undergraduate and Graduate Education:

- Doctor of Philosophy in Environmental Engineering,
  New Jersey Institute of Technology, Newark, NJ, 2005

- Master of Engineering in Civil Engineering,
  Maharaja Sayajirao University, Baroda, India, 2000

- Bachelor of Engineering in Civil Engineering,
  Maharaja Sayajirao University, Baroda, India, 1998

Major: Environmental Engineering

Presentations and Publications:

"Adsorption Filtration Process for Removing Viruses in Water Treatment."
Gawarikar, V. V., Labib, M. E., Dukhin, S. S.
Presented, Gradute Seminar in Civil & Environmental Enginnering, NJIT.
12/01/2003.

"Development of Adsorption Filtration Process for Virus Removal in Drinking Water Treatment." Labib, M. E., Gawarikar, V. V., Final Report, NJDEP, Contract # SR02-030, 06/15/04, 18 pages.

Dedicated to my mother, Vaishali Gawarikar and my father, Vijay Gawarikar.

ACKNOWLEDGMENT

I would like to express my sincerest gratitude to my advisor Dr. Mohamed E. Labib, whose expertise in several areas of science and practical approach have made this research experience very exciting and fulfilling. Dr. Labib also has been very encouraging and motivating throughout my studies. Many thanks to my co-advisor Dr. Taha F. Marhaba for all his advice and moral support during my studies at NJIT. I enjoyed several field trips organized by Dr. Marhaba which provided me a real world perspective in the field of environmental engineering.

A very special thanks to Dr. Stanislav S. Dukhin, for providing his deep insight in this area of research. Without Dr. Dukhin's invaluable help and expertise, the successful and timely completion of this research would not have been possible.

Special thanks to Dr. Jay N. Meegoda and Dr. Robert Dresnack for serving on my committee. I would also like to thank Dr. Thomas Atherholt of NJDEP for funding this research and actively serving on my committee. I also thank Dr. Hsin-Neng Hsieh and the Civil Engineering Department for providing me with financial support during my studies.

Many thanks to Mr. Eric Feerst and Mr. Bruce Hovendon of the Bureau of Marine Water Monitoring Lab at Leeds Point (NJ), who trained me to perform phage assay experiments for my research. I would also like to thank Mr. Chandrakant Patel of the Materials Characterization lab, Mr. Frank Johansson of the Civil Engineering machine shop, Mr. Robert Morris of the Civil Engineering computer lab, and the secretaries of Civil Engineering, Ms. Dallas Link and Ms. Marion Balavender, for providing me with all their help during my studies at NJIT.

I extend my sincere thanks to Mrs. Anita Labib for all her help in the numerous corrections she performed on the draft copy of the dissertation document. Many thanks to

Dr. Yacoob Tabani at Novaflux Technologies, Princeton (NJ), for all his help during my studies.

I would like to acknowledge my friends Jatin, Mahesh, Ashish, and Hiroshan who have been a source of support and inspiration throughout this study. I cannot thank enough my family (my mom, dad, wife, sister, and my brother-in-law) who have believed in me and who have stood by me throughout my life.

TABLE OF CONTENTS

TABLE OF CONTENTS
(Continued)

TABLE OF CONTENTS
(Continued)

Chapter **Page**

TABLE OF CONTENTS
(Continued)

TABLE OF CONTENTS
(Continued)

TABLE OF CONTENTS
(Continued)

LIST OF TABLES

LIST OF TABLES

LIST OF FIGURES

LIST OF FIGURES

LIST OF FIGURES

CHAPTER 1

INTRODUCTION

1.1 Virus Contamination in Groundwater

Groundwater (GW) is an essential source of drinking water in the State of New Jersey. Recent monitoring studies indicate that GW sources require effective means for removing or inactivating viruses (Atherholt et al. 2003). According to a recent report (Blackburn et al. 2004) on waterborne disease outbreaks for 19 states, five outbreaks affecting 727 people were of viral origin. Of the six outbreaks affecting the most persons reported in this report (Blackburn et al. 2004), five were of viral origin. New Jersey Department of Environmental Protection (NJDEP) monitoring data (2004), obtained as a result of the Private Well Testing Act, of over 5100 wells in NJ showed that 1.8 % of the private wells in the state contained fecal coliform or E. coli "indicator" bacteria and thus at least this many wells (and likely more) are likely to contain disease-causing viruses as well. The contamination rate in the northern part of the state (3.0%) was higher than in the southern part of the state (0.4%).

The virus contamination of GW used for drinking water thus poses a significant health risk. The following sections discuss the characteristics or viruses, virus transport in the aquifer and virus removal in water treatment.

1.2 General Introduction to Viruses

A virus includes genetic elements that can replicate only in a specific host cell. In order to multiply, the virus must enlist a specific cell in which it can replicate (Madigan et al. 2000). A virus can also be defined as an entity, which carries the genetic information

necessary for its own replication but does not possess the machinery for such replication by itself (Sterritt and Lester, 1988). All viruses are therefore obligatory parasites, and rely upon the machinery of the infected host cell, which is "borrowed" and reprogrammed, for the replication of viral nucleic acid (DNA or RNA), together with any structural proteins, which may be associated with the mature extra-cellular form of the virus (Sterritt and Lester, 1988). Viruses vary in size from 28 nm (poliovirus) to about 200 nm (Smallpox virus) (Maier et al. 2000). Viruses are known to cause a number of waterborne diseases and are classified in Table 1.1.

Table1.1 Some Waterborne Viral Illnesses

Virus	Illness	Size (nm)
Enteroviruses	From meningitis to hepatitis (Stannard, 2003)	27-32 (Stannard, 2003)
Enteroviruses Type 68-71	Meningitis, pneumonia, paralysis, common cold (Stannard, 2003)	---
Poliovirus	Paralytic poliomyelitis, meningitis (Stannard, 2003)	28 (Maier et al. 2000)
Echoviruses	Meningitis, encephalitis, diarrhea	---
Coxsackie A	Meningitis, hepatitis, pneumonia, diarrhea (Stannard, 2003)	---
Coxsackie B	Asthma, meningitis, pneumonia, hepatitis (Stannard, 2003)	---
Rotaviruses	Infantile diarrhea (Stannard, 2003)	70 (Madigan et al. 2000)
Adenoviruses	Gastroenteritis, acute respiratory disease, conjunctivitis	70 (Stannard, 2003)
Reoviruses	Mild upper respiratory and gastrointestinal illness	80 (Wagner and Hewlett, 1999)
Astroviruses	Gastroenteritis (Stannard, 2003)	28 (Stannard, 2003)
Hepatitis A Virus	Hepatitis A (USFDA,2003)	27 (USFDA, 2003)
Calciciviruses		
Hepatitis E Virus	Hepatitis E (Stannard, 2003)	32-34 (Stannard, 2003)
Norwalk Virus	Diarrhea, abdominal cramps and nausea (Maier et al. 2000)	26-35 (Stannard, 2003)

1.3 Structure and Classification of Viruses

Basic virus structure includes a protomer or capsomer protein coat and internal nucleic acid, either RNA or DNA (Maier et al. 2000). All viruses have a nucleic acid genome and an outer protein capsid, but some may also have protein and lipid envelopes, glycoprotein spikes or even more complex tails and sheath structures (Maier et al. 2000), as shown in Figure 1.1. The genome, capsid and envelope (where present) make up the virus particle or virion (Wagner and Hewlett, 1999). The genetic material encodes the capsid and viral proteins required for initiating the replication (Wagner and Hewlett, 1999). On the basis of the hosts they infect, viruses can be classified as follows (Madigan et al. 2000):

i) *Animal viruses*, e.g., Herpes simplex virus type I, Poliovirus.

ii) *Plant viruses*, e.g., cauliflower mosaic virus.

iii) *Bacterial viruses*: viruses that infect bacteria, also called bacteriophages or phages for short.

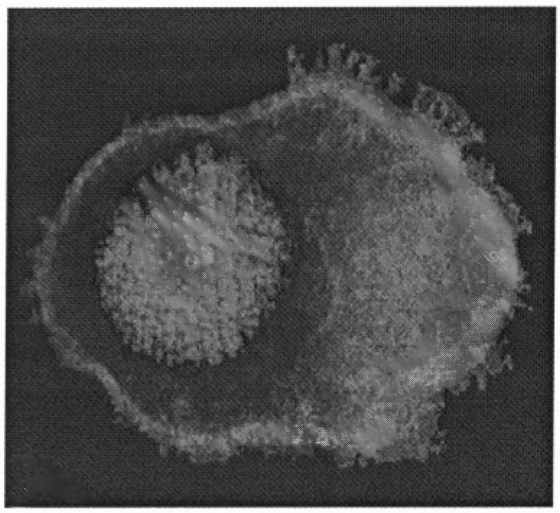

Enveloped Virus (Herpesvirus)
(Source: Stannard, 2003)

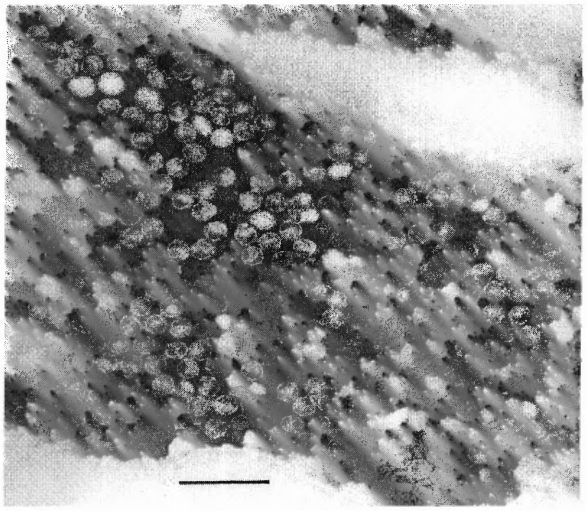

Non-enveloped Virus (MS2)
(Source: Ackermann, 2003)

Figure1.1 Enveloped and non-enveloped viruses.

On the basis of structural arrangement, capsid viruses can be classified as follows (Sterritt and Lester, 1988):

i) *Helical viruses*: The capsid consists of many identical protein subunits arranged regularly in a helix, with the nucleic acid embedded in a spiral groove.

ii) *Polyhedral viruses*: In these viruses, the capsid is a regular multi-faceted hollow structure in which there is nucleic acid. This is frequently in the form of an icosahedron, which has twenty equilaterally triangular faces.

iii) *Complex viruses*: These types of viruses have a polyhedral head connected to a helical tail, although the nucleic acid is found only in the head with the remainder of the particle being associated with the mechanism of entry into the host cell. Many of the bacterial viruses (they infect only bacteria), called bacteriophages or just phages, are of this type.

On the basis of nucleic acid type, viruses can be classified as follows (Madigan et al. 2000):

i) *RNA viruses*: Can have single-stranded (ss) or double-stranded (ds) RNA, e.g., Polio virus (ssRNA).

ii) *DNA viruses*: Can have single-stranded (ds) or double-stranded (ds) DNA, e.g., bacteriophage λ (dsDNA).

iii) *RNA - DNA* viruses: These viruses use both RNA and DNA as their genetic material, but at different stages of their reproductive cycle, e.g., ss RNA-Retroviruses, ds DNA –Hepadnaviruses.

Protonation and deprotonation of the functional groups of surface proteins are the basis of the outer surface charge of the virus. The ionizable groups are usually carboxyl, primary amine, guanidyl, imidazole, and phenolic hydroxyl (Taylor, 1981). The surface charge is developed by an acid-base reaction, as follows (Taylor, 1981; Taylor and Bosmann, 1981):

a) Carboxyl $-COOH \leftrightarrow -COO^- + H^+$

b) Amine $-NR_2H^+ \leftrightarrow -NR_2 + H^+$

c) Phenol $-Ph-OH \leftrightarrow -Ph-O^- + H^+$

The pH at which the net charge on the virus surface is zero is defined as the "isoelectric point" of the virus (IEP). At pH < IEP, the virus has a net positive charge, and at pH > IEP, the virus has a net negative charge (Elimelech et al. 1995). The surface charge and IEP of the virus particle are specifically important to this study since they determine the nature of adsorption onto the adsorbent particles during filtration.

1.4 Virus Transport in the Aquifer and Underlying Physical and Chemical Principles

Enteric viruses are the viruses that are found in the intestinal system of human beings and are transported by either food or water. The diseases caused by these viruses range from trivial to severe or even fatal (Maier et al. 2000). Viruses excreted by humans are considered a potential public hazard. It is believed that some viruses can survive in water or wastewater for as many as 41 days at 20° C (Metcalf and Eddy, 1991).

An infected person is a major contributor to the high number of infectious viruses in water and may excrete up to 10^{11} viral particles/gm of feces (Maier et al. 2000). In untreated domestic wastewater, enteric viruses may vary from 10-100 /ml (Metcalf and Eddy, 1991). In general, raw sewage can have about 10^5 - 10^6 viruses/liter, and after tertiary treatment and disinfection, the numbers can go down to as low as 0.7-170 viruses/liter (Maier et al. 2000), resulting in a logarithmic (log) removal of about 2.77 – 6.15. Viruses from septic tanks, treatment plant effluents, sewage sludge, leaking sewers, land application of effluents, and similar sources are the main sources of the pathogenic viruses present in GW.

Contrary to the assumption or belief of GW being free of microorganisms, a number of disease outbreaks have been traced to GW. Monitoring peak concentrations of

viral injections in sand and gravel aquifers indicate that the virus transport rate varies from as low as 0.2-1m/day (Bales et al. 1995; Peiper et al. 1997) to up to 300 m/day in highly permeable aquifers (Noonan and McNabb, 1979). Virus seeding studies indicate that viruses can travel up to 900 meters in a coarse grain aquifer (Noonan and McNabb, 1979). According to Keswick et al. (1982), viruses can be transported up to a distance of 1.6 km in fractured aquifers.

Recently, fecal contaminations of GW were detected when wells were systematically sampled in NJ, especially viruses (Atherholt et al. 2003). "Despite the fact that coliphages are present in un-disinfectioned fecal pollution sources at lower concentrations than indicator bacteria, coliphages may survive longer and travel further than indicator bacteria in GW" (Atherholt et al. 2003). Consequently, large attention has been paid in the literature to the detection of viruses in GW and to modeling their fate and transport in the aquifer. A recent review article summarizes the most relevant 150 studies in this field (Schijven and Hassanizadeh, 2000). These studies emphasize the importance of protecting, monitoring and treating GW sources to prevent viral contamination of drinking water.

Due to their small sizes, viruses are considered as colloids. Viral transport in GW or in the aquifer can thus be modeled as colloid transport, and this is fully elaborated in this study. The main processes for removing viruses in subsurface are adsorption and inactivation (Keswick and Gerba, 1980; Yates et al. 1987). In addition, virus transport is also attenuated by advection and dispersion effects (Schijven and Hassenizadeh, 2000). Advection is the horizontal movement, whereas dispersion is the spreading or scattering of viruses over an area or volume. Furthermore, adsorption of viruses can be irreversible

or reversible. In irreversible adsorption, there is no detachment from the surface of collector. On the other hand, reversible adsorption means that virus detachment takes place after a so-called residence time. The residence time is the time interval between adsorption and desorption, and it depends on virus-adsorbent interaction parameters, including surface forces, electrolyte concentration, pH, etc.

The modeling of virus transport in soil provides an explanation for outbreak episodes where GW infection is attributed to the mobilization of filamentous bacteriophages and viruses following prolonged rainfalls (Ryan and Elimelech, 1996). As GW passes through soil, a large accumulation of viruses takes place due to their irreversible attachment to positively-charged patches on soil particles (Loveland et al. 1996). This large amount of adsorbed viruses may be rapidly detached and mobilized due to the decrease of GW ionic strength (by dilution) and due to other chemical perturbations after rainfalls; these effects usually lead to an increase in the electrostatic repulsion forces between soil particles and adsorbed viruses (Ryan and Elimelech, 1996; Redman et al. 1999). The increase in the mobilized virus concentration in GW during those outbreaks can be orders of magnitude higher than normal levels since viruses have been accumulating in the aquifer for a period of time, depending on the season, before their immediate detachment by rainfalls.

Outbreaks may go undetected more often than not because most illnesses are mild enough that people do not seek medical attention or people see different doctors so no one doctor "sees" the outbreak. Also, routine sampling does not look for viruses for technical/cost reasons. Outbreak sampling sometimes, but not always, includes viruses. The high virus concentration during outbreaks has to be taken into account with respect

to virus removal from well water, especially when the latter is used to prepare drinking water.

Therefore, the transport of virus in porous media or aquifer depends on the grain size available for filtration, organic matter, temperature, pH, ionic strength, attractive and repulsive forces like van-der-Waals forces and electrostatic repulsions, respectively, and possibly other factors. According to Elimelech et al. (1995), chemical and physical perturbations can cause mobilization of colloids/viruses. Chemical perturbations like decreasing ionic strength, increasing pH and increasing the concentration of surfactants and dissolved solids, can mobilize colloids/virus transport. In additions, physical perturbations, like increasing the GW pumping rate above the natural flow velocity, can cause sufficient hydrodynamic shear to mobilize colloids/viruses. Also, rapid infiltration (naturally by rainfall or by artificial recharge) or flow in fractured media can result in velocities capable of mobilizing colloids/viruses. Virus transport can be quantified and modeled as 1-/, 2-/ or 3-dimensional depending on the subsurface hydrologic conditions (Schijven and Hassanizadeh, 2000). Given a set of conditions and factors, a virus can adsorb or desorb during its transport in the aquifer. If favorable conditions prevail, a virus can get into the GW pumping well used for making drinking water, and this normally takes place when GW is under the influence of surface water.

1.5 Current Regulatory Situation

The United States Environmental Protection Agency (USEPA) requires at least 4-log virus removal by treatment for public water systems that use surface water or Ground Water Under the Direct Influence (GWUDI) of surface water as their source of drinking

water (Federal Register, 1989). The federal rules for surface waters: SWTR (Surface Water Treatment Rule) (Federal Register, 1989), IESWRT (Interim Enhanced Surface Water Treatment Rule, (Federal Register, 1998) and LT1ESWTR (Long Term 1 Enhanced Surface Treatment Rule) (Federal Register, 2002) are administered by NJDEP. All surface waters must be filtered and disinfected to comply with the 4-log virus reduction requirement.

For ground waters currently there are no federal rules (although the USEPA proposed Ground Water Rule (Federal Register, 2000) is expected to become final by the end of 2005). The State of New Jersey Administrative Code (N.J.A.C. 7:10, 2004) specifies that community water systems (CWS) must have 0.2 - 0.4 parts per million (ppm) free available chlorine or 1-2 ppm combined chlorine (pH dependent) for at least five minutes contact time. There is a waiver provision for systems serving 100 or less service connections but the system must have a good total coliform (TC) bacteria history in its distribution system and must take at least two TC samples per month.

Non-community water systems (NCWS) such as those located at schools, factories, and parks (and private wells as well) are not required to disinfect but if a NCWS has a distribution system, it must have a detectable chlorine residual in it. NCWSs must also have quarterly or more often TC monitoring. NCWS must disinfect, if they have three monthly total coliform rule (TCR) maximum contaminant level (MCL) violations within 18 months (or two monthly violations and one acute violation in same period). The NJ Administrative Code also specifies various "setback" distance requirements from specified pollution sources such as septic tanks and the like. Some

CWS provide full treatment of GW (filtration and disinfection) while others just disinfect. Most NCWS systems either disinfect only or do not treat at all.

1.6 Virus Removal in Drinking Water Treatment

Virus removal can be calculated using the following equations:

$$\% \text{ Reduction} = 100 - (\text{Final population/Initial population} \times 100) \quad (1.1)$$

Or $\log_{10}$ reduction value (LRV) as

$$\log_{10} \text{reduction} = \log_{10} U - \log_{10} C \quad (1.2)$$

Where, C = average number of phages as counted in final population after treatment

U = average number of phages as counted in initial population before treatment

To achieve virus removal during water treatment, two fundamental processes are used:

i) *Physical processes:* These are based on physical exclusion of microorganisms by coagulation and flocculation, filtration, or by addition of an adsorbent to the water without causing a loss of virus viability.

ii) *Chemical processes*: These are usually achieved by adding a disinfectant, like chlorine or ozone, resulting in killing or inactivating the virus (i.e., rendering it non-viable).

1.7 Current Treatment Methods and Available Technologies for Removing Viruses from GW and SW

1.7.1 Conventional Water Treatment Train and Virus Removal

It has been reported that various treatment steps in conventional drinking water treatment for surface water sources achieve some level of virus removal/inactivation, as follows (Maier et al. 2000):

i) Coagulation – 88-95 %

ii) Rapid sand filtration – 10-99%

iii) Slow sand filtration – 85-99%

Bellamy et al. (1985) found that a new sand bed was able to remove 85% of source water coliform bacteria and 98% of Giardia cysts. As the sand bed matured biologically, removal of coliform bacteria can exceed 99% and the removal of Giardia may become virtually 100%.

For conventional and direct filtration processes, virus log removal is usually about 1 and 2, respectively (AWWA, 1999).

The combination of coagulation-settling-sand filtration together can remove from 98.6% to 99.987% of viruses. A typical conventional drinking water treatment for surface water sources is shown in Figure 1.2.

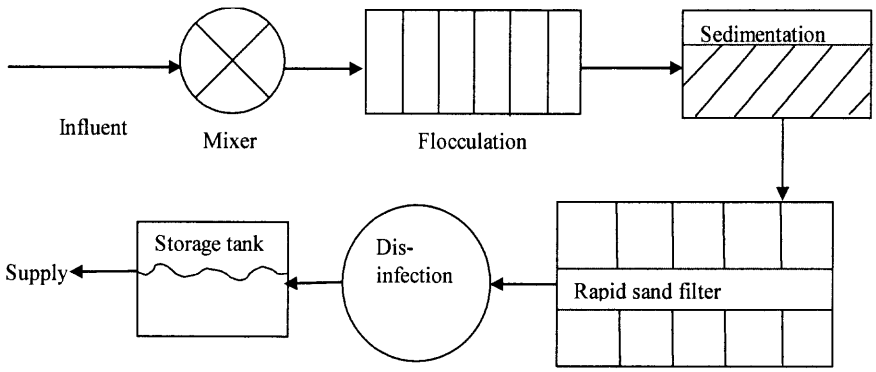

Figure 1.2 Conventional water treatment train for surface water.

Combining filtration and chlorination or ozonation enables one to provide virus removal of about 4 logs. However, this solution is often not considered satisfactory because of disinfection by products (DBPs) formation.

1.7.2 GW Treatment Processes for Preparing Drinking Water

Drinking water production form GW sources does not normally follow a specific treatment process due to difference in water quality of the sources used. Examples of GW treatment processes are shown in Figure 1.3. Some CWS water supply systems provide full treatment of GW (filtration and disinfection) while others just disinfect. Most NCWS systems either only disinfect the GW or do not treat at all.

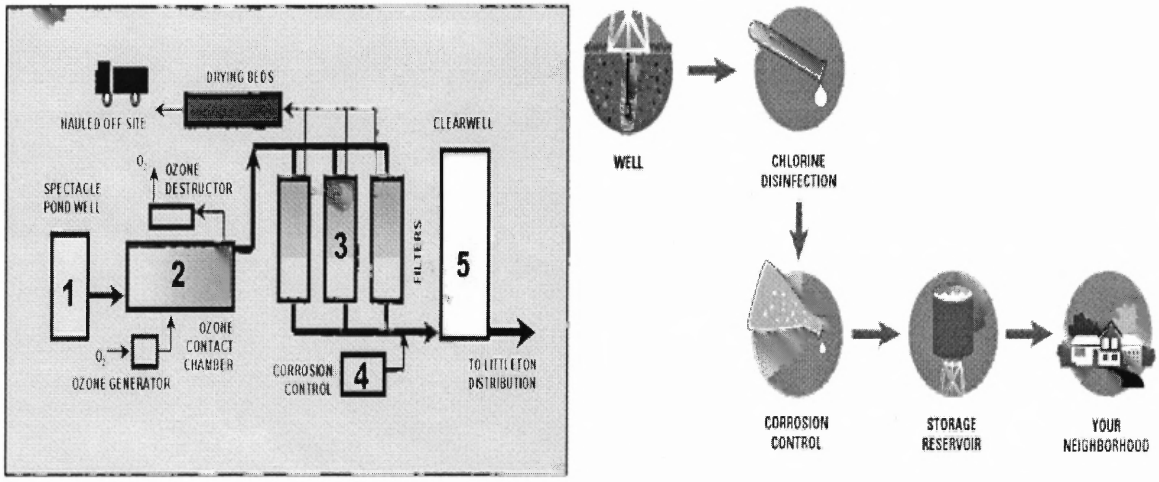

(Source: Littleton Water Department, 2005) (Source: United Water Company, 2005)

Figure 1.3 Examples of GW treatment processes

1.7.3 Technologies for removing viruses from GW and SW

Currently, there is no economical water treatment technology that is valid for achieving high logarithmic (high log) removal of viruses. Only the most effective membrane technology, reverse osmosis (RO), may in principle provide almost complete removal of viruses because the membrane pores are smaller than bacteriophages. However, the very small pore dimension of RO membranes causes a large hydrodynamic resistance that

necessitates the use of very high operating pressures (of the order of 100 psi). This high-energy consumption is unacceptable for a large-scale technology.

On the other hand, although nanofiltration and ultrafiltration can achieve 4-log removal or better removal of viruses (Jacangelo et al. 1995), the operational pressure remains high, namely 20-50 psi. In addition, some microorganisms may still pass through membrane systems through compromised seals or glue lines, and membrane imperfections (Gagliardo et al. 1996). Further, microfiltration (which is characterized by low operating pressure (10 psi) does not provide efficient removal of bacteriophages, only 1 log-removal for MS2 (States et al 2000). Although the advantages of reverse osmosis, nanofiltration and ultrafiltration with respect to virus removal are emphasized in many studies, microfiltration is always chosen in water treatment (States et al. 2000) because of its low head loss requirements. Correspondingly, post chlorination step following membrane filtration is used (States et al. 2000) for inactivating the remaining viruses (States et al. 2000), but only 4-log reduction is achieved with this practice. This means that water treated by microfiltration followed by chlorination (States et al. 2000) may become contaminated with disinfection byproducts (DBPs), which constitute another shortcoming of this strategy.

UV disinfection is one of the most economical technologies, but has technical issues which include the inability of UV to inactivate double-stranded DNA viruses like adenoviruses (except at unreasonably high doses). UV disinfection efficiency is also affected by the presence of particulate matter (turbidity) which can "shield" the target organisms and by the presence of dissolved substances like natural organic matter, iron and nitrate (Crittenden et al. 2005). Slow sand filters can achieve high log removal of

viruses but they have a small operational velocity of 0.05 m/h (0.001 cm/sec) to 0.2 m/h (0.005 cm/sec) (Crittenden et al. 2005), and thus have cost issues due to large space requirements.

1.8 Objectives of the study

One concludes that a new technology is necessary for GW disinfection with respect to virus removal because existing water treatment methods are either not economical (reverse osmosis, ultrafiltration) or do not provide high log removal with respect to bacteriophages/viruses. The proposed AF technology is expected to become a new option for removing viruses during GW treatment, with the promise of both high efficiency and low cost. The principles of this new process are elaborated in this dissertation.

Irreversible adsorption of viruses on the surface of small particle adsorbents (40-80 microns), under certain conditions, provides an opportunity to develop a new technology for efficient virus removal. However, this unique opportunity cannot be realized with the current conventional packed-bed adsorbers, such as sand filters (depth 1-1.5 m), due to the huge head loss expected if small adsorbent particles (about 40-80 microns) are used. Meanwhile, the use of such small particles is mandatory to enhance virus transport to the adsorbent particle surface, and thus it becomes a necessary requirement for achieving high log removal of viruses.

Combining features of adsorption technology with the modified hydrodynamic process configuration inherent in membrane filtration enables us to propose a new technology, i.e., Adsorption Filtration – AF, for achieving high log removal of viruses in water treatment. In the proposed AF technology, high log removal is provided by the

irreversible adsorption of viruses onto small particle size adsorbents, and a small head loss (in the order of 1-10 psi) is achieved by utilizing the modified hydrodynamic process configuration of membrane technology, i.e., large filtration surface area and small filtration depth.

The objectives of this study were to elaborate the relevant parameters that control virus adsorption process in packed-beds and to address key elements of the hydrodynamic configuration needed to develop the AF technology as they pertain to virus removal from water. The study includes experimental and theoretical aspects of the AF technology, and specifically addresses the removal of viruses from GW sources. The present study employs model viruses (bacteriophages) to test and define the practical aspects and conditions of this novel AF technology.

CHAPTER 2

PHYSICO-CHEMICAL KINETICS OF THE DEPOSITION OF COLLOIDAL PARTICLES AND VIRUSES IN PACKED-BED REACTOR -- A REVIEW

The theoretical approach to studying the effect of chemical-colloidal interactions on the attachment step during the deposition of particles (such as viruses and/or organic molecules) onto the surface collector in packed-beds combines fundamental theories of mass transfer in porous media, physicochemical hydrodynamics, colloidal stability and interaction at interfaces. A systematic elaboration of a model for colloidal particle deposition in a flow packed bed was accomplished by Elimelech and O'Melia (1990). This model, which directly pertains to the present study, is characterized below.

2.1 Theory

Colloid deposition is normally divided into two steps: 1) transport of the colloidal particle from the bulk solution to the vicinity of the collector, and 2) attachment of such particle to the collector.

The main mechanism of transport for Brownian particles is convection and diffusion. In contrast, transport of non-Brownian larger particles in a porous medium is controlled by physical forces including gravitational force and fluid drag force, and by physical interception due to the finite size of the particles (Yao et al. 1971; Tien, 1989). The chemical-colloidal interactions that act between particles and surfaces at short distances (in the order of nanometer distances) include electrical double layer, van der Waals interactions, hydrophobic interactions, effects of hydration and steric interactions.

A combination of the above effects determines the kinetics of particle/molecular

attachment to a collector. These interactions are controlled by the solution chemistry and the chemical characteristics of solid-solution interface of the colloids and collectors.

The following equation (Tien, 1989; Spielman and Friedlander, 1974) is used to describe the particle flux density j on a collector surface

$$j = D\nabla C - mC\nabla\Phi \tag{2.1}$$

where C is the concentration, D is the position-dependent diffusion coefficient, m is the particle mobility and Φ is the total colloidal interaction energy. This equation in its general form is commonly referred to as the transport equation or the convective diffusion equation. The diffusion coefficient at infinite separation can be found from the Stokes-Einstein equation (Yao et al. 1971; Spielman and Friedlander, 1974; Dahneke, 1974). The fluid velocity components are derived from the stream function around a spherical collector (Bird et al. 1960). The latter is obtained from the solution of the Navier-Stokes equation under the assumptions of steady and low Reynolds number flow. Happel's (1958) porous medium model is used to account for the disturbance of the flow field around a spherical collector by neighboring collectors.

2.1.1 Colloidal Interactions

Colloidal interactions play a significant role when a particle approaches a collector at short distances (several to a few nanometers) during the attachment step in deposition. In the Derjaguin Landau Verwey Overbeek (DLVO) theory of colloid stability (Derjaguin and Landau, 1941; Verwey and Overbeek, 1948), the total interaction energy as a function of separation distance is considered as the sum of van der Waals and electric double layer interactions. As the Brownian particles are much smaller than the collector, theoretical expressions for interaction energy between a sphere and a planar surface can

be used in colloidal deposition studies. Van der Waals interaction forces depend on the size (diameter) of the interacting particles, the distance of separation between particles and collectors, and the Hamaker constant which is related only to the properties of the interacting particles and the medium (Elimelech et al. 1995). Analytical expressions for these are available in the literature (Nir, 1976; Gregory, 1970; Gregory, 1981). The magnitude of the electrical double layer repulsion between similarly charged surfaces depends on the size of the interacting particles, the distance of separation, the surface potential of particles and collectors, and the electrolyte concentration and counter-ion valence. Quantitative theories for these interactions are available in the literature (Verwey and Overbeek, 1948; Hogg et al. 1966; Wiese and Healy, 1970).

2.1.2 Kinetics of Deposition

In deposition studies, the rate of colloid deposition onto a collector is usually expressed in a dimensionless form, using a common approach of the so-called single collector efficiency (Yao et al. 1971; Friedlander, 1958). It is defined as the ratio of the total particle deposition rate on the collector to the rate at which particles approach the projected area of the collector from the upstream. Thus the product of attachment efficiency (α) and a dimensionless deposition rate (η_T) gives the dimensionless deposition (or removal) rate of particles (η_R) as:

$$\eta_R = \alpha \eta_T \tag{2.2}$$

The attachment efficiency (α) accounts for chemical colloidal effects on the rate of deposition, while η_T accounts for physical effects (O'Melia, 1990). Thus, when chemical-colloidal interactions are favorable for deposition (i.e., in the absence of repulsive total interaction energies), the attachment efficiency approaches unity, and the

deposition rate is equal to the transport rate. In this case particle transport is the rate-determining step, and this case is generally referred to as a favorable deposition. When the chemical-colloidal interactions are unfavorable for deposition (i.e., repulsive colloidal interactions predominate), the attachment efficiency is smaller than one and particle deposition rates are hindered. This case is referred to as unfavorable deposition.

The dimensionless particle deposition and transport rates, η_R and η_T, respectively, can be evaluated from the solution of the transport equation. Levich (1962) solved the transport equation analytically for the concentration distribution and deposition rate on a spherical collector. In his solution, colloidal and hydrodynamic interactions were not included. In this case the deposition rate is equal to the transport rate. The analytical expression of Levich (1962) for the transport rate can be expressed in terms of dimensionless single collector transport efficiency (η_T), as follows (Yao et al. 1971):

$$\eta_T = 4.0 A_s^{1/3} Pe^{-2/3} \tag{2.3}$$

Where A_s is the porosity-dependent parameter of Happel's (Happel, 1958) porous medium model, and Pe is a dimensionless Pecklet number defined as $2a_c U / D_\infty$; a_c is the radius of the spherical collector, U is the approach velocity of the fluid toward the collector, and D_∞ is the diffusion coefficient of the colloid at infinite separation.

2.1.3 Chemical-Colloidal Effects on the Attachment Efficiency

The theoretical framework developed can predict the effects of solution chemistry and colloidal interactions on the attachment efficiency. Theoretical computations show the following relation for theoretical expression for attachment efficiency α_{the}:"

$$\frac{d \log \alpha_{the}}{d \log C_s} = -B(\psi_p, \psi_c, Z) a_p \tag{2.4}$$

in which C_s is the electrolyte concentration, B is a numerically evaluated function that depends on the surface potentials of particles and collectors (ψ_p, ψ_c, respectively) and the valence of the counter-ions (z), and a_p is the radius of the suspended colloids. As shown by the above equation, the slope of $\log\alpha_{the} - \log C_s$ curves is sensitive to ψ_p, ψ_c, z, and a_p. With this framework, theoretical predictions can be compared to experimental results.

2.2 Experimental Testing of Theory with the use of Model Colloid Particles

Results of systematic experimental testing of the above theory are presented in Elimelech and O'Melia (1990). In their study (Elimelech and O'Melia, 1990), surfactant-free polystyrene latex particles with sulfate functional groups were used as model colloids. The particles used were spherical and monodisperse with comparable chemical properties with three different diameters (0.046, 0.378, and 0.753μm). Spherical glass beads (0.2 and 0.4 mm in diameter) were used as model collectors for deposition studies. The glass beads were cleaned with a 1M HNO_3, rinsed with distilled de-ionized water and dried in an oven at 60° C. The collectors were packed in a cylindrical Plexiglas column to a porosity of 0.4.

KCl, and $CaCl_2$ salts were used as destabilizing electrolytes. Salt concentrations were varied over a wide range (0.001-0.3 M) so that favorable and unfavorable deposition could be studied. Latex particles were suspended in distilled de-ionized water. Dilute suspensions of particles (1-4mg/l) were used in the deposition studies. Suspensions were pumped through a packed-bed column at a constant flow rate, producing a linear velocity of 0.14cm/sec. The ζ potentials of the colloids and glass micro-spheres as a function of KCl concentration are presented in figure 2.1 below.

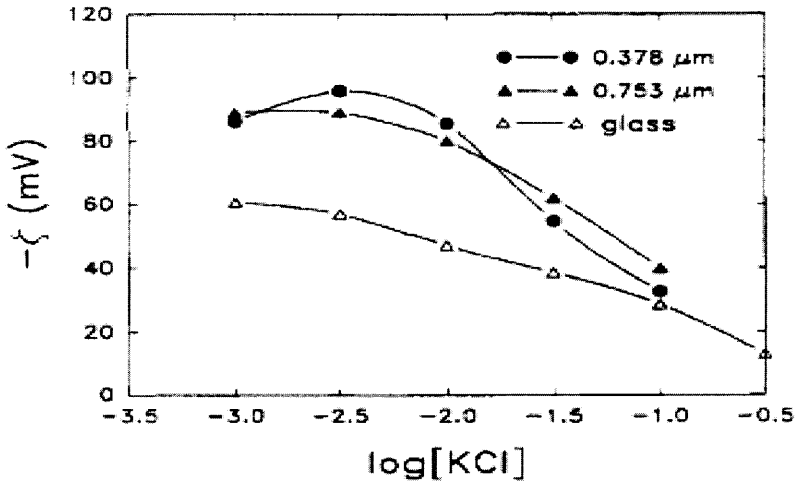

Figure 2.1 ζ potentials of latex colloids and glass beads as a function of log-molar KCl concentration (pH 6.7). The ζ potentials were calculated from the measured average electrophoretic mobilities.
(Source: Elimelech and O'Melia, 1990)

Typical particle breakthrough curves at different KCl concentrations are presented in Figure 2.2.

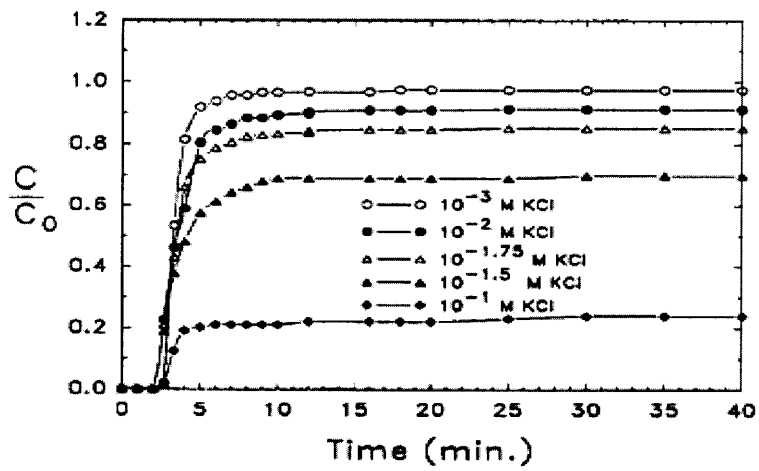

Figure 2.2 Particle breakthrough curves of the 0.753-μm latex particles with various concentrations of KCl. The residual particle concentration C/C_0 is plotted as a function of time. Experimental conditions were as follows: approach velocity 0.14cm/sec, bed depth 20 cm, collector size 0.2mm.
(Source: Elimelech and O'Melia, 1990)

As shown in Figure 2.2, particle deposition rates (or removal efficiencies) increase (C/C_0 values decrease) with increasing KCl concentrations when the physical flow conditions are similar. This finding is in qualitative agreement with the DLVO

theory. As the concentration of KCl in the solution increases, the diffuse double layer is compressed; the ζ potentials decrease (becomes less negative), and the electrical double layer repulsions are reduced. At a very low salt concentration, the repulsive electrical double layer interactions are very large and the removal is very low (C/C_o close to 1). Yao, (1968) obtained an expression that relates the experimental attachment efficiency, α_{exp}, to the initial (clean-bed) removal, $(C/C_o)_o$, by performing a mass balance of particles over a differential packed-bed volume and integrating over the entire bed depth

$$\alpha_{\exp} = -\ln(C/C_o)_o \left(\frac{4a_c}{3(1-\varepsilon)L\eta_T} \right) \tag{2.5}$$

where ε is the porosity of the bed, L is the media depth, and a_c is the collector radius. The clean bed removal efficiency, $(C/C_o)_o$, is determined from the particle breakthrough curves. The ζ potentials measured in this work were used in the constant surface potential interaction expression of Hogg et al. (1966) to calculate electrical double layer repulsion. The theoretical stability curves of the latex colloids investigated are presented in Figure 2.3.

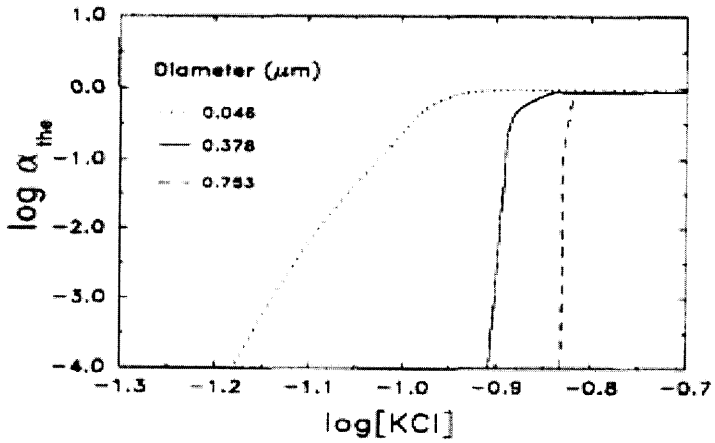

Figure 2.3 Theoretical stability curves of the model colloids employed in this research. The following parameters were used: KCl concentration in molar, surface potentials of particles and collectors were replaced by the measured mean ζ potentials, approach velocity 0.14 cm/s, porosity 0.4, collector diameter 0.2 mm, temperature 24° C.
(Source: Elimelech and O'Melia, 1990)

Theoretical and experimental stability curves of the 0.0416 μm and 0.378 μm suspensions are presented in Figure 2.4.

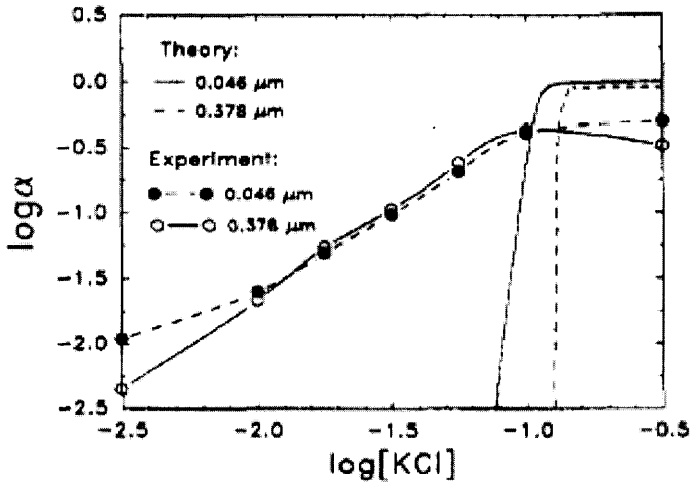

Figure 2.4 Comparison of theoretical and experimental stability curves of the 0.046 μm - and 0.378-μm suspensions.
(Source: Elimelech and O'Melia, 1990)

The mean ζ potentials of particles and collectors at a given KCl concentration were used as surface potentials in electrical double layer interaction calculations. Elimelech and O'Melia (1990) observed a common feature of the curves, as found in other studies (Ruckenstein and Prieve, 1973; Adamczyk et al. 1983; Wang, 1985): a drastic drop of the attachment efficiency practically to zero below a certain electrolyte concentration. This electrolyte concentration indicates the transition from favorable to unfavorable deposition condition and was referred to as the critical deposition concentration by Elimelech and O'Melia (1990). Above this critical deposition concentration, $\alpha = 1$, i.e., each collision between particles and collectors results in attachment. At electrolyte concentrations lower than the critical deposition concentration, the experimental attachment efficiencies were smaller that the theoretical values, which approach unity. Also, the experimental efficiencies decreased gradually with decreasing

KCl concentration, whereas theoretical values decreased sharply. This discrepancy may be attributed to the procedure used to calculate α_{exp} (equation 2.5). In this equation, α_{exp} is calculated from the ratio of the experimental single collector efficiency to the theoretical dimensionless transport rate η_T (equation 2.3).

Elimelech and O'Melia (1990) observed that the latter procedure might overestimate the real value since hydrodynamic interactions are not included in this derivation. As a result, experimental attachment efficiencies smaller than unity can be obtained. Gregory and Wishart (1980) also suggested a similar explanation, who obtained α_{exp} values smaller than 1 for deposition in the absence of energy barriers. It is also possible that the porosity-dependent parameter (A_s) used in equation (2.3) overestimates the effect of neighboring collectors (Elimelech and O'Melia, 1990). Experimental attachment efficiencies were orders of magnitude larger than predicted values in the unfavorable deposition region. Among the explanations given for the discrepancy between theory and observations are surface roughness of particles and collectors, heterogeneity of surface charge distribution, and interfacial electrodynamics of double layers during interaction (O'Melia 1987; Tobiason, 1989; Hull and Kitchener, 1969; Bowen and Epstein, 1979).

To distinguish from the discussion in Elimelech and O'Melia (1990) where main attention has been paid to the discrepancy between the theory and experiment, this study will underline the results which are significant for the adsorption filtration technology development, as follows: 1) Although the DLVO theory overestimates electrostatic repulsion and accordingly overestimates decrease in attachment efficiency below the critical deposition concentration, the measured decrease is large. The conclusion follows

that the suppression of electrostatic repulsion is important for enhancement of colloid removal, and 2) although measured α values do not equal exactly 1 when the electrostatic repulsion is suppressed, the difference from 1 is not large. This is a validation of equation (2.3), and a good approximation. This conclusion means that the equation can be safely used as the theoretical base for modeling the diffusion transport to a collector surface.

2.3 Experimental Verification of the Physico-Chemical Theory of Virus Attachment and the Basis for Adsorption Media Selection for Virus Removal

Regarding the transport stage of colloid-collector interface, the adsorbent (may also be referred to as collector/ adsorption medium (AM)) behavior is universal and the difference between them is not large for the same collector dimension if their shapes are not very different. There is not a very large difference in shapes for materials of different nature when the collector dimension of about of 100 microns is generated by means of mechanical milling processes. Hence, the selection of a proper adsorbent is determined by account of the virus attachment characteristics or sticking properties to the collector surface.

The first condition for successful virus removal is achieving the condition for irreversible attachment. As surfaces of viruses normally carry a negative charge (at the neutral pH), the electrostatic repulsion may prevent virus irreversible attachment to a collector surface, and would thus resulting in only a small removal efficiency ($\alpha << 1$). Virus attachment will become irreversible for solid collector surfaces (or patches on solid surfaces) that are positively charged due to the presence of iron oxide, aluminum oxide, or manganese oxide coating layer/s.

2.3.1 pH Influence on Virus Attachment

The net surface charge on viruses is caused by the ionization of the amino and carboxyl groups that comprise their surface proteins/glycoproteins and is a function of pH. The ionization of these surface functional groups yields viruses with an amphoteric surface that is characterized by the isoelectric points, pH_{IEP} (the isoelctric point is defined as the pH value at which the net surface charge is zero). The isoelectric point of viruses is normally in the range of 3 to 7 (Loveland et al. 1996). For example, model bacteriophages PRD1 (Loveland et al. 1996) and MS2 (Penrod et al. 1996) have isoelectric points between 3 and 4, whereas the bacteriophage SJC3 has an isoelectric point below 3 (Redman et al. 1999). In natural waters, pH is usually in the range of $4 < pH < 10$. At pH values above the virus pH_{IEP}, both virus and most mineral surfaces are negatively charged and removal by attachment may be diminished due to electrostatic repulsion as shown in Figure 2.5.

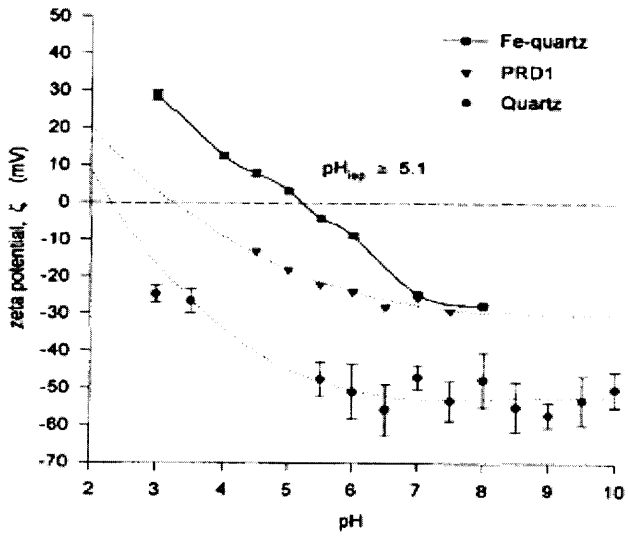

Figure 2.5 Plot of ζ potential of quartz, Fe-quartz, and PRD1 as a function of pH. The cubic polynomial curve fits for quartz, and PRD1 predicts pH_{IEP} values of 2.5 and 3.5, respectively.
(Source: Loveland et al. 1996)

Therefore, it can be expected that quartz (sand) is not an effective adsorption medium for viruses because its isoelectric point is even lower than that of the viruses, namely about 2 (Loveland et al. 1996). This is because both viruses and sand are negatively charged at the pH of water. For Fe-quartz (quartz coated with ferric oxyhydroxides), the isoelectric point is about 5 (Loveland et al. 1996), and this means that electrostatic repulsion is again possible when pH>5 and both the collector and virus are negative. A comprehensive literature review regarding virus-adsorbent interaction reveals that the attraction is generally suppressed if there is a strong electrostatic repulsion. One concludes that the proper adsorbent has to provide the electrostatic attraction at the pH condition of treatment. Accordingly, virus adsorption to sand was found to be greater at acidic rather than alkaline pH values according to (Nasser et al. 1993), as follows – see Table 2.1.

Table 2.1 Effect of pH on the Adsorption of F^+ Bacteriophages and Poliovirus onto Sand

pH	% adsorption in distilled water		% adsorption in tap water	
	F^+ phage	Polio 1	F^+ phage	Polio 1
4.0	99.9	92.0	89.6	98.1
5.0	41.3	61.5	64.4	98.1
6.0	26.9	42.3	40.3	95.8
7.0	12.6	7.7	49.5	60.4
8.0	8.2	3.8	32.3	60.4
9.0	5.9	3.9	25.4	37.2

(Source: Nasser et al. 1993)

At acidic pH conditions, ζ potentials of both sand and viruses are low, which causes a weak electrostatic repulsion. Accordingly, this weak electrostatic repulsion does not "completely" suppress virus attachment. With increasing pH, the absolute values of negative zeta potentials of both sand and virus increase. Due to the increasing electrostatic repulsion, a huge decrease in virus attachment occurs. At neutral and high

pH, the suppression of virus removal in tap water is not so pronounced as in distilled water (Table 2.1, above). This occurs because the electrostatic repulsion weakens when electrolyte concentration increases. Since the isoelectric point for Fe-quartz is much higher than that of sand (Figure 2.5), PRD1 attachment becomes possible at normal pH (Figure 2.6 and 2.7). Under definite conditions, attachment is possible even in the presence of electrostatic repulsion, i.e., when both the virus and mineral collector possess macroscopic negative charges. This occurs due to the universal molecular forces of attraction (van der Waals forces). At some distances between surfaces, such attractive forces exceed the repulsive forces at pH smaller and even larger than pH_{iso} of the mineral collector, if the difference between larger pH and smaller pH_{iso} does not exceed 2 pH units. This fact is in agreement with the DLVO theory and supported by experiment.

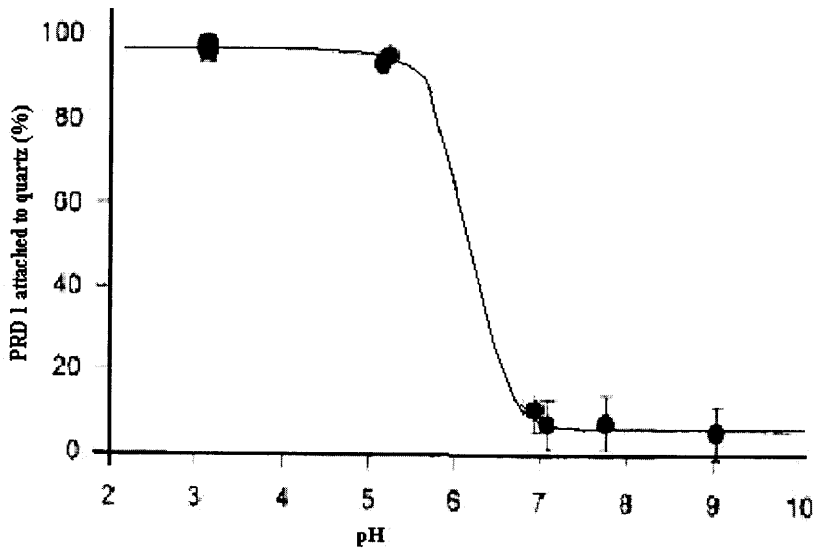

Figure 2.6 PRD1 attachment to Fe-quartz grain as a function of pH (attachment edge for PRD1 to Fe-quartz.
(Source: Loveland et al. 1996)

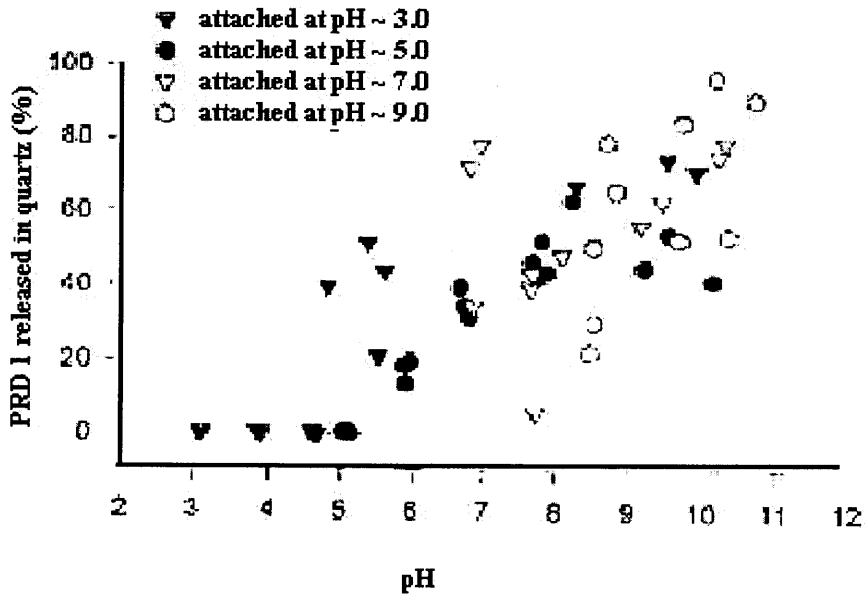

Figure 2.7 PRD1 detachment to Fe-quartz as a function of pH (detachment of PRD1 from Fe-quartz grains). Filled symbols represent irreversibly attached viruses. Empty symbols represent reversibly attached viruses.
(Source: Loveland et al. 1996)

A rapid decrease in virus attachment above pH about 7 occurs because both sand and virus are negatively charged. In experiments with other viruses (Farrah and Preston, 1985), it was found that their removal is poor at low pH, namely 3.5 and 5, in comparison with that of higher pH.

Table 2.2 Influence of pH on Adsorption of Viruses to Cellulose Filters Modified by In-situ Precipitation of Ferric and Aluminum Hydroxide

Virus	pH	Filters with Ferric and aluminium hydroxide		Untreated filters	
		% adsorbed	% eluted	% adsorbed	% eluted
Poliovirus 1	5	88 ± 3	81 ± 1	8 ± 5	9 ± 5
	7	86 ± 1	89 ± 1	10 ± 5	1 ± 1
	9	6 ± 3	7 ± 4	7 ± 6	0
Bacteriophage MS2	5	96 ± 1	56 ± 15	6 ±2	1 ± 1
	7	100	66 ± 5	3 ± 2	4 ± 1
	9	9 ± 1	5 ± 4	2 ± 1	2 ± 2

(Source: Farrah and Preston, 1985)

Although Table 2.2 relates to a cellulose filter, the same regularity has to be valid for sand coated by ferric or aluminum hydroxide, because the coating captures viruses

whereas sand or cellulose are only a substrate for the coating and may not have a direct role in capturing viruses, i.e., the process is dominated by the chemistry of the surface layer of collector.

In the case of sand, the attachment of phage particles is stronger when the absolute value of electrostatic repulsion is small at low pH (Table 2.2). For the case of metal-coated sand, the attachment of phage to collector is weaker at low pH and stronger at high pH because the electrostatic attraction is stronger for the latter (high pH condition), Table 2.2.

2.3.2 The Influence of Electrolyte Nature and its Concentration on Virus Attachment

The common trend in the experimental data considered below agrees with the theory of electrostatic interaction. The increase in electrolyte concentration and in counter-ion valence suppresses electrostatic repulsion and enhances virus removal. This regularity is well illustrated with the results shown in Table 2.3.

Table 2.3 Effect of Ion Concentration on Virus Removal

Cation	Concentration (Molar)	% adsorption in distilled water		% adsorption in tap water	
		Polio 1	F^+ phage	Polio 1	F^+ phage
None	0	46.4	28.3	88.3	81.7
NaCl	0.5	64.2	45.6	99.0	88.0
	0.05	64.2	34.7	96.0	83.7
$MgCl_2$	0.05	97.8	36.9	99.4	99.5
	0.005	85.7	32.6	86.8	96.6
$CaCl_2$	0.05	99.3	71.7	99.2	99.3
	0.005	98.2	52.1	95.7	98.6
$FeCl_3$	10^{-4}	99.9	97.4	98.6	99.5
	10^{-6}	99.8	60.8	81.7	88.3

(Source: Nasser et al. 1993)

It is noteworthy to mention that even high a NaCl concentration is not sufficient for a high virus removal. This may be better achieved with the use of divalent and trivalent cations. But even in the case of $FeCl_3$, the removal is many orders of magnitude smaller than that achieved by the AF technology under elaboration.

Information about the exact surface chemistry of sand, its origin and methods to prepare such surface for experiments were not detailed in the paper by Nasser et al. (1993). Meanwhile, the study by Litton and Olson (1993) emphasizes the enhancement of sand-virus attraction caused by impurities of natural sand surface. Accordingly, in subsequent papers (Penrod et al. 1996; Redman et al. 1999), large attention was paid to sand surface cleaning. When ultrapure quartz grains were used in a study by Penrod et al. (1996), the results confirm that α is very small, although it increases with increasing NaCl concentration, as shown in Table 2.4. The complete suppression of electrostatic repulsion at pH conditions near quartz isoelectric point is not sufficient to achieve α of about 1, although α increases as shown in Table 2.4. In these experiments, sand with rather small particle dimension, about 200 microns, was used.

Table 2.4 Experimental Conditions and Alpha Values for Filtration Experiments Involving the Virus MS2

pH	Electrolyte concentration (Molar)	α
5.0	0.010 M NaCl	0.009
5.0	0.10 M NaCl	0.09
5.0	0.30 M NaCl	0.04
3.5	0.010 M NaCl	0.12
3.5	0.30 M NaCl	0.16
5.0	0.30 CsCl	N.D*

*N.D., not determined because the breakthrough was complete; i.e. $PFU/PFU_0 \approx 1$
(Source: Penrod et al. 1996)

α was calculated in this and other research (Redman et al. 1999) using equations (2.3) and (2.5). Under the same packed bed filtration conditions, namely particle diameter

200 microns, water linear velocity 0.025 cm/sec, and l about 20 cm, effluent concentration was measured and α was estimated by (Redman et al. 1999). However, separate filtration experiments were conducted with three different salts (NaCl, $CaCl_2$, $MgCl_2$) at three different concentrations (1, 10, 100 mM). As seen from Figure 2.8, the suppression of electrostatic repulsion at high hardness (10 mM $CaCO_3$ or $MgCO_3$ or larger) provides α of about 1. This may create an illusion that sand is the proper adsorption media for virus removal. This topic is analyzed in the next subsection since the results are dominated by the use of multivalent cations in the influent..

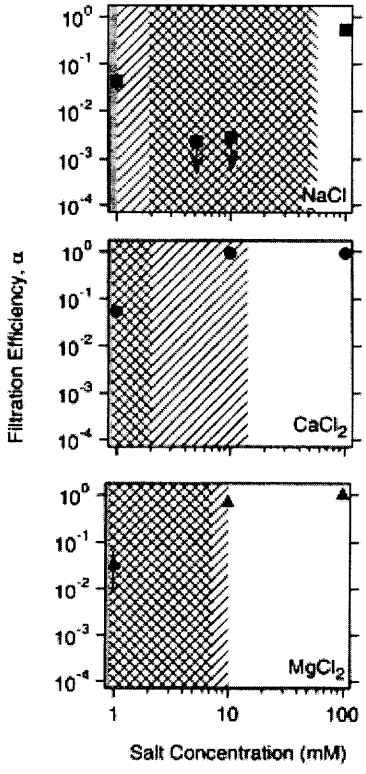

Figure 2.8 Filtration efficiencies estimated from the break-through curves, plotted as a function of salt concentration. The arrows on the 5 and 10 mM NaCl data indicate they represent upper bounds. Error bars represent one standard deviation. The hatched regions represent ranges of cations present in rainwater (shaded region, Berner and Berner, 1987), groundwater (forward hatching, Faust and Aly, 1981) and wastewater (back hatching, Chang and Page, 1985)
(Source: Redman et al. 1999).

2.3.3 Limitations Arising at Sand Application for Virus Removal

Although α about 1 is proclaimed in the study by Redman et al. (1999), a more certain statement, validated in this study (Redman et al. 1999), is that α approaches 1. First, the experiments are accomplished at pH = 7, whereas electrostatic repulsion essentially increases at larger pH. Second, the procedure of α calculation based on the measured breakthrough concentration is not sufficiently rigorous. Actually, equation (2.5) is used where all parameters are considered as known, while α is a single unknown value.

The citation (Penrod et al. 1996) shows that equation (2.5) cannot be considered as a sufficiently rigorous one, "…..difference of 100% between theoretical and experimental estimates of deposition rate are not unusual even when colloids in question are well characterized polystyrene microspheres" (Elimelech and O'Melia, 1990). In addition, equation (2.5) is derived for spherical monodisperse particles, while sand grains are not spherical and particle size distribution is not very narrow.

α about 1 is postulated (Redman et al. 1999) rather than proved. Perhaps α of about 1 maybe achieved at a $CaCO_3$ concentration much higher than 10 mM. But even 10 mM of $CaCO_3$ corresponds to a very high hardness. Water is qualified as soft if the hardness concentration is less than 70 mg/l as $CaCO_3$ and hard if the hardness concentration is higher than 150 mg/l as $CaCO_3$ (Murray and Parks, 1980). But 100 mg/l is 1 mM/ l, i.e., 10 mM/l corresponds to a huge hardness 1000 mg/l as $CaCO_3$. How unusual such a high hardness is can be seen from "USEPA 1998 Stage 1 Disinfection By-Product Rule (DBRP)," which classifies source water (mg/l as $CaCO_3$) in classes 0- 60, >60 – 120, > 120 (AWWA, 1999). A similar conclusion, that 10 mM $CaCl_2$ has unusual

high hardness, follows from the analysis of Figure 2.8 (Redman et al. 1999) as well. The hardness of rainwater and groundwater is ten times smaller (about 1mM $CaCl_2$). This means using sand as a filtration medium is possible if $CaCl_2$ in concentration larger than 10 mM will be fed into the influent.

Perhaps a $CaCl_2$ dosage of about 1 g/l is not acceptable for many reasons. First, very high hardness is not favorable for drinking water. Second, the consumption of a huge amount of $CaCl_2$ causes technological complications. For unclean sand, α is much larger than for clean sand. Nevertheless, even this α provides a possibility for virus removal. A large variety of sand due to the presence of different chemical impurities (composition) would possess different α. It is possible that different portions of sand obtained from the same location may provide different α. Therefore, the selection of proper sand composition with a consistent α value is expected to be a difficult task to achieve consistent virus removal.

2.4 Different Classes of Adsorption Media for Virus Concentration and Removal

Earlier information about virus adsorption was obtained when devices for virus concentration were being developed. Virus concentrators are necessary to determine virus concentration in natural and wastewater. Some materials such as coal-based media, clay minerals, metal oxides-hydroxides, and activated carbon could be used for virus removal. For example, 70% of bacteriophages (T4 and MS2) were removed from an aqueous solution by bituminous coal (Oza and Chaudhari, 1975, 1976).

Gupta and Chaudhuri (1995) reported that some coal-based media (bituminous coal and lignite treated with aluminum or ferric hydroxide) have very high sorption

capacities for polioviruses and sorption by these materials is very rapid. Clay minerals, kaolinite, and montmorillonite have also been found to have appreciable sorption capacities for reovirus, coliphages (T1 and T7), and bacteriophage MS2 (Schiffenbauer and Stotzky, 1982; Steven and Stotzky, 1983, 1984). Atherton and Bell (1983a, 1983b) reported that alkali-treated magnetite had high retention capacities for bacteriophage MS2. The removal of bacteriophages T1 and MS2 was also achieved by sorption to activated carbon (Cookson, 1967; Powell et al. 2000).

Insoluble salts of aluminum, calcium, and magnesium have been found to efficiently adsorb a variety of viruses (Farrah and Bitton, 1982; Farrah et al. 1976; Vilagines et al. 1982; Wallis and Melnick, 1967). Ferric chloride has been used to enhance the formation of virus-adsorbing flocs in solutions that have been used to elute viruses adsorbed to membrane filters (Payment et al. 1984; Sobsey et al. 1977).

Early researchers observed that poliovirus and influenza virus could be concentrated by adsorption to metallic precipitates such as calcium phosphate (Farrah and Bitton, 1982; Sabin, 1931; Stanley, 1945). Wallis and Melnick (1974) found that several viruses, including reoviruses and enteroviruses, could be efficiently adsorbed to aluminum hydroxide and other metallic precipitates. The ability of aluminum hydroxide and other metallic precipitates to efficiently adsorb viruses has led to their use in methods for the recovery of viruses from water. Aluminum hydroxide flocs have been used as virus adsorbent in the first or second stages of virus concentration procedures (Farrah et al. 1976; Walter et al. 1985).

Preformed magnesium hydroxide flocs have been used to further concentrate viruses eluted from micro-porous filters (Vilagines et al. 1982). Zeolites share many of

the surface properties of clay minerals (high specific surface areas and cation exchange properties), but can be prepared in a wide range of grain sizes.

Some researchers have used surfactant-modified zeolites (also called tailored zeolites) to remove heavy metals and organic contaminants from water (Cadena and Bowman, 1994; Bowman et al. 2000). Cationic surfactants are used to reverse the surface charge of zeolite collectors from negative to positive. Thus, this treatment may optimize the zeolite's ability to adsorb negatively charged pathogens in groundwater (Schulze-Makuch et al. 2003a). A high efficiency of virus removal coherent in surfactant-modified zeolite was proved in recent experiments (Schulze-Makuch, 2003a). Since metallic hydroxides have been found to efficiently adsorb viruses in water, attempts have been made to combine the filters to produce flowthrough systems that are capable of both processing large volumes of water and efficiently removing viruses from water (Farrah et al. 1991).

Seeley and Primrose (1979) coated microporous filters with aluminum hydroxide. Clogging of these filters produced slow filtration rates with distilled water and precluded their use with surface water. Wallis and Melnick (1974) combined ferric hydroxide flocs with 10-in. (25-cm) fiberglass filters. This combination of a filter with ferric hydroxide floc was reported to adsorb all of the poliovirus in 3.8 litres of water. Brown et al. (1974a, 1974b) found that coating diatomaceous earth with aluminum hydroxide flocs increased its ability to adsorb viruses from water. Two general problems have been found in attempting to combine aluminum hydroxide flocs with filters: (i) clogging of the filters (Farrah and Preston, 1985; Moeglich, 1977; Seeley and Primrose, 1979), and (ii)

poor adhesion of the floc to the filters (Brown et al. 1974b; Farrah and Preston, 1985; Toranzos et al. 1986).

Another approach was elaborated to enhance the adhesion of metal oxide coating and correspondingly to suppress its entrainment and loss (Farrah and Preston, 1985). Microporous and deep filters can be modified by in situ precipitation of individual metallic salts or combinations of two metallic salts (Farrah and Preston, 1985; Toranzos et al. 1986). The modified filters were capable of adsorbing viruses in water with little or no decrease in the flow rates through the filters. This procedure has been found to be capable of modifying diatomaceous earth (Farrah et al. 1988) and sand (Farrah and Preston, 1989) and increasing their ability to adsorb viruses in water.

There may be some concern with solubilization of aluminum during treatment. However, the use of aluminum precipitates has been an accepted component of water treatment procedures for years (Hoff and Akin, 1983). Also, the aluminum and ferric precipitates used in the above study are relatively insoluble. The solubility constants for aluminum hydroxide and ferric hydroxide are 5×10^{-33} and 6×10^{-38}, respectively (Hogness and Johnson, 1954). Not very satisfactory results were found (Ahammed and Chaudhuri, 1996) for iron hydroxide- and aluminum hydroxide-treated sand. Iron and aluminum levels in the effluents were 0.14 and 0.16 mg/l, respectively, and below drinking water guideline values (0.3 and 0.2 mg/l), as recommended by the World Health Organization (1984).

2.5 Reversibility of Virus Adsorption

Adsorption is called irreversible if the detachment of an adsorbed species is impossible, under a given condition. This is in contrast with the reversible adsorption where detachment occurs after some time; the latter is termed residence time.

In reversible adsorption, an adsorbed species may exist in the adsorbed state during the residence time only. Irreversible adsorption is an extreme case of the reversible adsorption corresponding to an infinite residence time. Reversible adsorption of viruses to an adsorbent surface implies that its transport is retarded but not attenuated. In the case of reversible adsorption, any virus will penetrate through an adsorbent; however, its average transport time through the adsorbent layer will be greater than that of water (water contact time). On the other hand, irreversible attachment will reduce the number of mobile viruses and completely remove them if enough attachment sites are available inside the adsorber, and if every virus collision with a site during contact time (time of water transport through an adsorber) leads to attachment.

According to the DLVO theory, adsorption irreversibility is controlled by the depth of the potential pit, which arises at the distance between the surfaces of adsorbent and virus. It is defined by the absolute value of the difference between van der Waals energy of attraction (which is negative) and the energy of the electrostatic interaction (which may be either repulsive for the case of similar signs of surface charges, or attractive for the case of opposite signs of surface charges). The adsorption is irreversible if the depth of the potential pit exceeds 5-10 KT (KT is the energy of heat movement, T is the absolute temperature, K is the Boltzmann constant). This occurs when adsorbent and virus electrokinetic potentials have opposite charges. When the difference between

solution pH and pH_{iso} of a mineral adsorbent is small (near the isoelectric point), its electrokinetic potential is small and correspondingly the electrostatic interaction is weak. In cases when the latter is weak and smaller than van der Waals attraction, the adsorption is irreversible, even at the repulsive electrostatic interaction that takes place as long as the difference between pH and pH_{iso} is small. This difference is specified in Loveland et al. (1996) to be about <2-2.5 pH units. Therefore, the first criterion for AM selection is that its pH_{iso} should be larger than 5 since pH of 6-7 is usual for GW.

The DLVO theory fails to quantify the inter-surface forces at rather small distances (less than 1nm). Also, this theory considers the surface as homogenous. Meanwhile, the notion of discrete adsorption sites is central in the theory of polymer and biopolymer adsorption onto a mineral surface, and this may not be completely described with the DLVO theory, and thus specific virus adsorption may be much stronger than the prediction of the DLVO theory due to the above situation. While the possibility of α for sand may not be very small in comparison with 1 at very high water hardness (which is confirmed by experiment), there is a large uncertainty regarding the residence time of adsorption.

The reversibility of virus attachment to sand surface is revealed in research studies by Loveland et al. (1996) and Murray and Parks (1980). Both small α as well as virus reversibility are found in research of transport and recovery of PRD1 in sand and gravel aquifer (Pieper et al. 1997). Table 3 in Pieper et al. (1997) demonstrates low α value, when the aquifer sand is contaminated with sewage derived organic matter. Although metal-coated sand may exhibit higher α values compared to ultrapure sand, only a portion of the surface has a metal coating, whereas the uncoated surface of sand

has a drawback similar to clean sand for virus removal. It is questionable that the residence time of virus adsorption onto the clean sand fraction of metal-coated sand grain is sufficiently long. Meanwhile, virus desorption from the clean portion of the sand grain surface makes it impossible to obtain a significant removal of viruses.

The selection of a specific adsorbent that provides strong virus adsorption improves the potential for effective virus removal with the AF configuration, especially in consideration of adsorbent and virus hydrophobic interactions. "Interaction between hydrophobic groups on the surfaces of viruses and solids may cause an increase in virus attachment when the silica beads were coated with C_{18}-trichlorosilane; 400 times more attachment took place, independent of pH" (Bales and Hinkle, 1991).

2.6 Effect of Competing Anions on Virus Sorption

Multivalent anions like SO_4^{-2} and HPO_4^{-2} compete effectively with MS2 for binding sites on layered double hydroxides adsorbents such as those used by You et al. (2003). At an MS2 influent concentration ~ 10^5/ml and in the presence of multivalent anions, the fraction of phage sorbed on layered double hydroxide collector decreased dramatically as shown in Table (2.5).

Table 2.5 Effect of Competing Anions on Virus Removal

Competing anions	Fraction sorbed %
NO_3^-	97
SO_4^{-2}	2.3+- 5.6
HPO_4^{-2}	4.8+-4.8

(Source: You et al. 2003)

2.7 NOM Influence on Virus Adsorption

If the amount of active sites needed for virus adsorption is not sufficiently large, the effectiveness of adsorption medium will be exhausted after a short time, i.e., the filter run will be short. Unfortunately, in experiments where the virus irreversible attachment was found, the fractional surface coverage by attached viruses f_{patch}, was very small. This was interpreted in the framework of the "surface heterogeneity model" which assumes that the attachment to the major part of collector surface is reversible and that irreversible adsorption takes place within small patches only. The latter was estimated as 10^{-7} of the surface area according to Loveland et al. (1996).

On the other hand, f_{patch}= 0.3 was determined for PRD1 interaction with iron-coated quartz in a systematic investigation (Ryan et al. 1999). To describe the collision efficiency for this situation, the following equation is used:

$$f_{patch} = f_{patch}\alpha_{patch} + (1 - f_{patch})\alpha_{qtz} \tag{2.6}$$

where the left hand side is the value measured by experiments of virus removal kinetics. The main part of the surface is characterized with the collision efficiency known as clean quartz surface with the same water properties α_{qtz}.

It is essential to note that for positively charged patches, $\alpha_{patch} \sim 1$ is determined. Consequently, α value about 1 may be predicted for iron oxide-coated sand, or for other positively charged adsorbents for the case of virus removal. This means that virus collision with a positively charged particle at any point results in irreversible attachment. Correspondingly, for modeling virus removal with AF, $\alpha \sim 1$ may be assumed for the entire surface, provided suitable positively charged adsorbents are selected. As the specific surface area is about a hundred times smaller for a nonporous adsorbent in

comparison with the activated carbon, the nonporous adsorbent exhaustion time has to be evaluated. After exhaustion time, the adsorbent surface is covered by an adsorbate (viruses or other molecules/ions) and further accumulation becomes impossible due to adsorbate-adsorbate repulsion.

The term adsorbent stability can be introduced in analogy to reactive media stability when a contaminant reduction seizes to adsorb because of surface blockage with reaction products (Gavaskar et al. 1998). Thus, low stability means a short exhaustion time. The expression for the virus amounts v which may be accumulated within $1 cm^3$ of adsorption media made of monodisperse spherical particles is the key value needed for the exhaustion time t_{exh} estimation:

$$v = \frac{3f}{d_c S_{vir}} \tag{2.7}$$

where $3/d_c$ is specific surface area (SSA), f is its maximal fraction, which may be occupied by viruses, S_{vir} is the surface occupied by a single virus.

The entire amount of water that flows through a $1 cm^2$ area of the AF front surface during time t_{exh} is ut_{exh}. Correspondingly, the amount of viruses removed is nut_{exh}. Assuming a uniform deposition of viruses along the water stream, one concludes that viruses are accumulated in AM volume l cm^3, where l is the filtration depth.

The maximal amount of viruses that may be adsorbed determine the maximal time of the adsorption

$$nut_{exh} = vl \tag{2.8}$$

$$t_{exh} = \frac{vl}{nu} = \frac{3fl}{d_c S_{vir} nu} \tag{2.9}$$

It turns out that this evaluation yields a very large value for the exhaustion time because S_{vir} is very small and virus concentration in water is usually not high. For $d_c = 40$ microns, f =0.1, l = 100cm, $S_{vir} = (20nm)^2 = 4x10^{-12}$, the equation above (2.9) yields $t_{exh} \sim 2.10^{15}/nu$

Even for unusually high virus concentration n=100, and u = 0.1 cm/sec, the estimation above yields $2x10^{14}$ sec, i.e., 10^6 years, which is not realistic because other sub-processes will control AM aging during the actual water filtration process.

Adsorption sites suitable for virus attachment are simultaneously valid for humic acid (a Natural Organic Matter (NOM) fraction). As the concentration of the latter is normally many orders of magnitude larger than that of viruses, the competition for virus adsorption sites with NOM for the same adsorption sites may significantly define virus removal/attachment. Therefore, the formation of NOM deposits on collector surface may control the adsorbent longevity with respect to virus adsorption efficiency.

Based on the literature review, there is no systematic investigation of NOM influence on virus removal treatment as it relates to packed bed filtration. However, some information regarding the effect of NOM may be inferred from research studies dealing with virus transport in the aquifer. "Some researchers have concluded that organic matter enhances virus transport by blocking virus attachment to mineral surfaces, while others suggest that organic matter inhibits virus transport by promoting hydrophobic interactions between the virus and grain surfaces" (Pieper et al. 1997).

Let us consider the worst situation for virus removal, namely, the possibility of virus removal suppression because of the blockage of the adsorption sites with NOM. "Bacteriophage PRD1 and silica colloids were co-injected into sewage-contaminated

aquifer and uncontaminated zones of an iron-oxide coated sand aquifer on Cape Cod, MA, and their transport was monitored over distances up to 6m in three arrays" (Ryan et al. 1999).

It turned out that the collision efficiency α in the contaminated zone was smaller than that in the uncontaminated zone. Analysis of this difference led the authors to the following conclusion: "It is reasonable to assume that adsorption of organic matter has blocked PRD1 deposition on the remaining 60% of the positively charged patches" (Ryan et al. 1999). This statement means that 40% of adsorption sites remain available for virus adsorption. At the same NOM concentration, the blockage may be smaller in the experiments with positively charged calcite (see Chapter 5) because much larger surface fraction, f_{patch}, for virus adsorption may be provided by the proper selection of the adsorption media for virus removal, compared to ~ 0.3 as determined in Ryan et al. (1999).

The virus-adsorbent bonding energy is very different for different viruses, i.e., virus and humic acid competition for adsorption sites is virus specific. Hence, the entire available information about NOM influence on virus removal can be used to conclude that this competition may complicate the development of the adsorption filtration technology for virus removal, therefore it deserves a special attention in this study.

The presence of organic matter in waste and surface water has been shown to interfere with the adsorption of enteric viruses to sand by competing for adsorption sites (Nasser et al. 1984). Bixby and O'Brien (1979) found that the adsorption of bacteriophage MS2 to loamy soil was inhibited by fulvic acid present in wastewater. Nasser et al. (1993) also observed appreciable interference due to the presence of humic

acid at only at high concentration about 10 and 100mg/l (Table 2.6), whereas lower concentration did not interfere with virus adsorption.

Table 2.6 Effect of Humic Acid on the Adsorption of F^+ Bacteriophages and Poliovirus onto Sand

Humic acid concentration, mg/ml	% adsorption in distilled water		% adsorption in tap water	
	Polio 1	F^+ phage	Polio 1	F^+ phage
100	19.1	16.2	22	16.4
10	34.5	27.9	42	25.4
1	45.7	36.7	55.5	31.3
0.1	45.0	39.7	75.5	44.7
0.01	54.9	45.6	80.0	53.7
0	42.0	47.0	88.8	56.7

(Source: Nasser et al. 1993)

In all experiments (Nasser et al. 1993), it was found that virus adsorption onto sand was greater in tap water than in distilled water. This fact emphasizes the importance of cationic concentration in the medium on the adsorption rates of viruses to sand since the latter possess net negative charge at the pH of water used. The higher adsorption of viruses from tap water can be due to the presence of divalent cations (Ca^{++} and Mg^{++}). These data substantiate the claim that freshwater with low ionic strength may enhance desorption and migration of viruses through sand filters (Nasser et al. 1989; Landry et al. 1979).

While the presence of divalent cations is favorable for virus removal from tap water in comparison with the distilled water, the concentration of NOM in tap water is larger than in distilled water. The Tables 2.3 and 2.6 show that the positive influence of divalent cations manifests itself at humic acid concentration lower than 1mg/ml.

However, 1mg/ml (1000mg/L) humic acid concentration (Table 2.3) is a concentration that exceeds the NOM content in surface water (about 10 mg/l= 10^{-2} mg/ml) by a hundred times. Hence, the studies of Nasser et al. (1993) demonstrate a

negligible influence of NOM on virus adsorption at the typical concentrations of NOM found in both surface and groundwater.

An opposite conclusion follows from Pieper et al. (1997). Because virus transport scenarios typically involve elevated concentrations of sewage-derived organic matter, the need to comprehend the role of organic matter on virus-aquifer grain interactions is necessary. To test the effects of sewage-derived organic matter on virus attachment, ^{32}P-labeled bacteriophage PRD1 was injected into sewage-contaminated (suboxic, elevated organic matter) and uncontaminated (oxic, low organic matter) zones of iron oxide-coated quartz sand and gravel aquifer on Cape Cod, MA. In the uncontaminated zone, 83% of the PRD1 was attenuated over the first meter of transport by attachment to aquifer grains. In the contaminated zone, 42% of the PRD1 was attenuated over the first meter of transport. Accordingly, $\alpha = 0.0014$ was found for the contaminated zone and 0.013 for the uncontaminated zone, respectively. These values are much lower than $\alpha =$ 0.59 to 0.94 for the same sediment in solutions free from organic matter. This difference in α suggests that even low concentrations of dissolved NOM (0.1-1.0 mg/l) in uncontaminated groundwater enhanced PRD1 transport.

2.8 Testing Different Adsorption Media for Virus Removal

The complete removal of MS2 bacteriophage using layered double hydroxide-coated sand is reported in You et al. (2003). No conclusion about the technological value of this research is possible because information about filtration velocity and particle dimension were not defined in the above study. Schulze-Makuch et al. (2003a) proclaim the

superiority of surfactant-modified zeolite (SMZ) in comparison with oxide-coated sand for virus and bacteria removal from groundwater.

Field experiments were conducted to evaluate the efficiency of iron-oxide-coated sand (ICS) and surfactant-modified zeolite (SMZ) to remove viruses and bacteria from groundwater. The reactive media were employed as filter packs of a pumping well that withdrew sewage effluent from a constructed wetland at a rate of 0.72L/min. The contact time of the pumped water with the filter pack (10 cm thick) was about two minutes. Upgradient of pumping well, the sewage effluent was spiked with MS2 bacteriophage and E-coli. While the employed ICS filter pack failed to remove viruses and bacteria to a significant degree, the SMZ filter pack removed more than 99% of the viruses and 100% of E-coli from the groundwater while fresh.

In an additional field experiment using the same configuration but leaving the filter pack in place for more than five months, the SMZ filter pack was still removing 100% of E-coli, but failed to reduce virus numbers to a significant degree. The grain size distribution used in this study (Schulze-Makuch et al. 2003a) was 80% gravel by weight with a diameter ranging from 0.25 to 1mm. The iron coating increased the surface pH_{iep} of the sand, which consisted of a mix of quartz and feldspars, from < 7 to ~ 8.5. A natural zeolite material, ~ 74% clinoptilolite by weight (obtained from St. Cloud Mining Co., Winston, New Mexico) was used in this study. It had an external (nonzeolitic) surface area of 14 m^2/g, an aggregate size of 1.4 to 2.4 mm, and a bulk density of 0.9 g/cm^3 (Bowman et al. 2001).

The high intra-aggregate porosity increases the zeolite's surface area about two orders of magnitude larger than that of the sand used in this study. Due to isomorphic

substitution of aluminum for silicon in their crystal structures, most zeolites have a net negative structural charge, which limits their capacity for adsorbing viruses. However, the charge on the external surfaces of zeolites can be modified by cationic surfactants.

For this study (Schulze-Makuch et al. 2003a), the untreated zeolite was modified by spraying a 29% aqueous solution (by weight) of hexadecyltrimethylammonium chloride (HDTMA-Cl) onto the zeolite, thoroughly mixing the slurry for 5 minutes, and drying the resultant surfactant modified zeolite (SMZ) at 150°C for 10 minutes. At pH~7 in this experiment, the difference between pH_{iso}~8.5 and 7 was rather small, and perhaps electrostatic attraction was weak. However, the main reason for small virus removal by sand may be attributed to the very slow transport at adsorbent particle surface with a dimension of about 250 microns. At l=10cm and u=0.1 cm/sec, the log removal calculated using equation (2.10) is low for the 250 micron collector. Meanwhile, the volume fraction of this smallest fraction is about 0.1, while removal by larger collectors is negligible.

Had the authors been more attentive to the colloid transport theory (Section 2.1), they would not have used such large sand collectors in their experiment. The same remark is not valid for zeolite collectors, because they mention "aggregate" size 1.4 to 2.4 mm. Virus removal by larger particle size (1000 microns) collectors, especially at rather large velocity of about 0.1 cm/sec in these experiments (Schulze-Makuch et al. 2003a), is negligible, which follows from the theory (Section 2.1) and from the experiment results of this study (Chapter 4). However, transport to an aggregate may be much stronger than that for a single particle of the same dimension and shape. This

perhaps may explain why virus transport was provided in spite of large aggregate dimension.

Let us consider, for example, a spherical carrier particle with a dimension of about 1 mm coated by collector spherical particles with a dimension of about 100 microns. Due to large collector particles, the pores between them are broad and a high velocity of about 0.1 cm/sec is possible at rather low pressure drop. While the velocity of 0.1 cm/sec in packed bed with a particle dimension of 100 microns corresponds to a pressure drop exceeding 1m of H_2O (water), this fast stream at low pressure is possible for aggregates. Rather rapid diffusion transport to 100 micron particles of aggregate provides effective virus removal. The authors mention a rather small aggregate density, $0.9 g/cm^3$, inherent in aggregates and specific surface area 12 m^2/g. The equation SSA=6 / d is well known for a powder consisting of spherical particles with diameter d. SSA=$12m^2$ yields d~0.5 microns.

One concludes that the zeolite aggregate has a fractal structure. However, the porosity of the fractal aggregate is very high (0.9 to 0.99). Perhaps information about the SMZ aggregate structure may be found in Bowman et al. (2000, 2001).

While the aggregates of optimal dimension with subaggregates of optimal dimension may provide a new and much higher level of achievement in high log removal, there is a harmful peculiarity in this new approach to water treatment. The filter media cleaning and regeneration are problematic because the aggregates may be destroyed. It is very unlikely that the optimal structure of aggregates will be restored after their destruction.

Perhaps there is another mechanism which enhances virus transport because the authors write: "As the HDTMA content on the surface decreases, the SMZ begins to lose its anion exchange characteristics (Li and Bowman, 1998). This decrease in anion exchange activity would have the strongest effect on MS2 retention, given MS2's small size and hydrophilic nature". Zeolites are ion-exchange resins. Ion exchange occurs through diffusion transport. When diffusivities of cations and anions are not equal, the electrical field arises, which is localized within the diffusion layer with the thickness δ. This electrical field enhances virus transport through the diffusion layer. This is equivalent to an increase in virus diffusivity. However, it occurs if the electrical field (of diffuse origin) pushes the negative virus towards the ionite surface.

A harmful peculiarity of this mechanism is a rapid exhaustion of ion-exchange capacity. After a period of five months there was no significant removal of viruses by SMZ, while removal of the E-coli was 100%. Better E-coli removal in comparison with viruses indicates that SMZ aggregates consist of collectors of optimal dimension. As the E-coli dimension exceeds the MS2 dimension by about 100 times, their diffusivity is 100 times smaller. Accordingly, E-coli's diffusion may not provide for its rapid deposition. Hence, the main mechanism of E-coli transport seems to be interception because if the collector dimension is about 1000 microns (Schulze-Makuch et al. 2003a), the collision efficiency due to diffusion is too small at collector dimensions of about 1000 microns.

Farrah et al. (1991) and Lukasik et al. (1999) have developed systematic investigations aimed at elaborating flow packed bed technology for virus removal over the past 20 years on the basis of in situ precipitation of ferric and aluminum hydroxides. Metal oxide-coated sand sieved to a size less than 150 microns with a column length of

35 cm at a velocity of 0.3 cm/sec was used in experiments (Lukasik et al. 1999). This column reduced E coli, V. cholera and MS2 by several orders of magnitude. This high log removal was achieved due to large α value for coated sand, while virus transport was provided due to small collector dimension and sufficiently large depth l. The experiments were accomplished with tap water over a period of a month. The authors did not detect a decrease in flow rate through the column throughout this long-term experiment.

This causes the illusion that the problem of coated sand deactivation and clogging does not exist. But this is not so because water treatment was accomplished during a short time every day. During the course of a month, the entire amount of treated tap water was 200 liters. Taking into account the column cross-section of about 20 cm^2 and the velocity of 0.3 cm/sec, it is revealed that the water was treated for only about 10 hours during the month. Hence, the coated sand is not tested with respect to its performance during a long period of time.

Another essential shortcoming of this research is the very high pressure drop. Values of pressure drop have not been mentioned in Lukasik et al. (1999). An estimate according to Ergun equation for l = 30 cm, d_c = 150 microns, u = 0.3 cm/sec yields a pressure drop of 100 cm H_2O. But in reality it may be upto 3 to 10 times higher because a rather broad fraction may be obtained when the sieving range of AM < 150 microns. This yields an increase in pressure drop by about 4 times. Also, the so-called shape factor for sand, which is squared in the Ergun equation, might increase the head loss by 3 to 5 times. This shortcoming of the packed bed design in this work may be eliminated by means of a velocity decrease of 3 to 5 times because a velocity of about 0.1 cm/sec is typical in rapid filtration. During long-term treatment, the gradual NOM and other

contaminant deposition will block the metal oxide surface which will decrease α and increase the pressure drop. At high velocity, and accordingly at high viscous stress, the deposit may be removed and these difficulties may be overcome.

Another usual approach in water treatment is AM regeneration by means of backflush. But oxide coated-sand backwash is problematic because the coating may be removed due to attrition. It took many years to provide the stability of the metal oxide coating with respect to the filtration flow. It is obvious that attrition during backflush is much more harmful. There is no mention of this in any of the papers devoted to metal oxide-coated sand because this is the main obstacle for the development of technology based on this kind of filter media. This explains why there is no development based on the patent (Lukasik et al. 2000) and that it took four years before the next step in the development of this technology was published (Scott et al. 2002).

The operational parameters of the experiments in this study (Scott et al. 2002) were essentially changed. While the sand was again coated with aluminum chloride and ferric chloride, the media size was changed from < 150 microns in the previous study (Lukasik et al. 1999) to a range of 600-700 microns, and the velocity was maintained at about 0.14 cm/sec. These parameters lie within those used in large-scale municipal and industrial water filters. Similar to rapid filtration, cake formation is eliminated at this large grain dimension and velocity.

However, the problem of gradual film clogging and metal oxide deactivation perseveres. Nevertheless, information about the long-term testing of new operational parameters is absent in this paper, which advertises the new technology for virus removal. The backflush is mentioned (Scott et al. 2002), but its possibility without the

coating loss is not discussed. In this study (Scott et al. 2002) the uncoated sand removes about 15% of viruses, while the increase in removal up to 50% is achieved due to metal oxide coating. *l* in this experiment was 50 cm. Table 2.7 contains the operational parameters and other characteristics of a new rapid deep filtration device for municipal / industrial filtration (Scott et al. 2002).

Table 2.7 Cost of Using Coated Sand for Municipal/Industrial Filtration

Filter coefficient	1.2 m^{-1}
Bed depth	1.0 m
Initial virus removal	70%
Porosity	0.35
Bed cross-sectional area	1.0 m^2
Bed depth	1.0 m
Bed volume	1.0 m^3
Media weight (specific gravity of sand = 2.65	1722.5 kg
Unit coating cost	$ 0.07/kg
Coating cost for 1.0 m^3 bed	$ 120.57
Superficial velocity	1.4 mm/s
Volume treated 1 month	3498 m^3
Unit cost	3.4 cents/m^3
Typical U.S. delivered municipal water cost (conventional filter media)	40 cents/m^3

(Source: Scott et al. 2002)

Calculations of α using data about the virus removal, d_c, *l* and u given in Table (2.7) and Figure 1 of this study (Scott et al. 2002) revealed value of $\alpha = 0.15$ and $\alpha = 0.2$. These are rather small values for the coated sand. Accordingly, the planned initial virus removal for municipal filter (Table 2.7 in Scott et al. (2002) is only 70%. It is proposed to replace the uncoated sand in the rapid sand filter by metal oxide-coated sand to provide virus removal of about 70%. Hence, the earlier task, namely the technology elaboration for providing very high log removal of viruses of about 6, is not solved in spite of about 20 years of effort. Finally, the authors (Scott et al. 2002; Lukasik et al. 1999; Farrah et al. 1991) replaced this challenge by a simpler task, namely modest removal of viruses by 70%. This happened because they were unable to maintain operational parameters for

smaller dimensions of collector, even though smaller collector dimension is essential to increase log removal.

The authors (Scott et al. 2002; Lukasik et al. 1999; Farrah et al. 1991) started from a collector dimension smaller than 150 microns and replaced it by a collector of 600-700 microns. It seems that the authors (Scott et al. 2002; Lukasik et al. 1999; Farrah et al. 1991 were unable to accept the effective small collectors due to the shortcomings inherent in coated sand, namely because of the coating loss during the backwash. The smaller the collector, the more rapid is its clogging, and accordingly, the shorter is its filter run. The shorter the filter run, the larger is the amount of backwash needed per year. As coated sand loses coating during every backwash, this becomes the main limitation. These disadvantages inhibit the use of effective small collectors in water treatment.

2.9 Conclusion

The basis for modeling virus and bacteria removal is the colloidal filtration theory, which emphasizes the role of electrostatic repulsive forces and the role of colloidal transport. Colloidal particle filtration and molecular (ion) adsorption are 2-step processes, as follows:

1) The first step is colloidal transport, namely, particle (virus) transport from the water stream to the surface of collectors which form the flow packed bed (FPB).

2) The second step is the attachment of particle (virus) to the collector's surface in FPB.

As surfaces of viruses and bacteria (like any surface) carry a negative charge (at neutral pH), the electrostatic repulsion retards the deposition at their approach to the

collector surface which results in insignificant removal. For bacteriophages, this was experimentally verified by Redman et al. (1999). The authors generalize similar publications and proclaim that electrostatic suppression of virus removal is a general phenomenon. Redman et al. (1999) measured "filtration efficiency" (part of collisions with collector surface which lead to virus attachment). With the decrease in virus electrokinetic potential to zero, "filtration efficiency" increases and almost all collisions lead to attachment.

Although the DLVO theory overestimates electrostatic repulsion, and accordingly overestimates the decrease in attachment efficiency below the critical concentration of deposition, the measured decrease is large. The conclusion follows that the suppression of electrostatic repulsion is important for enhancement of colloidal removal. On the collector surface, this is provided with the use of the mineral collector particle with a positive charge (calcite, for example) or metal- coated sand.

The mechanism of colloid (biocolloid) transport to collector (adsorbent) surface is well documented, quantified and verified by experiments (Elimelech et al. 1995). For viruses and small bacteria, the gravitational settling and the interception mechanisms are negligibly weak because of their small dimensions. The deposition due to Brownian diffusion predominates. Collision efficiency provided with one collector due to Brownian diffusion of viruses or bacteria is:

$$\eta_T = 4A_s^{1/3}\left(\frac{D}{ud_c}\right)^{2/3}\alpha \tag{2.10}$$

Although the measured values do not equal exactly 1, when the electrostatic repulsion is suppressed, the difference from 1 is not large. This is validation of equation

(2.3) by Loveland et al. (1996) as a good approximation. This conclusion means that equation (2.3) may be the theoretical base for modeling the diffusion transport to a collector surface. As a virus or a bacterium flows with water through a column with length l, it meets l/dc grains, and correspondingly, the log removal increases proportional to this huge multiplier:

$$\ln\left(\frac{N_c}{N_o}\right) = 6A_s^{1/3}(1-\varepsilon)\frac{l}{d_c}\left(\frac{D}{ud_c}\right)^{2/3}\alpha \tag{2.11}$$

Although in some research a sufficiently large log removal of viruses was obtained, this was achieved when the operational parameters were not suitable for water treatment, namely at too low filtration velocity or at high pressure drop. When high log removal was provided, rapid filter clogging occurs.

Both small column experiments with tap water and the monitoring of subsurface transport of viruses reveal the same main regularities of virus NOM competition for the adsorption sites, as follows: a) The attached efficiency α decreases with increasing NOM concentration. However, α does not become zero even at high but realistic NOM concentration. This means that NOM in particular may not prevent virus adsorption, but NOM might retard the kinetics of virus deposition. b) While α increases and approaches almost to 1 due to metal oxide coating at low NOM concentration, it essentially decreases at larger NOM concentration. The experiment with tap water and the surface water yields $0.15<\alpha<0.4$.

Among the many candidates for virus adsorbent, the best results are obtained for metal oxides and tailored zeolites. Simultaneously, the authors proclaim that their cost is acceptable. As to tailored zeolites, their main shortcoming is not discussed by the authors

(Schulze-Makuch et al. 2003a). It is questionable whether their regeneration will be possible because the favorable aggregate structure of zeolites will be destroyed during backwash. Although the field experiments with tailored zeolites were accomplished, down-gradient to a septic system, their value is low because information about the duration of the filter media exposition to the contaminated stream with respect to viruses is lacking. At least it is shorter than 1 week.

An even worse situation is inherent in the so-called long-term monitoring of metal oxide sand, i.e., the duration of metal oxide sand exhibition to the tap water for only 10 hours. Although α may approach 1 for clean metal oxide sand, it decreases to about 0.1-0.3 for surface water and tap water due to NOM accumulation. Even in tap water at a sufficiently high concentration of divalent cations, α increases but at a sufficiently high concentration of sulfate and phosphate ions, it decreases.

There is a shortage of research devoted to the adsorbent consisting of the entire metal oxide. Perhaps α may be larger than in the case of metal oxide-coated sand. The latter demonstrates low α in the presence of divalent anions, at pH below 4 to 5 and above 7 to 8. It is very probable that the metal oxide coating is lost during backwash. This is perhaps the reason why the authors (Scott et al, 2002; Lukasik et al. 1999, Farrah et al. 1991) who 5 years ago demonstrated virus log removal larger than 6 using collectors smaller than 150 microns, now present a technology for virus removal of only 70%. This low virus removal is caused by the use of coated sand particles larger than 600 microns.

The evolution in research by Scott et al. (2002), Lukasik et al. (1999), and Farrah et al. (1991) leads to an important conclusion. To achieve log removal of 6 with respect

to viruses, it is not sufficient to have perfect properties of adsorbent surface only. The use of the optimal adsorbent surface has to be combined with optimization of the hydrodynamic process configuration. It has to be optimized in a way that the use of the collectors of smaller dimension is possible without an essential increase in the pressure drop. In the next Chapter, an advanced hydrodynamic process configuration is proposed, which creates a perspective to provide log removal of about 6, rather than a longer filter run and the possibility of adsorbent regeneration by means of backwash.

CHAPTER 3

CONCEPT OF ADSORPTION FILTRATION PROCESS FOR VIRUS REMOVAL

3.1 Concept of Adsorption Filtration and its Quantification

At least two peculiarities cause large difficulty in drinking water preparation requiring necessary low virus content. First, an unusually high log removal greater than 6 is necessary, while smaller log removal is sufficient with respect to other contaminants. Second, virus transport to the collector with a typical dimension (about 1mm) is very slow. It must be emphasized that the transport stage has to be enhanced, while proper collectors for virus irreversible adsorption are known. Metal oxides, or sands coated by metal oxides, are promising adsorbents for virus removal.

An overview of the literature (Chapter 2) shows that an attachment efficiency of about 1 can be achieved. However, in those experiments, when log removal of about 6 was achieved, the operational parameters were unacceptable for the elaboration of large-scale technology. Another conclusion following from analysis of the literature is that the existing theory of virus transport to a collector (for example, equation (2.10)) or for entire virus removal (for example, equation (2.11)) within Flow Packed Bed (FPB) is not used to estimate the possibility of large-scale technology elaboration. Meanwhile, the paper by Elimelech et al. (1990) demonstrates that these equations are rather reliable and their use is reasonable to estimate a perspective for large-scale technology for virus removal.

In the process of the application of equation (2.11) for estimating the possibility of a large-scale technology elaboration for high efficiency virus removal, it turned out that this may be possible when the entire process of filtration is revised with respect to

virus removal. As result, a concept for a new water treatment process was elaborated, which will be referred to as adsorption filtration (AF). In this process, virus removal is achieved due to adsorption on collector particles. However, the operational parameters of filtration, which effect virus transport, undergo a cardinal revision.

3.2 Revision of Adsorbent Grain Dimension with respect to Virus Removal

It can be easily seen from the reliable equation (2.11) that a tremendous increase in log removal is possible with the use of smaller particle adsorbents since the log removal is inversely proportional to $d^{5/3}$. "Filters with small grains can result in high log removal of particles. However, the use of small grains is not recommended in water treatment since it results in higher head losses, clogging of filters, and shorter filter runs" (Elimelech et al. 1995). This statement is valid for conventional filtration for removing coarse particles or for adsorption of smaller molecules from water, but is not valid for viruses.

Commercially available particle sizes of granular activated carbon (GAC) range from 0.55 mm to 1.35 mm. This size range provides a reasonable compromise between good hydraulic characteristics and higher adsorption rates" (Faust and Aly, 1987). The compromise is reasonable with respect to small organic molecules whose diffusion is rapid but this compromise is not reasonable with respect to viruses or bacteria whose dimensions are 100-1000 times larger, and correspondingly, their diffusivity and adsorption rates are 100-1000 lower. The compromise is especially not reasonable with respect to viruses because the unique large log removal may not be provided.

A significant increase in contaminant removal is possible with the use of smaller grain particle adsorbents. But this will be accompanied with a significant increase in the

head loss, according the Ergun equation (3.1) (Cooney, 1999), below. By decreasing adsorbent particle dimensions to about 100 microns, the head loss increases about a hundred fold, which is not acceptable for practical applications.

$$\frac{\Delta p}{l} = \frac{180(1-\varepsilon_o)^2 \mu u}{\varepsilon_o^3 d_{FPB}^2 \rho_L g} \tag{3.1}$$

where μ is viscosity, ε_o is porosity and u is linear flow rate.

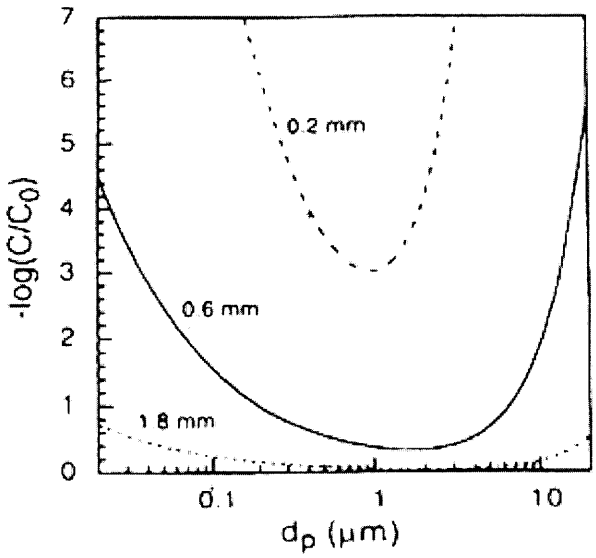

Figure 3.1 Log removal of particles as a function of particle diameter calculated for three different filter grain sizes (diameters) using equation (2.5). The following parameters were used: $\alpha = 1.0$, U = 0.14cm/s, L = 60cm, f = 0.4, T = 293 K, A = 1 x 10^{-20}J, and $\rho_p = 1.05 g/cm^3$.
(Source: Elimelech et al. 1995)

The need for using a small adsorbent particle dimension to remove viruses from water is universal. However, the fundamental difficulty is that although a small adsorbent particle size is needed for high log removal, the head loss increase that accompanies the use of small particle size makes it difficult in large-scale applications. This controversy cannot be eliminated with the improvement of adsorption properties of the surface

because the universal law of convective diffusion transport will control the entire process rate. The single possibility of avoiding this dilemma is by the cardinal revision of the entire hydrodynamic process configuration of flow packed bed (FPB) adsorber. The concept of AF is elaborated by means of this revision, with the use of small particle size absorbents.

3.3 Revision of the Entire Hydrodynamic Process Configuration of Adsorber with respect to Virus Removal

The main components of the entire process configuration are particle dimension and hydrodynamic process configuration. The main parameters of the hydrodynamic process configuration are filtration area (S) and filtration depth (*l*). The latter two parameters and the adsorbent particle dimension determine the overall flow rate (q) for an adsorber as shown in equation (3.2).

$$q = Su = \frac{S}{l} d^2 \Delta p A \tag{3.2}$$

where A may be considered as invariant.

$$A = \frac{\rho_L q \varepsilon_o^3}{180(1-\varepsilon_o)^2 \mu} \tag{3.3}$$

The revision of the entire process configuration of FPB includes 2 main steps, as follows:

i) The decrease in adsorbent particle size by about 10 times yields an increase in adsorption rate by about 30 times, but at the same time increases the head loss by about 100 times -- or flow rate decreases about 100 times at the same head loss; and

ii) The increase in the filtration area (S) *n* times enables one to decrease filtration velocity '*u*', '*n*' times, while the volumetric velocity preserves its necessary large value. Simultaneously, the filtration length may be decreased. The decrease in both the filtration velocity and the filtration length

compensate for the pressure increase, caused by the particle dimension decrease of about 10 times. This procedure may be quantified using equation (3.2), namely its group $(S/l)d^2$. The decrease in d, for example, 10 times, and the simultaneous increase of the ratio S/l 100 times, provides the same volumetric velocity 'q' without any increase in the pressure drop.

In principle, a plate-type adsorber (single layer) with decreased adsorbent particle dimension, increased S and decreased l, which can increase the adsorption rate about 30 times without any change in head loss, flow rate, and adsorber volume, is possible. However, space limitation may prevent the use of a large diameter (S) plate adsorber, although a tremendous increase in the adsorption rate may be achieved.

3.4 Combining Adsorber with Modified Hydrodynamic Process Configuration of Membrane Technology – AF Design

A typical membrane module consists of a feeding channel, permeate channel and a membrane layer between them (Figure 3.2). The membrane hydrodynamic permeability (per unit surface area) is extremely low because of its very small pore dimensions. Nevertheless, the flow rate (i.e., superficial or operational velocity) through a finished membrane device (module) is reasonable due to the small thickness of the asymmetrical membrane active layer and due to the hydrodynamic porous configuration effected by its extended surface area.

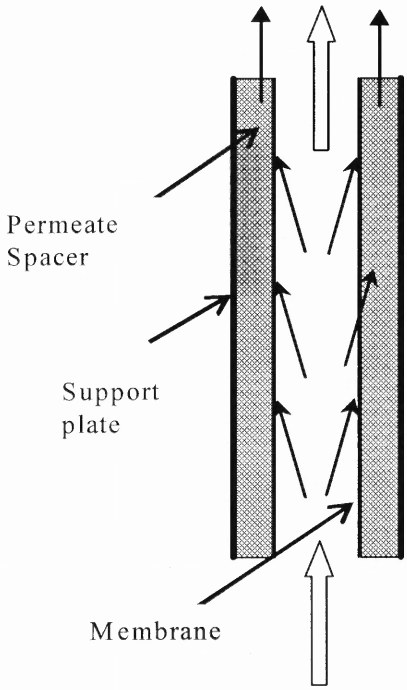

Figure 3.2 Schematic showing hydrodynamic configuration of Membrane Filtration module

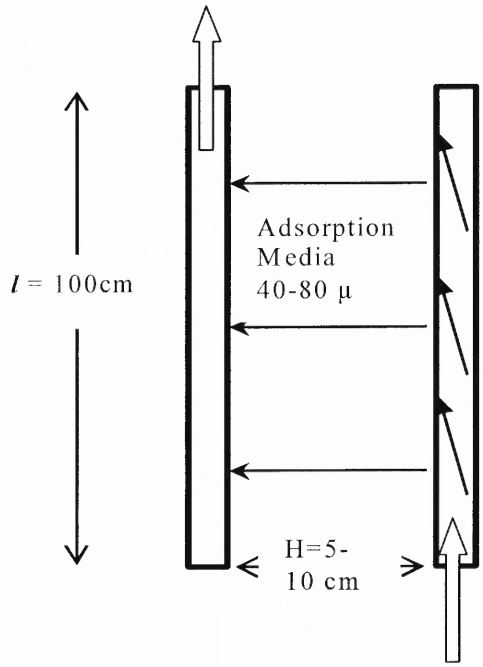

Figure 3.3 Schematic showing hydrodynamic configuration of Adsorption Filtration module with one feeding and one receiving channel and an adsorbent layer between them

The incorporation of the two modifications into the plate-type membrane module (Figure 3.2) yields a plate-type module for adsorption filtration (Figure 3.3) by incorporating the following: i) closing the feeding exit channel; and ii) incorporating an adsorbent media layer instead of the membrane. The adsorbent is confined between two perforated, firm, plastic plates with the perforation diameter about 20 microns. AF of any overall flow rate may be fabricated by means of uniting several AF modules.

A significant increase in Hydraulic Conductivity (HC) can be achieved by incorporating into the Flow Packed Bed (FPB) body two arrays of transport channels, that is, transition to AF hydraulic process configuration. One array of channels (feeding channels) is connected with the upstream face, and the second one (receiving channels) with the downstream face, as shown in Figure 3.4. Feeding and receiving channels

alternate along the AF front surface. As the pressure in the feeding channels is almost the same as the pressure before AF, and the pressure in the receiving channels is almost the same as behind the AF, water filtrates through the Adsorption Media (AM) from a feeding channel to the nearest receiving channels and flows out along them.

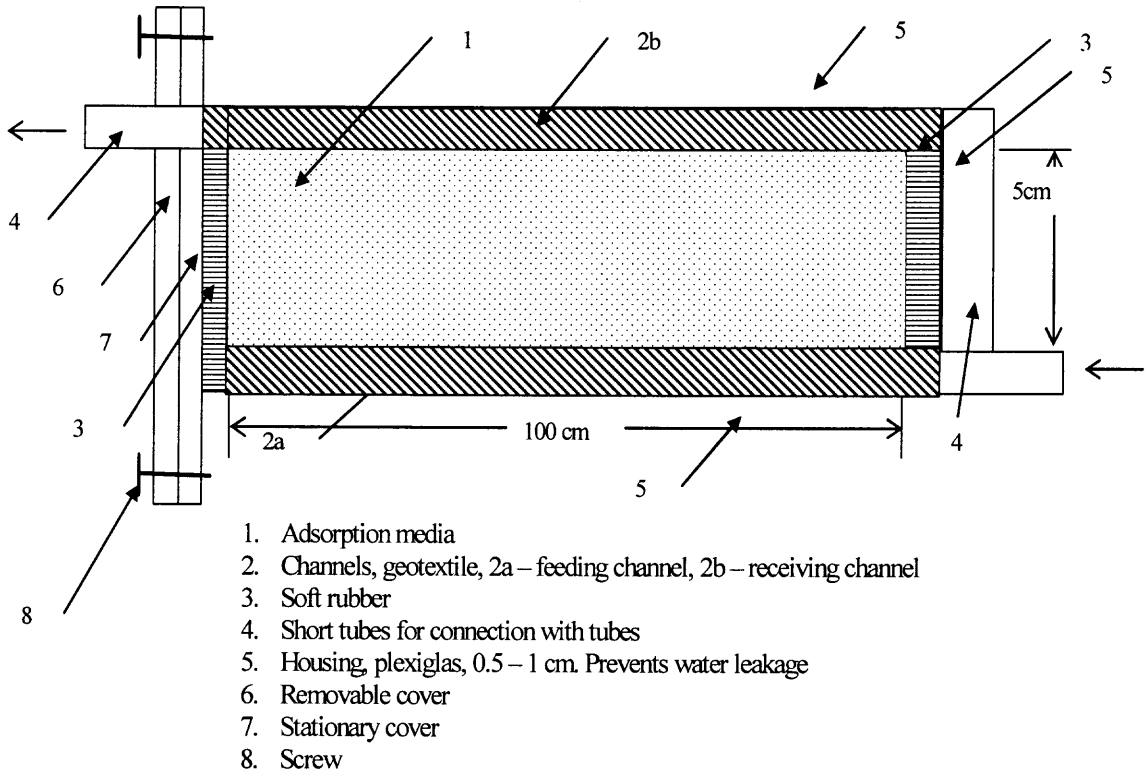

Figure 3.4 Adsorption filter with one set of feeding and receiving channels.

3.5 The Decrease of Adsorbent Particle Size and its Implications

HC increase is provided by an increase in filtration surface and a decrease in filtration length (thickness h of AM between feeding and receiving channels), and is proportional to the ratio of increased filtration area to decreased filtration length. For the sake of brevity, let us consider the AF as a parallelopiped with its length l and square cross-section with linear dimension l_1^2. Thus the filtration area for one channel is $2ll_1$ because

the liquid filtrates in the neighboring channels through both the lateral surfaces of the channel. The number of the feeding and receiving channels is the same and equals to $l_1/2h$. The entire filtration area in per l_1^2 of the front surface of the installation is the filtration area per one channel multiplied by the number of channels.

$$S_{AF} = \frac{2ll_1^2}{2h} = \frac{l}{h} S_{FPBR} \tag{3.4}$$

because $S_{FPBR} = l_1^2$ i.e.

$$\frac{S_{AF}}{S_{FPBR}} = \frac{l}{h} \tag{3.5}$$

The entire flux crosses the front surface of AF(S_{AF}) and its filtration area. One concludes that superficial velocity through AF is increased l/h times in comparison to the velocity through AM (u_{AF})

$$v = u_{AF} \frac{l}{h} \tag{3.6}$$

The filtration length for FPB and AF are l and h respectively.

The smaller the distance h between channels, and correspondingly, the smaller the hydrodynamic resistance of the AM layer between channels, the smaller particle dimension d_{AF} in AF may be used in comparison with particle dimension d_{FPB} in FPB

$$d_{AF} = d_{FPB} \frac{h}{l} \tag{3.7}$$

This recommendation for the selection of d_{AF} follows from comparison of AF and FPB at the same crossection, i.e., same head loss conditions:

$$S_{AF} = S_{FPB} = S, \Delta p_{AF} = \Delta p_{FPB} = \Delta p \tag{3.8}$$

Afterwards, equation (3.2) is specified for AF and FPB

$$q_{FPB} = \frac{S}{l} d_{FPB}^2 \Delta pA \, , q_{AF} = n_{ch} \frac{S_1}{h} d_{AF}^2 \Delta pA \tag{3.9}$$

where the channel amount

$$n_{ch} = \frac{l_1}{2h}; S_1 = 2ll_1, S = {}_1^2 \tag{3.10}$$

equation (3.7) follows from equation (3.9) at the condition

$$q_{FPB} = q_{AM} \tag{3.11}$$

one concludes that hydrodynamic process configuration allows for the decrease in adsorbent particle diameter d_{AF} according to equation (3.7) at the same operational parameters of FPB and AF, i.e., at the conditions (3.9), (3.11), and their same volume

$$V = l_1^2 l \tag{3.12}$$

A more simple AF design is possible. AF may be fabricated as a rectangular plastic housing with a removable flat roof. The array of plane parallel perforated plates (transport channels) may be installed through the roof, and the gaps between plates may be filled with adsorbent powder through the roof (Figure 3.5). This is similar to the experimental laboratory module (already constructed) that was used in this research.

3.6 Hydrodynamics of Transport Channels and Selection of their Width

At L ~ 1m, h ~ 5cm, the overall HC increase of 400 times at the transition of FPB to AF is possible according to equation (3.9) and at $d_{AF} = d_{FPB}$. This large advantage, and correspondingly, equation (3.12) will be valid if hydrodynamic process configuration for AF satisfies the condition

$$\frac{p_{ch}}{p} << 1 \tag{3.13}$$

where p is the entire head loss and p_{ch} is head loss along a channel. This condition has to be expressed through the main parameters of AF design l and h. With this purpose, the condition of the liquid conservation at the steady flow may be used, namely the water flux entering into a channel equals the flux entering into AM through both the channels. The water flow density is expressed through the pressure gradient within the channel entrance according to Darcy's Law. The gradient in this equation cannot be expressed as the ratio p_{ch} to 1 because the pressure distribution along the channel p(x) is not linear. The condition in equation (3.13) is used to simplify the expression for the density of flow into the AM layer through the permeable channel wall.

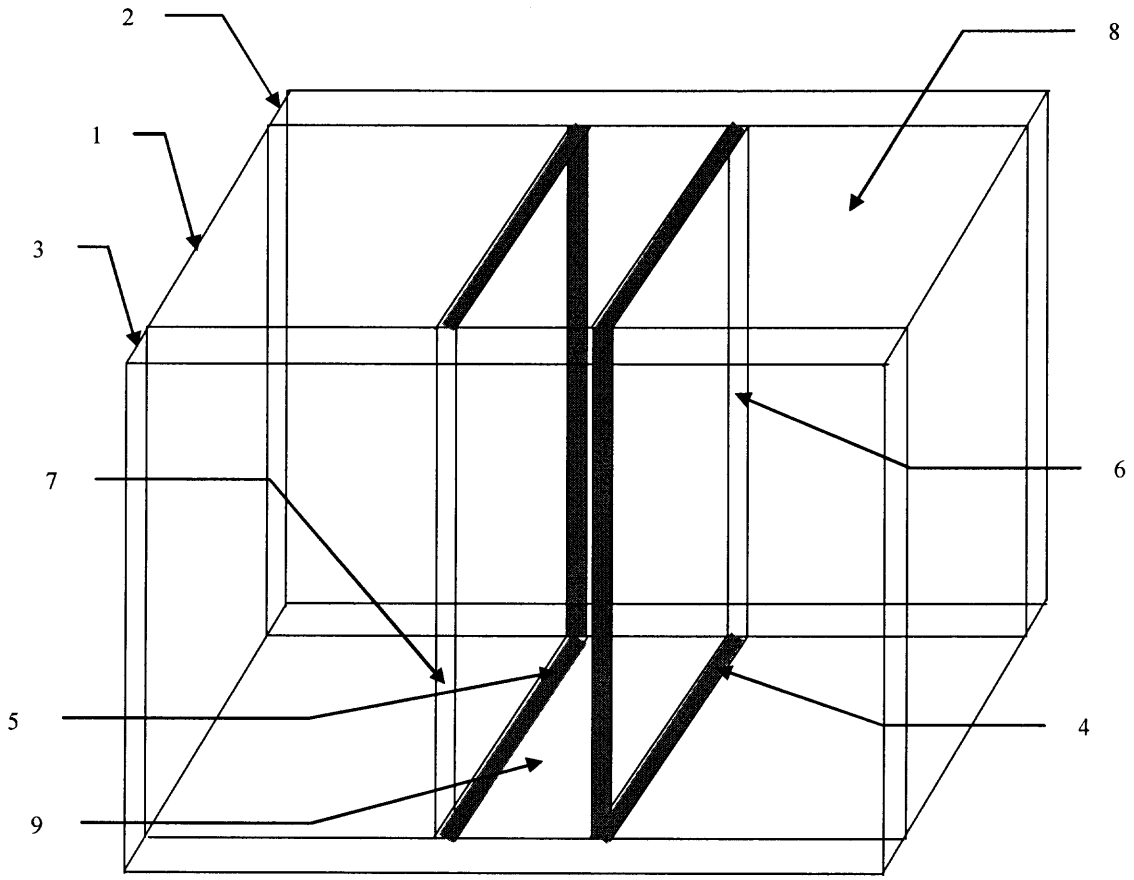

1. Housing
2. Feeding chamber
3. Receiving chamber
4. Feeding channel with permeable walls made as rigid perforated plates
5. Receiving channel with permeable walls made as rigid perforated plates
6. Entrance into feeding channel
7. Exit of receiving channel
8. Removable cap
9. Adsorption media between perforated plates

Figure 3.5 Adsorption Filter with multiple removable feeding and receiving channels.

$$f(x) = \frac{K_{AM}}{h}[p_f(x) - p_r(x)] \cong \frac{K_{AM}}{h} p_o \tag{3.14}$$

with account for representations

$$p_r(x) << p_o \tag{3.15}$$

where p_o is pressure before AF, p = 0 behind it, $p_f(x)$ and $p_r(x)$ are pressure distributions along the feeding and receiving channels, respectively.

$$p_f(x) - p_o << p_o \text{ and } p(x) << p_o \tag{3.16}$$

follow from condition (3.13)

water flux decreases along the channel because water flows out through the permeable wall:

$$-\eta h_{ch} K_{ch} [\frac{dp}{dx}(x) - \frac{dp}{dx}(x + \Delta x)] = 2\eta K_{AM} \Delta x \frac{p_o}{h} \tag{3.17}$$

or

$$S^2 \frac{d^2 p}{dx^2} - p_o = 0 \tag{3.18}$$

or

where

$$S^2 = h h_{ch} \frac{K_{ch}}{K_{AM}} \tag{3.19}$$

The boundary condition at the channel end is necessary for equation (3.18) integration. Two extreme cases are possible, namely flow absence or same flow density, as through AM. For these different boundary conditions, the difference in final results is not large.

$$\frac{dp}{dx} = \frac{p_o}{S^2}(x - 1) \tag{3.20}$$

$$p(0) - p(1) = \frac{p_o}{S_1^2} \frac{l^2}{2} \tag{3.21}$$

i.e.

$$\frac{p(0)-p(l)}{p_o}=\frac{l_2}{S^2 2}<<1 \tag{3.22}$$

This yields for the condition (3.13) taking into account equation (3.22)

$$\frac{K_{ch}}{K_{AM}}>>\frac{l^2}{h_{ch}h^2} \tag{3.23}$$

K_{ch} is the maximal for empty channel.

Another extreme case corresponds to a channel filled with large monodisperse spherical particles with a diameter equal to the channel width. The necessity in these spheres may appear if the screens which form the porous wall of channels are not very rigid. At large surface area of these walls of about $1m^2$, the elasticity of thin screens may cause an uncontrolled decrease in the channel thickness. Taking into account that screens are not rigid, the spheres may prevent screen deformation if their diameter is about h. In other words, the spheres may be used as spacers. In this case, $K_{ch}h_{ch}$ is HC, as expressed by the Ergun equation. The porosity of channels may almost be the same as the porosity of the AM in the channels. This simplifies the right hand side of equation (3.23)

$$\frac{h_{ch}^2}{d^2}>>\frac{l^2}{h^2} \tag{3.24}$$

$$h_{ch}>d\frac{l}{h} \tag{3.25}$$

with $l/h \sim 100$ and d = 100 microns, the equation (3.25) yields

$$h_{ch}>1cm \tag{3.26}$$

The width of the empty channel may be smaller, namely

$$h_{ch} \sim d(l/h) \sim 1cm \tag{3.27}$$

One concludes that the adsorption filter volume increase due to the incorporation of channels is approximately 15%, when h_{ch}~ 1cm, and that channel thickness can be disregarded in comparison with h ~ 5cm. This justifies manifold simplifications.

3.7 Enhancement of Virus Removal by Adsorption Filtration

At the same operational parameters and contact time, a very large decrease in the adsorbent particle dimension is possible according to equation (3.7). The contact (residence) time is the time of liquid (impurities) movement through the filter. This time increases with an installation dimension increase and with a decrease in volumetric velocity, and is equal to the ratio of volume to volumetric velocity. Comparing FPB and AF, their volumes and volumetric velocities are the same. Consequently, the contact time, which is time available for the impurities transport to the adsorbent, is the same.

$$t_{AF} = \frac{h}{u_{AF}}; t_{FPB} = \frac{l}{u_{FPB}} = \frac{l}{v} = \frac{lh}{u_{AF} l} \tag{3.28}$$

where equation (3.6) is accounted for equation (3.28) shows that

$$t_{AF} = t_{FPB} \tag{3.29}$$

when

$$v = u_{FPB} \tag{3.30}$$

The amount of collectors is the same as well. This is seen from equation (3.7). Better removal occurs due to the enhancement of the diffusion transport to a single collector because the colloid particle has to travel smaller distance to the collector as compared to the collectors with larger diameter. Also, velocity decreases with decreases

in particle size, which provides for additional time to complete the transport step. At the same operational parameters, the log removal for AF may be quantified by means of the substitution of d_{AF} and u_{AF} instead of d_{FPB}, l, and of u_{FPB} into equation (3.31) as specified for FPB

$$\ln\left(\frac{n_e}{n_o}\right)_{FPB} = -B\frac{l}{d_{FPB}}\left(\frac{D}{2u_{FPB}d_{FPB}}\right)^{2/3} \text{ (FPB)} \tag{3.31}$$

$$\ln\left(\frac{n_e}{n_o}\right)_{AF} = -B\frac{h}{d_{AF}}\left(\frac{D}{2u_{AF}d_{AF}}\right)^{2/3} \text{ (AF)} \tag{3.32}$$

$$\ln\left(\frac{n_e}{n_o}\right)_{AF} = -B\frac{h}{d_{AF}}\left(\frac{D}{2u_{AF}d_{AF}}\right)^{2/3} = -B\frac{l}{d_{FPB}}\left(\frac{D}{2u_{FPB}d_{FPB}}\right)^{2/3}\left(\frac{l}{h}\right)^{2/3}\left(\frac{d_{FPB}}{d_{AF}}\right)^{2/3}\frac{h}{l}\frac{d_{FPB}}{d_{AF}} =$$

$$= \ln\left(\frac{n_e}{n_o}\right)_{FPB}\left(\frac{l}{h}\right)^{4/3} \tag{3.33}$$

where the conditions (3.6) and (3.7) are used.

The second multiplier in equation (3.33) is about 5 to 10^2. Consequently, very high log removal can be achieved at adsorption filtration in spite of very low log removal in the case of FPB at the same operational parameters.

3.8 Longevity of Adsorption Filtration

In addition to the AM stability parameter, which characterizes AM aging due to the accumulation of micro-pollutants such as viruses on adsorbent surface, the term "longevity" (Gavaskar et al. 1998) describes an aging parameter affected by much larger concentrations of other contaminants like turbidity. There are two processes that control longevity and correspondingly determine the filter run, i.e., time period after which head

loss will exceed a definite value. First, a cake is formed on adsorbent surface and grows with time. Second, contaminants of different nature form deposits on the surface of adsorbent particles that lead to the blockage of the adsorption sites for viruses and to the suppression of virus' diffusional flux. The contaminant amount (volume) accumulated within 1 cm^3 of adsorbent is equal to the product of SSA (specific surface area) and W (thickness of deposit). These amounts and these products are equal to FPB and AF.

$$SSA_{AF} W_{AF} \sim SSA_{FPB} W_{FPB} \tag{3.34}$$

where W is the thickness of contaminant deposit on adsorbed surface for AF and FPB, respectively.

Consequently,

$$\frac{W_{AF}}{W_{FPB}} \sim \frac{SSA_{FPB}}{SSA_{AF}} \sim \frac{d_{AF}}{d_{FPB}} \sim \frac{h}{l} \sim 0.03 \tag{3.35}$$

Due to the transition from FPB to AF, the simultaneous decrease in the deposit (cake) thickness and in pore dimension takes place. The deposit thickness decrease leads to the filter run increase, and the pore decrease leads to the filter run decrease. However, accounting for these two factors is not sufficient to conclude that the AF longevity will be better. There are two other factors that are favorable for the longevity of AF. First, the filtration velocity through AM (u_{AF}), is *l/h* times smaller at the same volumetric velocity for FPB and AF according to equation (3.28). Second, because AF application is for GW treatment the turbidity may be an order of magnitude smaller as compared to a rapid filter or adsorber for surface water treatment.

In spite of these favorable factors, the longevity may be short because the enhanced transport on adsorbent grains promotes cake formation. When the collision efficiency is small, a small portion of contaminant is collected near the first layers and the

contaminant majority penetrates deep into the AM (deep filtration). But the larger the collision efficiency, the larger the portion of impurities accumulates within surface layers. This leads to rapid cake formation (surface filtration). This will happen in the case of adsorption filtration because the adsorbent particle decrease and the filtration velocity decrease promote the collision efficiency increase.

In Chapter 5 it will be shown that metal-coated sand or calcite with a dimension of about 600 microns, which is typical in the case of rapid sand filters for municipal water treatment, may be promising candidates for pretreatment with respect to NOM and turbidity removal. Although the viruses are removed as well, their transport is weak and the achieved log removal is low. The major portion of NOM and turbidity may be accumulated with a prefilter, which does not participate in significant virus removal. This will decrease the contaminant loading on the virus adsorption filter.

Removal of cryptosporidium by slow sand filtration was studied by Schuler et al., (1988). The pilot slow sand filter achieved log removal of 3.7 or higher when the filter was operated at 0.11gpm/ft^2 (0.26m/hr), using 0.27mm effective size sand. This means that AF, proposed for virus removal, will provide a necessary high log removal of about 4 for bacteria because AF is more effective than slow uncoated sand filtration.

According to Hozalski and Bouwer (1998), water backwash was not effective at removing bacteria from the filter media with only 20-40% removal during 10 min backwash cycles. If this difficulty arises in the case of AF, another mode of backwashing will be used. The study by Ahmad et al. (1998), showed that a combination of air plus sub-fluidization water flow, called collapse pulsing, gives optimum cleaning of sand, dual-media, and GAC filter-adsorbers. A version of this method has been systematically

investigated in collaboration with Novaflux Technologies (Princeton, NJ), which has successfully developed this method for removing foulants from membrane. The use of this air scouring approach is expected to be effective for the periodic cleaning of AM of AF.

At first glance, it appears that the problem related to microorganism multiplication may aggravate the operation of the AF because the AM particles and the pores between them are 10 times smaller than conventional GAC. However, only 1 among a million microorganisms penetrates through the cake of diatomaceous earth filter (Fulton, 2000), and this may be the case with AF. However, this small amount of microorganisms may multiply with time causing local pore clogging because the overlap of two microorganisms would occupy comparable pore dimension.

Fortunately, microorganism multiplication (clogging) in the filter is rather a slow process – about three months were required for the biological colonization of GAC filters in drinking water treatments (Servais et al. 1994). These data are in agreement with the maximum growth rate of 0.15 hour of aquatic bacteria (Billen et al. 1998) at an operating temperature of 12°C. If at high temperatures the rapid multiplication of microorganisms penetrating the front surface of AF occurs, feeding chlorine or another disinfectant can be used to suppress such growth. Correspondingly, a rather long filter run for AF may be provided.

A very low disinfectant dose is necessary to prevent growth of bacteria within the distribution system. However, an additional chlorination dose is necessary to prevent microorganism multiplication within AM of AF. But this dose may be minimized by means of pulsive feeding of disinfectant into AF. For example, the ozone pulse with a

duration of 1 hour was sufficient (Weber-Shirk and Dick, 1997) to kill fixed bacteria. Perhaps even shorter pulses of chlorine may be sufficient because chlorine is a much stronger oxidant than ozone (Fulton, 2000). The pause between disinfectant pulses is expected to be long (weeks to months) because the clogging rate is rather slow.

3.9 Applicability Area of FPB and AF for Virus Removal

3.9.1 Advantages and Disadvantages of FPB

Advantages:

Simple design and lower capital cost.

Simple backwashing.

Large adsorbent particle dimension.

Disadvantages:

High pressure drop, which forces one to use large particles.

Insufficient log removal due to large particle dimension.

How serious large disadvantage is depends on α and virus dimension. The smaller the α is and the larger the virus is (the smaller its diffusivity), the lower log removal is. Log removal becomes unacceptably low at sufficiently small α or sufficiently large virus.

3.9.2 Advantages and Disadvantages of AF

Advantages:

High log removal. It can be almost in the order of magnitude larger than that in the case of FPB.

Low pressure drop, which can be 1 or 2 orders of magnitude smaller than that in the case of FPB.

High HC, which may be in 1 or 2 orders of magnitude larger than in the case of FPB.

Disadvantages:

More complicated design and larger capital cost.

Possibility of more complicated backwash.

Possibility of higher operational costs.

Comparison between FPB and AF is made at the same installation volume and the same volumetric velocity and the same AM, while particle dimensions are smaller in the case of AF. Regarding more complicated backwash there is uncertainty for comparison. This necessitates additional analysis and experiment. Also, there is uncertainty regarding higher operational costs. Smaller head loss or larger HC decreases the operational costs in the case of AF. But more difficult AM replacement may increase operational costs.

3.9.3 Applicability Area for FPB and AF

When log removal predicted for FPB is sufficient and the head loss acceptable, FPB may be preferable due to simpler design and smaller capital cost. But when log removal is too low or pressure drop is too high, AF is preferable. In other words, AF is valid for solutions of the most difficult tasks of water purification, when FPB is not valid. For easier tasks, FPB is preferable. There are two difficult scenarios for applicability of AF namely 1) During virus outbreaks, when virus concentration increases significantly, log removal of about 6 might be necessary even though it exceeds the regulatory requirements (EPA requires at least 4-log removal) and 2) when the virus is extremely dangerous and it becomes necessary to eliminate as many viruses as possible.

3.9.4 Quantifying Conditions when FPB has to be Replaced by AF

The smaller the α is and the larger the virus is (the smaller its diffusivity), smaller adsorbent particles are necessary to provide log removal of about 6. The smaller the particle dimension, higher pressure drop is necessary and this may exceed 1m H_2O. This may be the critical condition for the preference of AF.

Hence, the equation (2.11) can be used with definite values for all parameters with the exception of d_c. d_c may be expressed as a function of these parameters for l=100cm, u = 0.1 cm/sec, ε = 0.4 and $ln\ n_i/n_c$ = log removal 6 × 2.3 = 13.8. This yields the critical d_c value as a function of D and α

$$6 \times 2.3 = 6 \times 0.6 \times 3.32 \times 100 \times D^{2/3} \alpha / d_c^{5/3} u^{2/3} \tag{3.36}$$

or

$$d_c = 3.6 \times \alpha^{0.6} D^{0.4} \tag{3.37}$$

The critical value calculation is illustrated in Table 3.1 for 2 values of α and 3 dimensions of viruses: 27 nm (MS2), 80 nm (rotavirus), 200 nm (smallpox)

Table 3.1 Alpha (α) Values for Three Viruses of Different Dimensions

D, cm^2/sec	α	d_c, micron	P_{FPB}, cm H_2O
1.5×10^{-7}	0.4	400	62
	0.1	180	300
5.25×10^{-8}	0.4	260	150
	0.1	120	700
2×10^{-8}	0.4	160	390
	0.1	75	1800

The Ergun equation can be used for pressure calculation, which corresponds to the calculated adsorbent particle dimension. The almost identical Kozeny equation is more convenient for calculations, namely equation (8.2) in AWWA (1999).

$$\frac{h}{l} = \frac{k\mu}{g\rho} \cdot \frac{(1-\varepsilon)^2}{\varepsilon^3} \left(\frac{a}{v}\right)^2 u \tag{3.38}$$

where h is head loss in the cm, k is the so-called Kozeny constant commonly found close to 5, g = 980cm^2/sec, ρ is water density, a/v is grain surface area per its volume. For a sphere the ratio of surface area to volume is 6/d. In the case of water the equation (3.38) transforms into the equation

$$\frac{h}{l} = 10^{-2} \frac{u}{d_c^2} \tag{3.39}$$

where u and d_c are expressed in cm/sec and cm, respectively.

Consideration of the data given in the last column of Table 3.1 leads to the conclusion that with the exception of the easiest case, which corresponds to α = 0.4 and smaller virus dimension, too large a pressure is necessary to provide log removal 6 or larger at l = 100cm, u = 0.1 cm/sec with the use of FPB. In other cases, AF is necessary. But even in the easiest case, the pressure may be larger than that given in Table 3.1.

The powder particles are not spherical and not smooth which corresponds to the higher head loss. The head loss increases with time due to gradual clogging of packed bed Even with respect to MS2 and AM with α ~ 0.4, α is smaller at a larger salt concentration of about 0.1M / l and in the presence of sulfate (SO_4^{2-}) or phosphate (PO_4^{3-}) ions (You et al. 2003). Also, α decreases with time. This occurs perhaps due to the gradual increase of NOM concentration, which blocks adsorption sites for viruses. In the presence of the NOM prefilter, the rate of NOM loading on the virus filter will decrease. Nevertheless, a slower gradual decrease of α will preserve.

3.10 Adsorption Filter with a Simplified Design

The analysis in Section (3.8) showed that the conditions necessary to provide log removal 6 using FPB with dimension d_c = 400 micron, is mainly not satisfied. On the other hand, the use of adsorbent with dimension about 100 microns is sufficient to provide log removal of about 6. This corresponds to pressure increase less than 4 times. This pressure increase may be eliminated with the use of AF with a not very large l / h ratio, and consequently, with a small amount of channels per m^2 of the filtration area of about 3 to 4. In turn, this leads to an essential simplification in AF design. The AM thickness may be increased to 20-30 cm. This decreases the possibility of channeling and simplifies the filling with AM.

Perhaps the horizontal orientation of the packed bed is reasonable. As channeling at this thicker packed bed is less probable, the uniform particle distribution within the packed bed horizontal plane may occur under gravity action. Perhaps packed bed vibration at its formation may be helpful. As the channel amount may be small, any channel has one permeable wall and another one impermeable wall. This make a module consisting of feeding channel, receiving channel and AM between them completely independent.

In an alternative design, when a very large surface area and many channels are necessary and many channels, every channel belongs to two AM layers.

In a simplified design with three to four channels, a module consists of housing with an impermeable roof and bottom, the feeding channel and receiving channels, and AM between them. At a horizontal orientation (Figure 3.6), the mesh to support AM is necessary on its bottom only. The AM top may be free, i.e. not covered by a permeable

roof. The feeding channel roof has to be removable for filling with AM and for its periodical replacements.

In a simpler design, channels are combined in a vertical direction, when the bottom of higher modules lies on the roof of the lower module. For the filling, the modules are disjoined from each other. A single complication is that they are rather heavy, namely hundreds of kilogram at $ll_1 = 1\text{m}^2$ and h ~ 20cm.

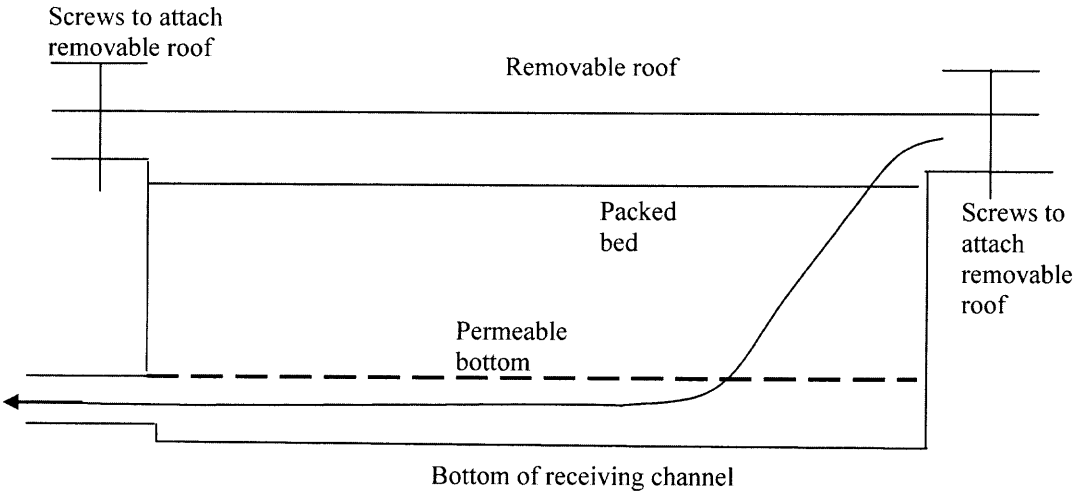

Figure 3.6 Simplified AF design.

A separate module is filled and emptied when the removable roof is opened. The filling and emptying may be easily accomplished by hand similar to the removal of the contaminated thin upper layer in slow filter. The procedure of AM replacement for 1 module may take about 1 hour. AM replacement for the entire filter with $l^2 l_1 = 1\text{m}^3$ may take 1 working day.

There is a possibility of a module without roof. The bottom of the higher module may have the roof perimeter of the lower module as a support, while the roof inside the perimeter is absent. In this case, the water level inside the feeding channel is lower than

the roof, i.e., a gap filled with air exists between free water layer and the roof level. Although this design is even simpler (no removable roof), its disadvantage is the necessity of an exact horizontal orientation of the packed bed

The equation (3.39) shows that

$$h/l \sim 0.25 \tag{3.40}$$

has to be chosen to increase log removal 4 times in comparison with FPB at the same installation volume, pressure drop and volumetric velocity. The equation (3.7) shows that $d_{AF} \sim 0.25 d_{FPB} \sim 100$ μm.

3.11 Conclusion

A cardinal revision of the entire hydrodynamic process configuration of flow packed bed (FPB) adsorber is necessary for virus removal.

The need for using a small adsorbent particle dimension to remove viruses from water is universal. However, the fundamental difficulty is that although a small adsorbent particle size is needed for high log removal, the head loss increase that accompanies the use of small particles makes it difficult in large-scale applications. This controversy cannot be eliminated with the improvement of adsorbent properties of the surface because the universal law of convective diffusion transport will control the entire process rate. The single possibility of avoiding this dilemma is by the revision of the entire hydrodynamic process configuration of FPB adsorber. AF design combines adsorber with modified hydrodynamic process configuration of membrane technology and provides the pressure loss decrease up to 10 to 100 times.

A significant increase in hydrodynamic conductivity (HC) can be achieved by incorporating into the FPB body two arrays of transport channels, that is transition to AF hydraulic process configuration. One array of channels (feeding channels) is connected with the upstream face, and the second one (receiving channels) with the downstream face. Feeding and receiving channels alternate along AF front area. Water filtrates through adsorption media (AM) from a feeding channel to the nearest receiving channel and flows out along it. The filtration area is increased (filtration velocity decreases) and filtration depth is decreased at the same dimension and volumetric velocity as in FPB case. Pressure drop decreases due to decrease in both the filtration velocity and the filtration length.

AF can provide the increase in log removal by 10 to 100 times for viruses in comparison with FPB at the same operational parameters (pressure drop, linear and volumetric velocity, contact time). This may be achieved due to decrease of particle dimensions and due to the advanced hydrodynamic process configuration. The later compensates the increase in pressure drop, caused by the smaller particle use.

CHAPTER 4

EXPERIMENTAL PROCEDURES AND RESULTS

The main aim of this chapter was to test and validate the adsorption filtration (AF) technology with respect to removing viruses by column experiments under various conditions of treatment. The experiments were designed to simulate the theoretical conditions as well as the new hydrodynamic parameters of adsorption filter, especially filtration depth, particle size of the adsorption medium and filtration flow rate (linear velocity). During the initial phases of this study, model colloids with a negative charge and size (polystyrene latex spheres) were considered as model for viruses for the filtration experiments.

However, unlike model colloids, viruses do not have uniform surface charge distribution and their adsorption may deviate from the known behavior of model colloid particles with the same size and charge density. On one hand, the surface charge on viruses is caused by the ionization of the amino and carboxyl groups (see Chapter 1) that comprise their surface proteins/glycoproteins and the number of charges is a function of pH, and the ionization of these surface functional groups yields viruses with an amphoteric surface – i.e., may be positive or negative depending of pH.

On the other hand, viruses are known to undergo inactivation (become non-infective) when exposed to chemical and physical conditions during filtration. Hence, to accurately predict virus removal effectiveness and behavior, it was necessary to select a model bacteriophage to represent virus removal. MS2 was used as the model phage in this study and other water-related investigations because it meets the requirements for a worst-case model virus (see Section 4.1). In addition, MS 2 has been used in several

previous studies (Penrod et al., 1996; Lukasik et al., 1999; You et al., 2003; Zhaung and Jin, 2003) to investigate virus removal. Equation (5.1) was used to calculate the experimental attachment efficiency of viruses in the experiments.

$$\alpha_{\exp} = -\ln(C/C_o)_o \left(\frac{4a_c}{3(1-\varepsilon)L\eta_T} \right) \tag{5.1}$$

In this chapter experimental results of the effect of the iso-electric point and particle size of different adsorption media (adsorbent) on virus removal have been presented. The selection process of calcite as an adsorption media for the adsorption filtration technology has also been discussed. The chapter also presents the results of parametric studies performed to investigate the effect pH, ionic strength, concentration of divalent anions, and filtration velocity on the virus removal efficiency.

4.1 Model Viruses

According to Mossel (1982), a model organism needs to include two distinct functions:

1) An index function, and
2) An indicator function.

The index function relates to health risk or occurrence of the pathogen (virus) directly or indirectly, and when selecting a model organism for experiments, the ecology and resistance of the index organism selected need to be similar to that of the pathogen under consideration. The indicator function to be considered relates to the effect of the treatment process on the model virus selected. Simple laboratory methods and similar resistance are the criteria of concern for indicator organism.

MS2 is an F-specific phage belonging to the leviviridae family, and it has single-stranded RNA as its genetic element. It specifically adsorbs to F- or sex-pili coded by a

plasmid (a genetic element separate from the bacterial chromosome) that is found in a number of strains of E.coli (Birge, 1981). MS2 has an icosahedral geometry with a size of about 27 nm. Though less than 10% of tested human fecal samples contain F-specific phage (Havelaar et al. 1990), sewage is an environment where multiplication can take place, and hence is an abundant source of F-specific phages (IAWPRC, 1990). Thus F-specific phage is an index organism of sewage pollution rather than of feces pollution (IAWPRC, 1990). Sobsey (1989) experimented with different disinfectants like chlorine, chlorine dioxide, ozone, and chloramines, and found that viruses are usually more resistant than E-coli. Also, it was found (Sobsey, 1989) that the RNA phage MS2 showed more resistance to some disinfectants, similar to that of Hepatitis A virus and Rotavirus SA -11, whereas Helmer and Finch (1993) found that MS2 to be more sensitive to disinfection by ozone than poliovirus.

In various groundwaters, the temperature dependent survival of MS2 was shown to be similar to echovirus 1 and poliovirus 1 by Yates et al. (1985), concluding that MS2 can be used as a model virus for animal virus survival in groundwater.

The retention of virus to soils also depends on the isoelectric point (iep) of the virus. The poliovirus strains have iep ranging from 3.5 and 8.5 (Vaughn and Landry, 1983), while bacterial viruses MS2 and fr have iep of about 3.5 and 9.0, respectively (Overby et al., 1966; Marvin and Hoffman-Berling, 1963). Such differences among viruses make it difficult to predict virus movement in groundwater (aquifer). Nasser et al. (1989) compared transport for various viruses like hepatitis A virus, Poliovirus 1, echovirus1 and MS2, and found that MS2 reduction was less than the enteroviruses, and hence MS2 can be used as an indicator for enteroviruses. An major advantage of MS2

and other bacteriophages in general is they are non-pathogenic to humans. Moreover, MS2 can be grown in high numbers for seeding experiments to measure high log removal levels, and can be assayed relatively easily while assaying pathogens can be complex (Schijven and Hassanizadeh, 2000). MS2 is also more resistant to inactivation compared to many pathogenic viruses; it gets inactivated faster at higher temperatures but at a temperature of 7°C the rate of inactivation is very low (Yates et al., 1985; Yahya et al., 1993; Blanc and Nasser, 1996; Schijven et al., 1999). The excellent review by Schijven and Hassanizadeh (2000) provides a comprehensive justification for why MS2 satisfies conditions for a model virus.

4.2 Materials and Methods

Since NJIT did not have a microbiology facility prior to this study, a microbiology laboratory had to be set up for the sole purpose of this project, and for continuing this line of research in the future. This effort took more than seven months of preparation before some experimental results to test virus removal were generated with actual phages. The following equipment was purchased, tested and validated to perform the plaque-forming-unit (pfu) assays used in the study:

1) Napco 9000 DSE Autoclave,
2) Edge Guard Laminar Flow Hood (Model #EG 4252)
3) Thermolyne Type 37900 Culture Incubator
4) Kenmore Refrigerator (Model # 98291)

In order to perform phage experiments at NJIT, request was reviewed and permission was obtained from the Office of Health and Safety. Mr. Eric Feerst at the

Bureau of Marine Water Monitoring Lab of NJDEP at Leeds Point, NJ, provided excellent training for performing and validating the phage assay used in the study.

4.2.1 Materials and Supplies

All the materials and supplies required to perform the Double Agar Overlay assay method according to Adams (1959), were procured and stored according to manufacturers' specifications.

A) Materials

Tryptone (Peptone from casein), yeast extract, sodium chloride (NaCl), calcium chloride ($CaCl_2$), magnesium chloride ($MgCl_2$), magnesium sulfate ($MgSO_4$), dextrose (glucose), streptomycin sulfate (Omnipur), tween (Omnipur), and glycine (Omnipur) were purchased from EM Science. Difco plate count agar (Beckton and Dickinson company), humic acid sodium salt (Sigma Aldrich Chemicals), magnesium carbonate ($MgCO_3$, Alfa Aesar, Ward Hill, MA), pure silica (GFS chemicals), and ampicillin sodium salt (Shelton Scientific).

The MS2 phage stock was obtained from American Type Culture Collection (ATCC), was assayed in the *E-coli* F amp (bacterial host for male-specific coliphages) obtained from the Bureau of Marine Water Monitoring Laboratory (NJDEP). The bacteriophage host strain *E. coli* HS(pFamp)R, also known as *E. coli* F amp, (Debartolomeis and Cabelli, 1991) was provided by the Bureau of Marine Water monitoring Laboratory (NJDEP).

Free samples of crushed calcite (Snow white-21 PT, Snow white-30 PT, Omyacarb 100 PT, Omyamarble - PT, Snow white 350) were provided by (Omya NA, Alpharetta, Georgia).

B) Supplies

Disposable polystyrene sterile plugged pipettes (1ml and 5 ml), Petri dishes (100 x 15 mm), safety bulbs, autoclave bags with indicator, cryogenic tubes (2 ml), and 5-gallon carboys were obtained from VWR Scientific. Sterilization filter units with 0.45-micron cellulose nitrate membranes were purchased from Nalge-NuncInternational. Chromatography columns (Flex-column, Kimble-Kontes) in sizes 2.5 x 20cm, 2.5 x 30cm and 2.5 x 50cm were purchased from VWR Scientific.

4.2.2 Methods

A) Phage Assay Preparation

MS2 was obtained in a freeze-dried form from ATCC. MS2 was extracted with growth broth and then diluted several times with de-ionized water before assaying in host *E. coli* F amp. This host was used, as it is resistant to ampicilliin/streptomycin, the addition of which would reduce contamination by other bacteria. The Double Agar Overlay method (Adams, 1959) was used to assay MS2 in *E. coli* F amp.

Solutions of glucose, $CaCl_2$, $MgSO_4$, and streptomycin/ampicillin were prepared as per the methodology (Adams, 1959) and stored at 4°C in a refrigerator. Growth broth, top agar and bottom agar were also prepared according to the above method, sterilized in during autoclaving and then cooled. After cooling, glucose, $CaCl_2$, $MgSO_4$, streptomycin/ampicillin was added. Growth broth and top agar were prepared in larger quantities and stored in the refrigerator (for less than one week). This was done when experiments were done continuously and when each media was being used up every day. Additionally, top agar was again autoclaved on the same day of plating. Petri dishes with bottom agar layer were also prepared in advance and stored in the refrigerator. On the day

of the experiments, the plates were warmed up in the incubator before pouring the top agar layer. A day before plating, *E. coli* F amp stock (0.2-0.5 ml) was added to growth broth (50-100 ml) and put in an incubator at 37°C to ensure the host was in log growth phase for the day of plating. Next day, a change in appearance of growth broth from clear to cloudy indicated the growth of the host.

B) Stock Preparation

E. coli F amp stock was prepared by taking about 2 ml of the log growth phase in a vial supernatant and storing it in a freezer at -4° C. This stock seemed to work fine in the experiments. Instead of propagating the phage, fresh stock was prepared from new vials purchased from ATCC and refrigerated at -4° C.

C) Assay

Before starting any experiments, the bench and hood surfaces were disinfected with disinfectant wipes and/or disinfectant spray. Reusable glassware and supplies were first cleaned, rinsed with de-ionized water the then sterilized using the autoclave for at least 20 minutes at 121°C and 15 psig pressure. Sterilized single-use supplies like pipettes and Petri dishes were used once in the experiment to reduce risk of contamination. The laminar flow hood was used during serial dilutions and during pouring top and bottom agar layers to prevent contamination from the surrounding air environment. To perform the actual assay, the water samples (influent and effluent) were serially diluted with sterile de-ionized water (Figure 4.1). 1 ml of the latter was added to tubes that were previously filled up to the 9 ml mark. After adding 1 ml of sample to the dilution tube and before transferring 1 ml from this tube to the next dilution, the dilution tube was closed with a rubber stopper and vigorously shaken to ensure that MS2 did not aggregate

and that proper serial dilution effect could be measured. 1ml disposable sterile polystyrene pipettes were used for serial dilutions, and the discarded every time. Agar for the top agar layer was also autoclaved and then kept in a waterbath at 42-44.5°C to prevent it from solidifying during the experiment. Just before plating, 1 ml of antibiotic (streptomycin/ampicillin solution) was added to each 100 ml of top agar taken.

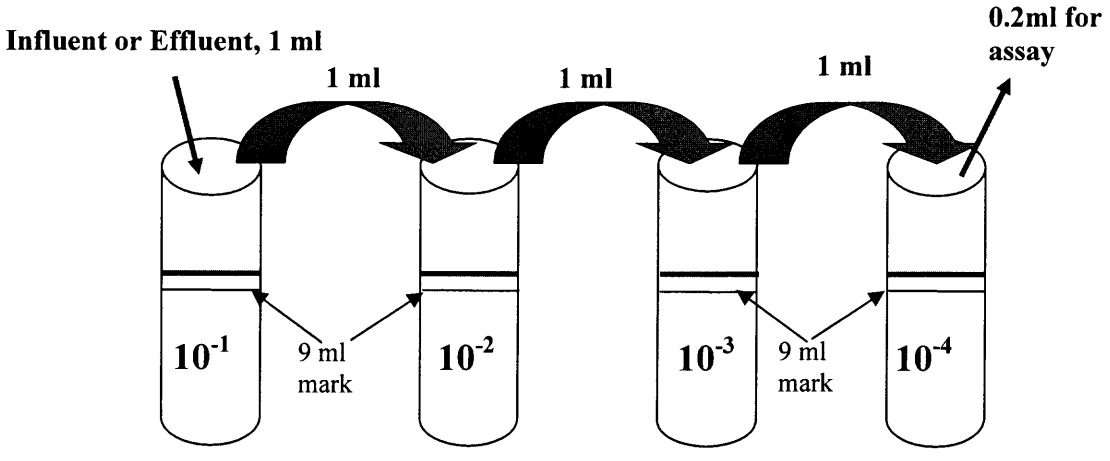

Figure 4.1 Serial dilutions procedure.

For plating, 0.2 ml of required MS2 dilution was added to 0.1-0.2 ml of *E. coli* F amp (in log growth phase) to 3 ml of top agar, which was kept at 42-45°C in the water bath. This agar layer containing MS2 and *E. coli* F amp was then poured over the single agar layer (Figure 4.2). The Petri dish was swirled to evenly distribute the top agar layer and then allowed to solidify. The dishes were then inverted and incubated in the oven for 24 hrs at 37°C.

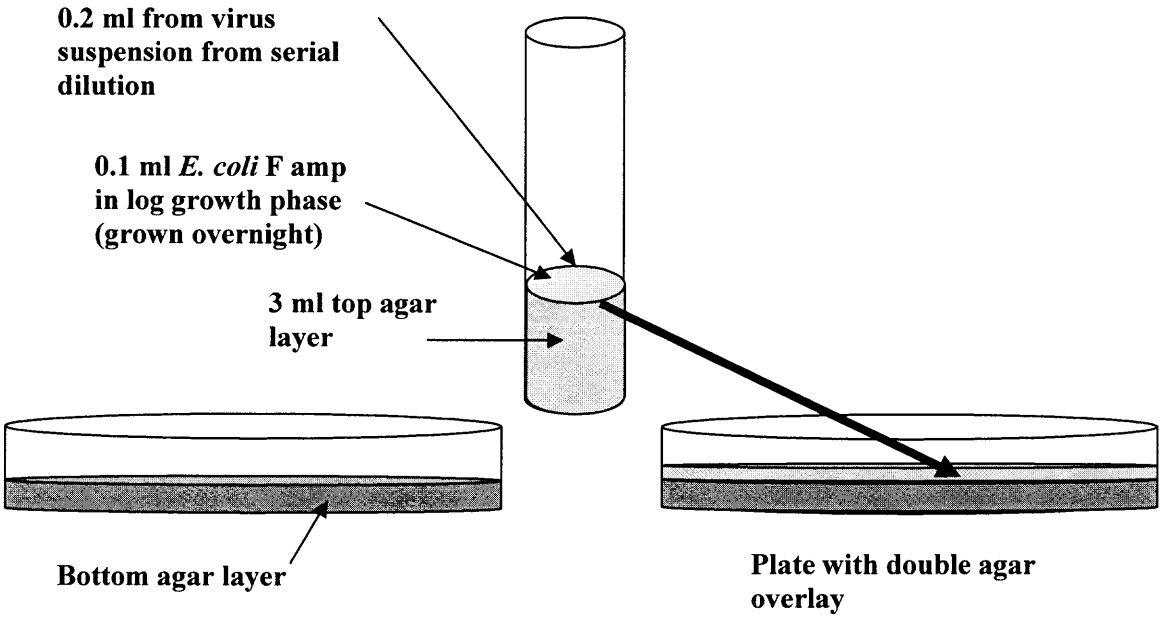

Figure 4.2 Plating the MS2 on a bottom agar layer.

Distinct lysis was visible on the next day as clear to hazy circular plaques are seen in the *E. coli* F amp full lawn; Each plaque, or zone of lysis in the host "lawn" of *E. coli* F amp bacteria, originates from either a single bacteriophage (probably in most cases) or (in some cases) from more than one phage stuck together. Because a plaque can theoretically be derived from more than a single phage, the zones are counted and designated as "plaque forming units" (PFU) rather than as "phage". The number of pfu corresponding to MS2 serial dilutions are shown in Figure 4.3.

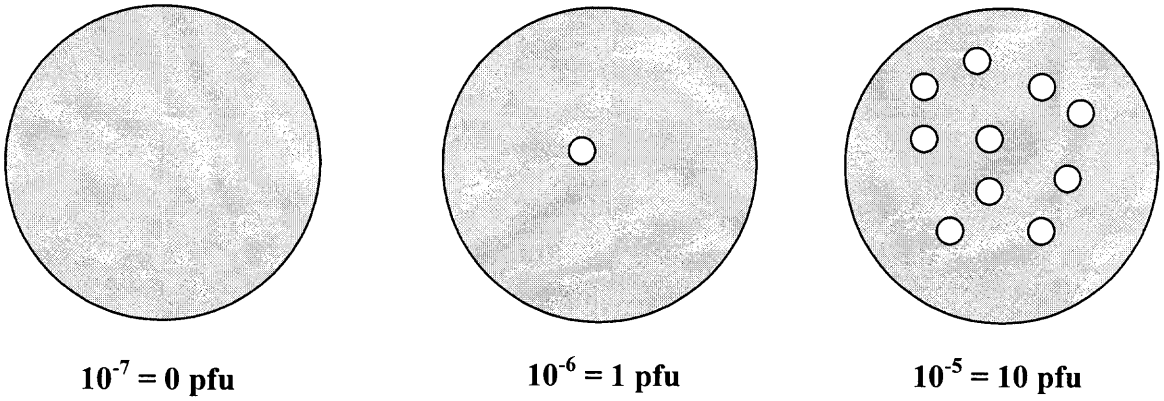

Figure 4.3 Double agar layer plates grown overnight show lysis (plaques) as per the dilutions.

The samples were plated in triplicate for at least three dilutions. Even though samples were plated during serial dilution, one undiluted influent sample was always plated to compare the difference between complete lysis (influent) and no lysis (effluent), and to measure concentration of pages in the control sample (influent). One blank plate (only *E. coli* F amp, no MS2) was also plated to ensure there was no contamination from broth or top agar, which would otherwise give false counts (false positive). After each experiment, all the supplies and waste were autoclaved in an autoclave bag with a sterilization indictor for safe disposal.

4.2.3 Column Preparation for Filtration Experiments

A) Bed Formation

To simulate the filtration process and hydrodynamic conditions of AF, chromatography columns were filled with the required adsorption media to a filtration depth of about 3 to 5 cm. These columns have a polyethylene porous bed support with 20 micron-pore size, which does not allow the adsorption media from passing while providing water flow in a downward direction without imparting any resistance to flow. The column experiments permit testing and validating the concept of AF technology without the need to build the final prototype. Therefore, these column experiments are more manageable and easily duplicable during the laboratory phase of the study. Moreover, the columns could be emptied, cleaned and refilled with ease. The results of column experiments can be scaled up for final testing or modeling of the AF technology since the main physical requirements of the adsorption layer will be the same, namely: particle size, filtration depth, and flow rate (linear velocity).

In the earlier filtration experiments, 10-20 grams of filtration medium was placed in the chromatography column followed by the addition of some de-ionized water, and the column was then compacted with the application of pressurized air for a period of time. However, as soon as the air valve was closed, visible cracks developed in the filtration bed made this procedure. Hence, other methodology had to be developed to prevent virus bypassing through such cracks during filtration, a condition that would invalidate the results.

To reduce the crack formation and to ensure reliable filtration results, the column was prepared by a different method. De-ionized water was first added to 10-20 grams of filtration medium to sufficiently fill up the entire column. The column was then vigorously shaken to ensure that all particles were in suspension. The adsorption media was then allowed to settle for 30-45 minutes, and then the column was compacted by applying pressurized air. In the latter method, the application of pressurized air was not necessary, especially when the average particle size of the adsorption medium was about 100 microns and larger. Columns prepared by this method had much better flow rate, lower pressure drop and showed no crack formation during long-term experiments (days to weeks). The success of this procedure for preparing and compacting the column was attributed to the initial settling of heavier particles first to the bottom of the column, followed by finer particles in the top layer. This sedimentation profile appeared to result in a filtration bed formation similar to that of sand filters used in conventional water treatment.

Although following this column preparation procedure resulted in a somewhat lower pressure drop, the pressure drop was still much higher than that predicted by Ergun

equation. Careful observation indicated that a visible layer of fines (2-5 mm) formed on top of the filtration bed (3 cm) after initial settling, and when the flow started, some of these fines would settle in the pores of larger particles and some would remain on top of the bed. The presence of the fines' layer developed after almost 90-95% of the bed had been formed suggested that its presence many influence the filtration results.

To correct for this possibility, the media were sieved for a longer time to ensure that considerable amounts of fines were removed. Columns prepared in this manner (i.e., after sieving for a longer time) had lower pressure drop compared to those prepared without removing the fines. For example, the velocity for similar hydrostatic head and column depth for 75-106 microns particle size increased from 0.0018 cm/sec to about 0.049 cm/sec.

B) Column Experiments to Test and Verify the Applicability of AF Technology

Once the columns were formed, influent water seeded with MS2 was filled in a holding container and the water wall allowed to flow at a predetermined rate. The flow rate (linear velocity) was controlled: 1) application of air pressure: pressurized air was used only in filtration experiments when very small adsorbent particle size or higher velocities were investigated, 2) adjusting the hydrostatic head: in this case increasing or decreasing the head of water above the column was employed as the main parameter to control linear velocity. The column filtration setup used in the experiments is depicted in Figure 4.4.

On the day of the experiments, frozen MS2 suspension was taken from the refrigerator and allowed to liquefy. The amount taken for the suspension varied depending on the strength of the stock (dilution of MS2 pellet) and the quantity of influent water required for the filtration experiment. Usually 0.5-1.5 ml of this suspension

was then added to 200-500 ml of water to achieve high log (10^6 – 10^7 phage/ml) concentration of MS2 in the influent. The water used for the experiments included: de-ionized water, tap water or saline water depending on the experiments performed. This water seeded with MS2 was then passed through the column filter (prepared as described above).

After commencing filtration, some volume of initial effluent was allowed to flow out to ensure that the sample taken to perform the assay truly represent the treatment desired for the experiment. Influent and effluent were collected in a sterile beaker. And then diluted for plating as described above. Effort was made to perform the experiments on the same day in a very short time to reduce the chances of inactivation of MS2. The average flow rate (linear velocity) through the column was calculated by measuring the amount of effluent collected over a period of 10-60 minutes.

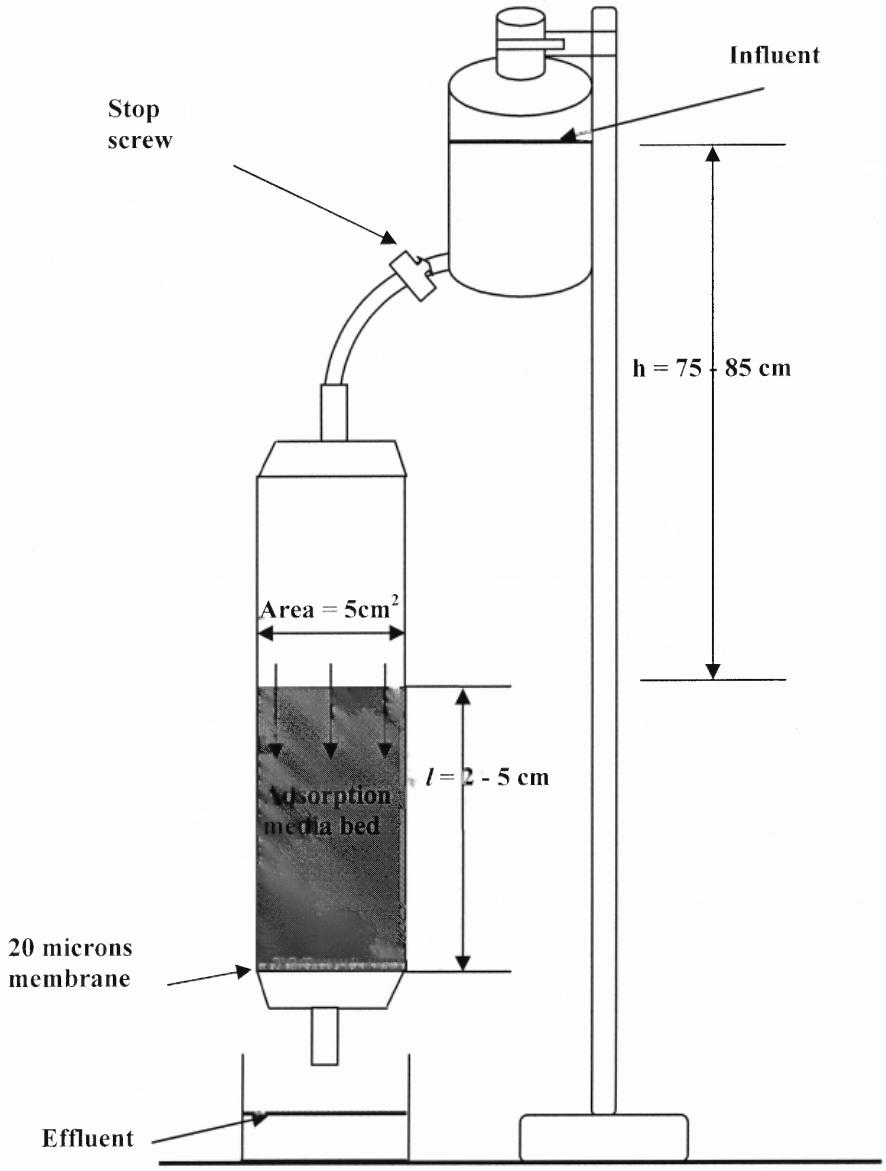

Figure 4.4 Setup of column experiment used in the laboratory.

4.3 Selection of Adsorption Media

At least 3 criteria have to be satisfied for selecting the optima: i) the adsorption of virus to AM surface needs to be essentially irreversible; ii) the amount of adsorption sites of AM should be sufficient to achieve reasonable filter run times, i.e., large adsorption capacity with respect to viruses is needed; and iii) the amount of adsorption sites of AM for viruses has to be sufficient even in the presence of NOM -- the latter competes with virus adsorption as elaborated in Chapter 5.

Additionally, the AM should be cost effective and easily available for an economical technology. The effects of parameters like isoelectric point; particle size, pH, ionic strength and presence of competing anions have been discussed in detail in Chapters 2 and 3. According to the DLVO theory, adsorption irreversibility is controlled with the depth of the potential energy pit, which arises at a distance between the surfaces of adsorbent and the virus. This energy pit is defined by the absolute value of the difference between van der Waals energy of attraction (which is negative) and the energy of the electrostatic interaction (which may be either repulsive for the case of similar signs of the surface charges, or attractive for the case of opposite signs of the surface charges).

The adsorption is irreversible if the depth of the potential pit exceeds 5-10 KT (KT is the energy of heat movement, T is the absolute temperature, K is the Boltzmann constant). This occurs when adsorbent and virus electrokinetic potentials have opposite charges. Irreversible adsorption may also arise if the pH of water is within 2-2.5 units from the iso-electric point of the adsorbent, Loveland et al. (1996) (Figure 4.5). When the difference between solution pH and pH_{iso} of AM is small (near the isoelectric point), its electrokinetic potential is small, and correspondingly, the electrostatic interaction is

weak. In cases when the latter is smaller than van der Waals attraction, the adsorption becomes irreversible, even if the repulsive electrostatic interaction is present. Therefore, the first criterion for AM selection is that its pH_{iso} should be larger than 5.0, since pH of 6-7 is usual for GW.

The selection of a specific adsorbent that provides a strong virus adsorption improves the potential for effective virus removal with AF, especially when if adsorbent and virus hydrophobic interactions can be taken into consideration. "Interaction between hydrophobic groups on the surfaces of viruses and solids may cause an increase in virus attachment. When the silica beads were coated with C_{18}-trichlorosilane, 400 times more attachment took place, independent of pH" (Bales and Hinkle, 1991).

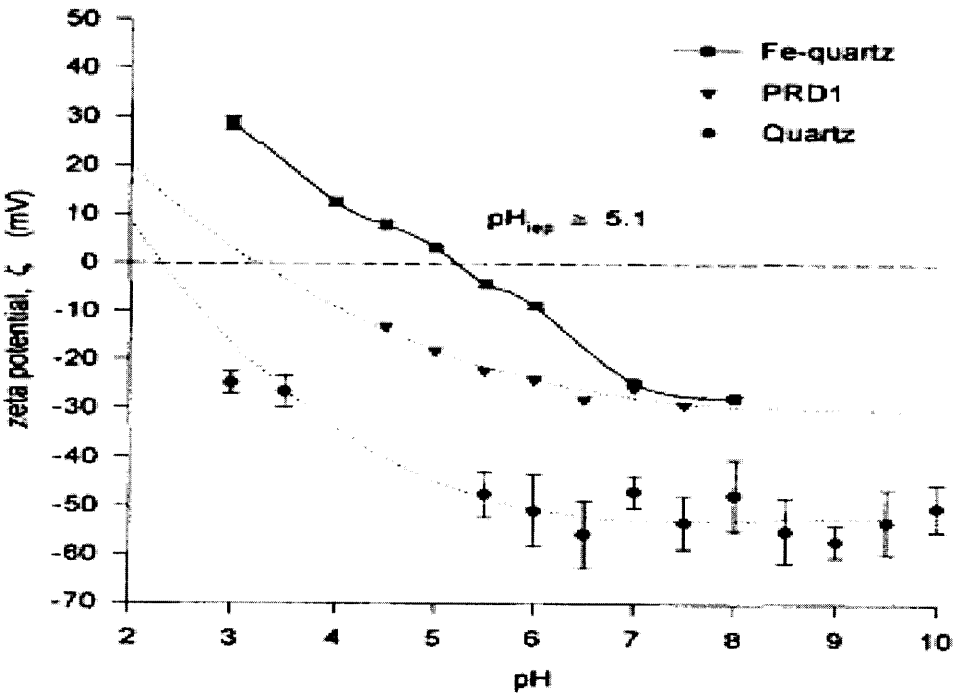

Figure 4.5. Plot of zeta potential of quartz, Fe-quartz, and PRD1 as a function of pH. The cubic polynomial curve fits for quartz and PRD1 predict pH iep values of 2.5 and 3.5, respectively.
(Source: Loveland et al. 1996)

In this study, two classes of adsorbents were screened using the short-column experiments, including: i) Adsorption media having isoelectric points > 5, such as alumina (iep = 9.2) and Calcite (iep = 8.2), and ii) hydrophobic adsorbents like silica (iep = 2.0). Once the AM was chosen, the adsorption capacity for virus removal using water quality similar to GW sources was determined. The effect of pH, salinity (ionic strength), effect of anionic strength and influence of NOM (see Chapter 5) on virus removal were investigated.

4.3.1 Experiments to Investigate the Effect of Isoelectric Point

The effect of isoelectric point (iep) on the log removal of viruses was investigated (Tables 4.1-4.3) for adsorbents having iep in the range between 2 (pure silica) and 11.5 ($MgCO_3$). Table 4.1 summarized the adsorption filtration media used in the study and their iso-electric points.

Table 4.1 Isoelectric Points of Various Adsorbents Tested

Medium	Size range	Isoelectric point
Sand	212-250	2.5-3.0 (Schulze-Makuch et al. 2003b)
Al_2O_3	74-177	9.3 (Roberts, 2005)
$CaCO_3$	212-250	8.3 (Roberts, 2005)
$MgCO_3$ (40-43.5%MgO)	20-80	12.5 (MgO) (Persson, 1994)

As seen from Figure 2.1 (see Chapter 2), the zeta potential of an adsorbent having iep less than neutral water pH is negatively charged below this pH value. In this case, both MS2, as well as adsorbent, are negatively charged, a condition that reduces electrostatic attraction and hence gives lower removal. The MS2 log removal efficiency of the adsorbent increases with the increase in the isoelectric point (at approximately the same particle size), as seen in Table 4.2.

Table 4.2 Effect of Isoelectric Point on Log Removal of Viruses

212-250 microns pure Silica (iep-2.0)	Linear velocity cm/sec	Influent concentration (log_{10} pfu/ml)	Effluent concentration (log_{10} pfu/ml)	Log_{10} removal pfu/ml	Volume of water treated ml	α
	0.0021	6.67	6.5	0.17	48	0.049
	0.0088	6.67	6.67	0	78	0
	0.0159	6.7	6.3	0.4	94	0.059
	0.016	6.0	6.3	-0.3	118	0
212-250 microns Natural sand (iep - 2.0 - 2.5)						
	0.003	6.40	2.7	3.7	70	0.11
	0.0126	6.40	5.7	0.7	112	0.24
Fresh column						
	0.0014	6.04	1.37	4.67	29	0.186
	0.0035	6.04	2.23	4.67	52	0.234
	0.016	6.5	6.5	0	122	--
	0.022	6.5	6.65	0	130	--
212-250 microns $CaCO_3$ (iep-8.3)						
	0.004	6.3	0.4	5.9	78	0.41
	0.013	6.3	2.55	3.75	118	0.54
Fresh Column						
	0.0018	6	0	6	32	--
	0.0031	6	1.4	4.6	42	0.31
	0.0168	6.06	3.85	2.2	124	0.38
	0.022	6.06	4.7	1.36	130	0.27
74-177 microns Al_2O_3 (iep-9.3)						
	0.01	5.5	0	5.5	35	--
	0.017	7.32	2.66	4.65	30	0.56

Table 4.2 indicates that adsorption media with higher isoelectric points give higher log removal for approximately the same particle size. During the study, it was important to choose an adsorbent that could give high log removal without any adverse effects on the water quality.

Other requirements for a successful adsorbent were: i). Commercial availability at the required particle size distribution, ii). possibility of backwashing, and iii). low cost to justify use in the adsorption filtration technology. Once the possible adsorption media with high isoelectric points were identified ($CaCO_3$, $MgCO_3$, Al_2O_3), attention was paid to their capability with respect water treatment and the quality water produced. Special Attention was given to health-related effects that might be caused due the dissolution of the media, change in pH and/or increase in hardness.

Systematic filtration experiments were performed with Alumina (Al_2O_3), Calcium carbonate ($CaCO_3$) and Magnesium carbonate ($MgCO_3$). The results are presented in Table 4.3 and Figures 4.6 and 4.7.

Table 4.3 Experiments to Compare Log Removal by Adsorbents with High Isoelectric Points

Adsorption media	Linear velocity cm/sec	Influent concentration (log_{10} pfu/ml)	Effluent concentration (log_{10} pfu/ml)	Log_{10} removal pfu/ml	Volume of water treated ml	α
74-177 microns Al_2O_3 (iep-9.3)	0.01	5.5	0	5.5	35	--
	0.017	7.32	2.66	4.65	30	0.56
30 microns (mean size) CaCO3 (iep-8.3)						
DI water	0.014	7.3	0	7.32	43	--
Tap water (Low salt and NOM)	0.013	6.5	0	6.5	40	--
40 microns (mean size) $MgCO_3$ (iep-12.5)						
DI water	0.002	7.78	0	7.78	--	--
Tap water (Low salt and NOM)	0.00085	6.67	0	6.67	18	--

Table 4.3 summarized the results of all three adsorption media, i.e., Al_2O_3 (iep 9.5), $CaCO_3$, (iep 8.3) and $MgCO_3$ (iep 12.5). For these three adsorption media (Table 4.3), high log-removal of MS2 was found for de-ionized water and tap water; the latter include low ion concentration and residual amount of NOM. Alumina was deemed unacceptable for two reasons: 1). High cost as an adsorbent, and 2) dissolution of aluminum ion may take place with low pH water and this will have associated health risks including Alzheimer's disease. It is clear from the results that sand, either pure or natural, does not satisfy the iso-electric requirements or the log removal levels requirements of the AF technology. This leaves $CaCO_3$ and $MgCO_3$ as potential AM candidates.

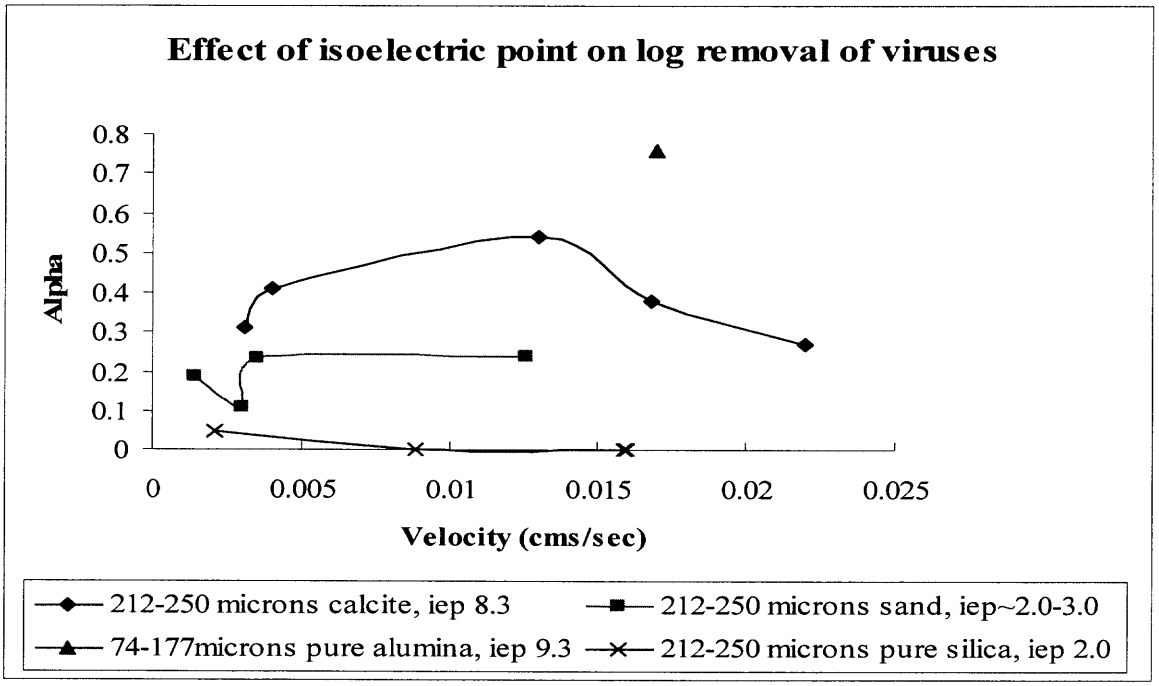

Figure 4.6 Effect of isoelectric point on log removal

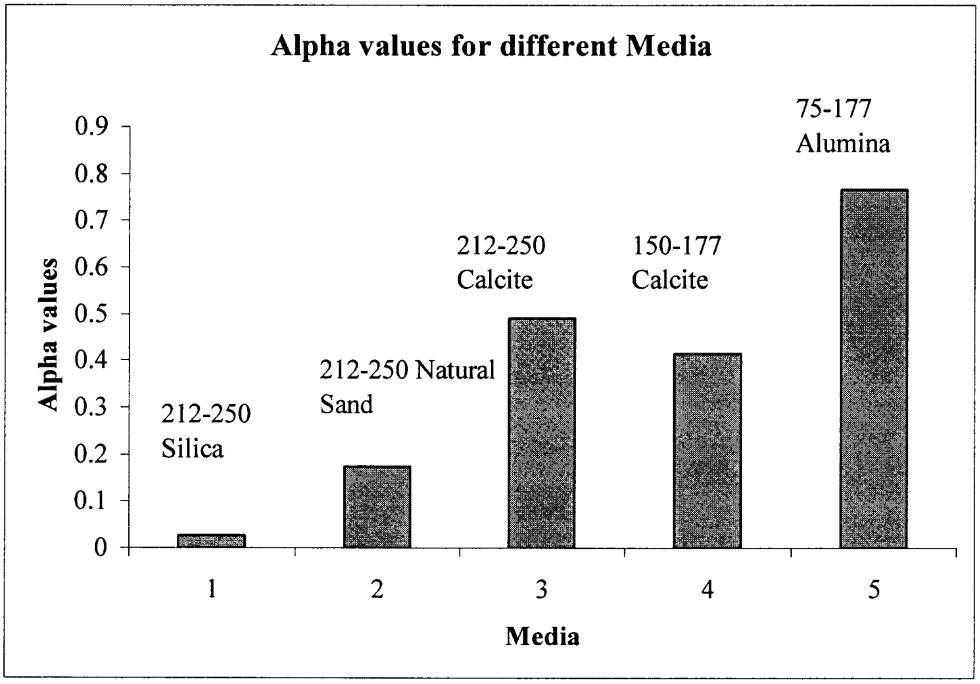

Figure 4.7 Average α values for different media

4.3.2 Selection of $CaCO_3$ over $MgCO_3$

$MgCO_3$ and $CaCO_3$ differ from conventional filter media (sand or carbon) in the sense that both have a small but finite solubility in the water. Therefore, there is always some dissolution of Mg^{++} and Ca^{++} ions, and this will change the effluent water quality (pH, hardness). The latter effect may however be advantageous since positive divalent cations are known to neutralize negatively charged virus/ NOM and reduce the repulsion with AM surface, thus increase the attachment efficiency. The results (Table 4.3) indicate that both $MgCO_3$ and $CaCO_3$, can give large removal, but the conductivity measurements indicate higher solubility of $MgCO_3$ (Table 4.4) compared to $CaCO_3$ which can give more hardness as compared to $CaCO_3$.

This means a post treatment step of hardness removal might have to be used when $MgCO_3$ is used. For DI water, pH increase was high for $CaCO_3$ as well as $MgCO_3$ (Table

4.4). However, when tap water was used, the pH of the effluent was about 8.3-8.5 for $CaCO_3$, which is acceptable for drinking water (USEPA, 1992).

Table 4.4 Conductivity and pH Measurements for $CaCO_3$ and $MgCO_3$

Type of water	Conductivity μmhos/cm	pH
Tap water	192	7.8
Passing through $CaCO_3$	73	9.5-10.0
Passing through $MgCO_3$	344	9.5-10.0

4.3.3 Effect of Particle Size on Virus Log Removal Efficiency

The purpose of these experiments was to determine optimal adsorbent particle size for effective high-log virus removal with the AF technology. As discussed in Chapter 3, increasing the hydraulic conductivity (HC) of AF, by incorporating the transport channels, allowed the decrease in particle size (d_c) of the adsorbent and achieved a significant increase in the log removal of viruses at reasonable head loss.

Having selected $CaCO_3$ (calcite) as an adsorption medium for the adsorption filtration technology, experiments were performed to establish the necessity of reducing the particle size of AM in the AF. Table 4.5 and Figure 4.8 show the effect of particle size on the efficiency of virus removal. There is an increase in the removal efficiency with a decrease in the size of the adsorbent. Log removal of > 6.0 was obtained for the particle size range of 75-106 microns or less. The efficiency of log removal in the particle size range of 75-106 microns at the first instant seemed unusual. The initial theoretical modeling of AF required that the particle size be reduced to about 40 microns to achieve high log removal. The experimental data generated directed us to examine the assumptions made during the initial modeling of the AF technology.

Upon analysis of the experimental results, it was observed that α value (removal efficiency factor) for calcite was 0.4-0.6, rather 0.1 which used in the modeling study. The 40-micron size range was first arrived at during the initial modeling when α was assumed to be 0.1. Because of the high alpha values (0.4-0.6), it is thus possible to use larger size and achieve log removal of viruses during AF.

Another assumption made in the initial modeling relates to using mono-disperse particles size adsorbents. However, the experiments performed with calcite were done using a size range (75-106 microns) rather than a mono-disperse system. Moreover, seeking mono-disperse calcite mineral from natural source is not feasible from cost point of view. It was realized that high log removal efficiency of MS2 could be achieved with a narrow particle size range. Thus, because of the values of α in the range of 0.4-0.6, and the use of $CaCO_3$ having a narrow particle size range, allowed an increase in the mean particle size from 40 microns to about 100 microns and still achieve high log removal of viruses. Hence, subsequent experiments were performed with 75-106 microns fraction. The increase in particle size range also allow for smaller pressure drop while maintaining > 6.0 log removal as would be indicated in the later results.

Table 4.5 Effect of Size on Log Removal of Viruses (with DI water)

Adsorption media	Linear velocity cm/sec	Volume of water treated ml	Influent concentration (log_{10} pfu/ml)	Effluent concentration (log_{10} pfu/ml)	Log_{10} removal pfu/ml	α
30 microns (mean size) $CaCO_3$						
	0.014	43	7.32	0	7.32†	--
< 75 microns $CaCO_3$	0.0016	25	6.73	0	6.73†	--
75-106 microns $CaCO_3$	0.0009	16	6.4	0	6.4†	--
	0.0018	33	6.5	0	6.5†	--
Fresh column						
	0.006	110	6.2	0	6.2†	--
150-177 microns $CaCO_3$						
	0.0058	78	6.7	0	6.7†	--
	0.013	102	6	1.62	4.38	0.4
	0.02	120	6.7	1.5	5.2	0.63
	0.025	112	6	2.95	3.05	0.43
212-250 microns $CaCO_3$						
	0.004	78	6.3	0.4	5.9	0.41
	0.013	118	6.3	2.55	3.75	0.54
Fresh column						
	0.0018	32	6	0	6†	--
	0.0031	42	6	1.4	4.6	0.31
	0.0168	124	6.06	3.85	2.2	0.38
	0.022	130	6.06	4.7	1.36	0.27

† It is difficult to provide reproducible high concentration in the influent. Complete log removal is obtained at this log concentration. Perhaps complete removal is possible even at higher influent concentration but it is difficult to prepare influent with higher phage titer.

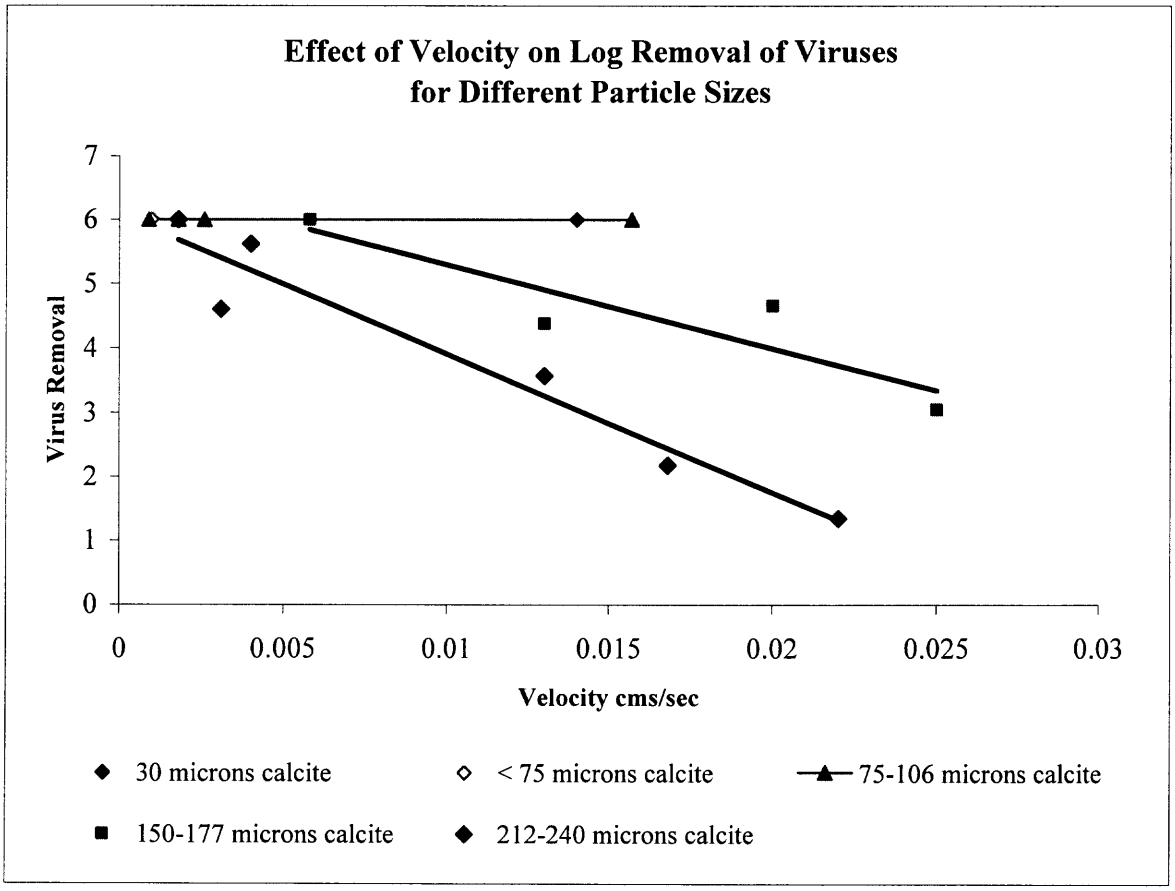

Figure 4.8 Effect of particle size on log removal.

4.4 Parametric Studies to Verify Log Removal Efficiency

4.4.1 Effect of Velocity on Log removal

Theoretical modeling of AF (Eq. 5.1) suggests that the log removal is proportional to $1/(u)^{2/3}$. Figure 4.9 depicts the change in log removal efficiency as a function of linear velocity. As expected from theory, an increase in velocity decreases the log removal. The Figure (4.9) shows a comparison of theoretical and experimental log removal at the same linear velocities (used in the experiment) for the particle size ranges of 150-177 microns and 212-250 microns calcite. For the theoretical predictions, α was assumed to be 1.

Experimental values for log removal were adjusted based on normalized log removal obtained in the experiment and assuming the influent concentration as 6.0 logs. A good agreement was obtained between theoretical prediction and experimental values for the same conditions. The particle size range of 75-106 microns provides > 6.0 log removal beyond the velocity (0.005) that was assumed during the AF design.

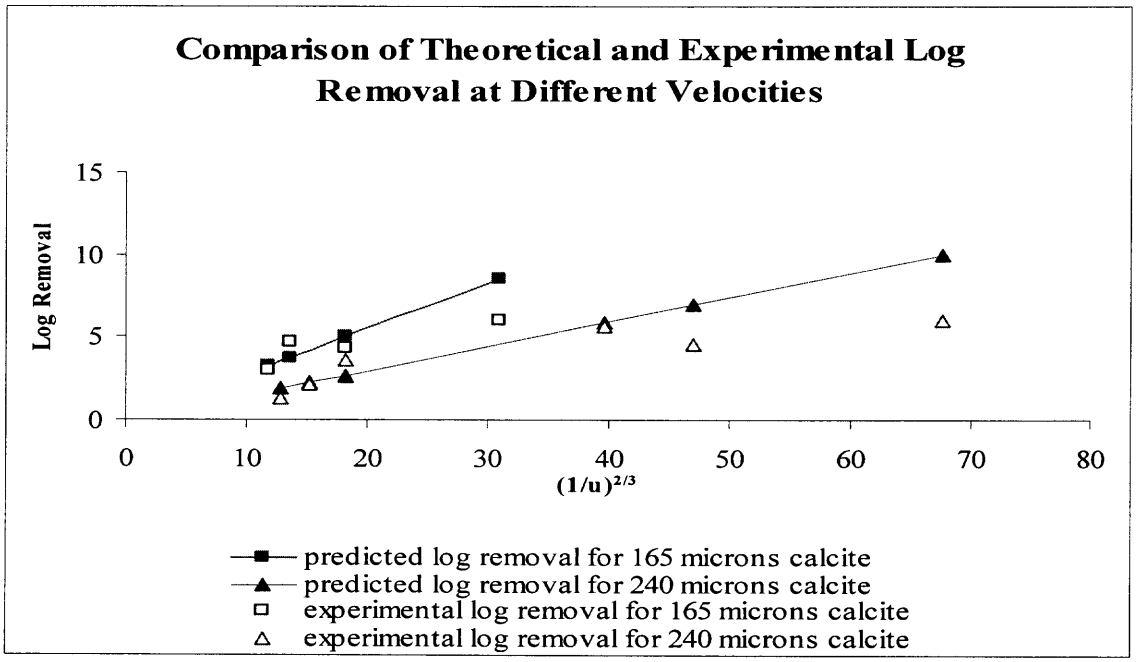

Figure 4.9 Comparison of predicted theoretical and experimental log removal. Experimental log removal has been adjusted by normalized log removal, assuming influent log concentration is 6.0 logs. For theoretical calculations, $\alpha = 1$, $\varepsilon = 0.4$, $l = 5.0$ cm.

4.4.2 Effect of pH and Ion Concentration

Depending on the source, groundwater varies in the pH as well as in ion concentrations. The effects of pH and ion concentration on the adsorption of viruses have been discussed in Chapter 2. Experiments were arranged to test the efficiency of AF at extreme pH's (2.6-11.9) and at ion concentrations ranging from ~ 0.0M (DI water, see Table 4.7) to

0.1M. pH was adjusted with hydrochloric acid (HCl) and Sodium hydroxide (NaOH). Sodium chloride (NaCl) was used to study the effect of ion concentration.

The results are tabulated in Tables 4.6 and 4.7. Complete log removal is preserved in this pH range (2.9-10.9) because at extreme pHs the ionic force is higher and accordingly electrostatic interaction is suppressed. Experiments at various ion concentrations did not seem to have a measurable effect of the efficiency on MS2 log removal. It seems that the screening of surface charge caused by increasing ion concentration, in this case (negative colloid and positive AM), is not sufficient enough to provide for electrostatic interaction. Thus, high log removal is maintained for NaCl concentration up to 0.2 M.

Table 4.6 Effect of pH on Log Removal of Viruses

Adsorption media	Influent pH	Volume of water treated ml	Linear velocity cm/sec	Influent concentration (log_{10} pfu/ml)	Effluent concentration (log_{10} pfu/ml)	Log_{10} removal† pfu/ml
< 75 microns $CaCO_3$ (1 layer NOM filter)	2.9	150	0.004	5.64	0	5.64
< 75 microns $CaCO_3$ (2 layer composite filter)	4.5	94*	0.0053	5.74	0	5.74
75-106 microns $CaCO_3$	6.7	110	0.006	6.2	0	6.2
75-106 microns $CaCO_3$	10.9	46	0.002	5.4	0	5.4
	10.9	116	0.0157	5.4	0	5.4

† - See comment for Table 4.5. * Presidential lakes field sample, NJ.

Table 4.7 Effect of Ion Concentration on Log Removal of Viruses

Adsorption media	Electrolyte concentration (Molar) M	Linear velocity cm/sec	Volume of water treated, ml	Influent concentration (log_{10} pfu/ml)	Effluent concentration (log_{10} pfu/ml)	Log_{10} removal† pfu/ml
30 microns (mean size) $CaCO_3$	DI water	0.014	43	7.32	0	7.32
75-106 microns $CaCO_3$	DI water	0.006	110	6.2	0	6.2†
30 microns $CaCO_3$	Tap water (low ion)	0.013	40	6.5	0	6.5
	NaCl					
	0.013	0.008	25	6.41	0	6.41
	0.0085	0.017	52	6.22	0	6.22
< 75 microns $CaCO_3$ (2 layer composite filter)	Field Sample* (low ion)	0.0053	94	5.74	0	5.74
75-106 microns $CaCO_3$	NaCl					
	0.2	0.019	94	6.13	0	6.13
	0.2	0.042	101	6.13	0	6.13
Fresh Column						
	0.2	0.03	116	5.65	0	5.65†
	0.2	0.049	117	5.65	0	5.65

† - See comment for Table 4.5. * Presidential lakes field sample, NJ.

4.4.3 Effect of Divalent Anions

Negative divalent anions have also been shown to reduce virus removal efficiency of Mg/Al layered double hydroxides (You et al., 2003), especially sulfate (SO_4^{2-}). The effect of sulfate anions was tested at 0.025 M as in You et al. (2003). Virus removal of about 6-logs was achieved at a velocity of about 0.028 cm/sec. For a second sample in the same

column log removal was still greater than 5.5 at a much higher velocity (0.043 cm/sec). Even at twice (0.05 M) the concentration used in You et al., (2003) a complete log removal was achieved with calcite (see Table 4.8 and Figure 4.10).

Table 4.8 Effect of Divalent Anions on Log Removal

Adsorption media	Na_2SO_4 concentration (Molar) M	Linear velocity cm/sec	Volume of water treated ml	Influent concentration (log_{10} pfu/ml)	Effluent concentration (log_{10} pfu/ml)	Log_{10} removal pfu/ml
75-106 microns $CaCO_3$						
	0.025	0.028	136	6.0	0	6.0†
		0.043	128	6.0	0.22	5.78
Fresh Column						
	0.05	0.02	128	5.74	0	5.74†

† - See comment for Table 4.5.

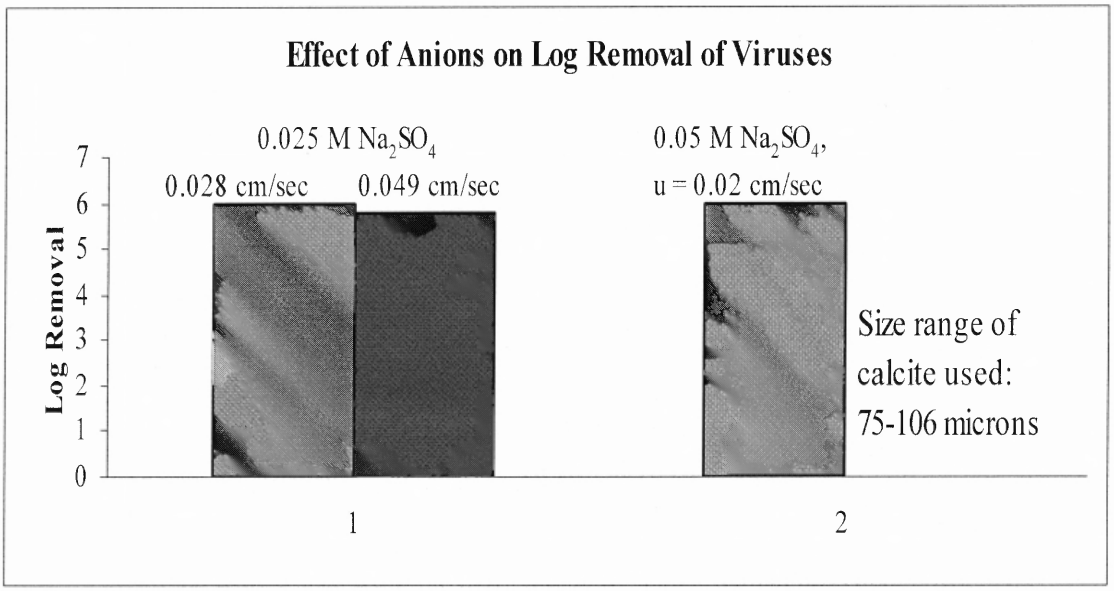

Figure 4.10 Effect of divalent anions ($SO4^{2-}$) on virus removal by calcite.

4.5 Reversibility of Virus Adsorption in AF

The first condition for successful virus removal is achieving the condition for irreversible attachment. As surfaces of viruses normally carry a negative charge (at the neutral pH), the electrostatic repulsion may prevent virus' irreversible attachment to a collector surface, and thus resulting in only a small removal. Virus attachment will become irreversible for solid surfaces (or patches on solid surfaces) that are positively charged due to the presence of iron, aluminum, or manganese oxide coating.

The iso-electric point of viruses is normally in the range of 3 to 7 (Loveland et al., 1996). At pH values above the virus pH_{IEP}, both virus and "most" mineral surfaces are negatively charged, and removal by attachment is mostly diminished due to net electrostatic repulsion (Figure 4.5).

Under definite conditions, irreversible attachment is possible even in the presence of "some" electrostatic repulsion, i.e., even when both the virus and mineral collector possess negative charges. This occurs due to the universal molecular forces of attraction (van der Waals forces). At some distances between surfaces, such attractive forces exceed the repulsive forces at pH smaller and even at somewhat larger than pH_{iso} of the mineral collector, if the difference between larger pH and smaller pH_{iso} does not exceed 2 pH units. This fact has been proven with the DLVO theory and supported by experiments (Loveland et al., 1996). The latter study proved that the irreversible attachment of the bacteriophage PRD1 to iron-coated quartz takes place if the pH of water does not exceed 7 (pH_{iso}=5). It should be noted that under the condition of irreversible adsorption, virus transport to the mineral collector surface is the rate-limiting step (Ryan and Elimelech, 1996).

Reversibility was studied for a period of about 4 days. For the first two days, AF was dosed with influent water seeded with MS2 and virus removal was studied. After two days, the dosing was stopped and sterilized DI water was passed through the virus contaminated AF column for about two more days to test the reversibility. Results indicate no desorption of MS2 for the given period of time (Table 4.9 and Figure 4.11). The total amount of MS2-contaminated liquid passed through this column was about 750 ml.

Table 4.9 Phage Removal and Reversibility of Virus Attachment (Initial titer - 6.24 log)

Hours	Percentage phage remaining in influent	Percentage phage removal
1.73	100	100
7.18	98.5	100
23.92	90.5	100
30.55	76.2	100
49.08	68.2	100
Total amount of MS2 seeded water passed = 750 ml		
Deionized water		Phage in effluent
1.45	--	0
2.45	--	0
21.76	--	0
26.01	--	0
43.84	--	0
Total amount of deionized water passed = 3300 ml		

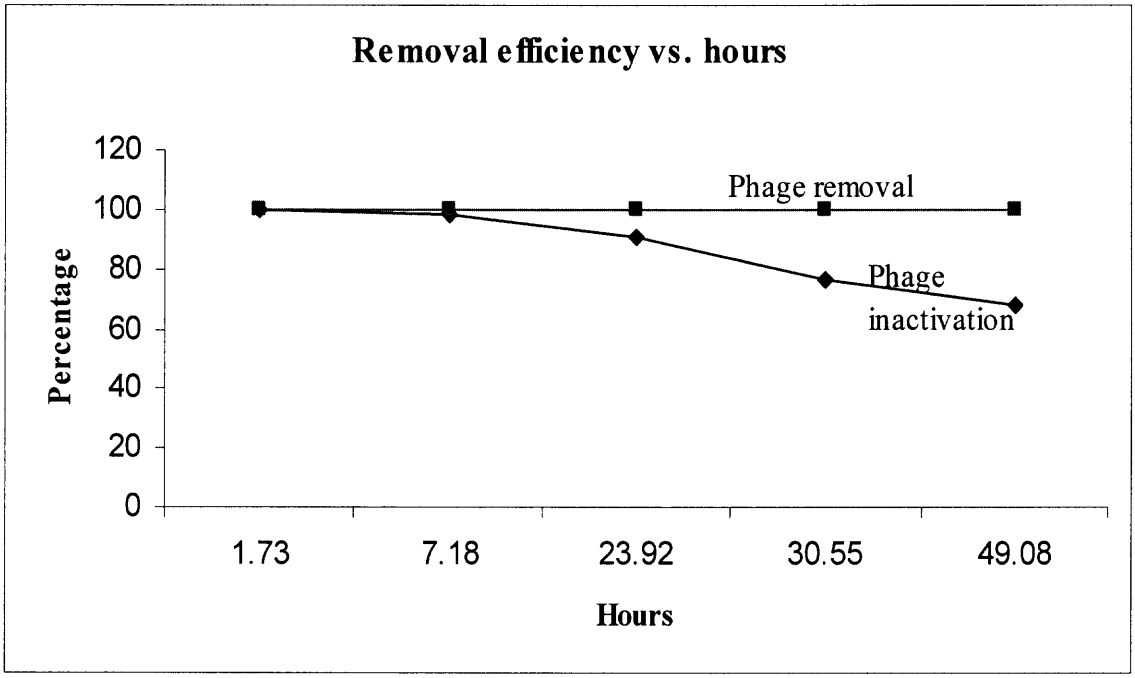

Figure 4.11 Removal efficiency of viruses during testing of reversibility of virus attachment.

A second experiment (new column) was performed to test the reversibility of the virus adsorbent, calcite. The calcite column was dosed with MS2-seeded water for about seven days. The total amount of water seeded with MS2 passed through this column was about 2500 ml in about seven days. After seven days this contaminated calcite column was removed and shaken in a glass flask having sterile water (100 ml). The media was allowed to settle for about 1.5 hours and then the supernatant was taken for analysis. Results are presented in Table 4.10 and Figure 4.12. Both columns were actively removing MS2 for the indicated time and no reversibility was observed in the above two cases.

Table 4.10 Results of Second Set for Virus Removal and Reversibility of Virus Attachment (Initial titer ~ 6.47 log)

Hours	Percentage phage remaining in influent	Percentage phage removal
1.5	100	100
24.5	87.3	100
47.25	76.9	100
96.73	57.6	100
120.53	46.3	100
Total amount of MS2 seeded water passed = 2500 ml		
Deionized water		Phage in effluent
Supernatant of column after shaking	--	0

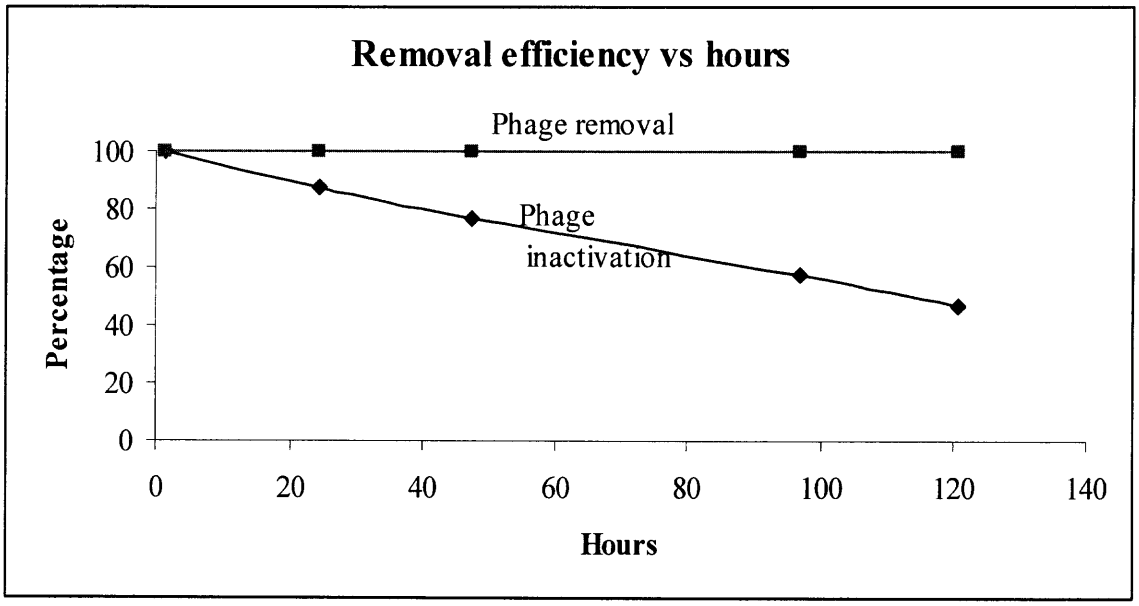

Figure 4.12 Second set for removal efficiency of viruses during testing of reversibility of virus attachment.

4.6 Discussion

The theory of colloid particle transport was verified by AF experimental results for virus removal. The analysis of the results indicates good agreement between the theoretical prediction and experimental with respect to MS 2 log removal. A novel AM (calcite) was selected after investigating different adsorbents ranging from silica (iep 2.0) to metal

oxides (8.3-12.5) with respect to virus removal efficiency. The results are summarized in Table 4.11.

Table 4.11 Summary of Alpha (α) values of different adsorbents

Adsorbent (size in microns)	Velocity, cm/sec	α
Pure silica, 212-250, mean particle size		
0.024	0.0021	0.04989
0.024	0.0088	0
0.024	0.0157	0
0.024	0.016	0
Natural sand, 212-250, mean particle size		
0.024	0.003	0.11
0.024	0.0014	0.186
0.024	0.0035	0.234
0.024	0.0126	0.24
0.024	0.016	0
0.024	0.022	0
Calcite, 150-177 , mean particle size		
0.0165	0.013	0.40255
0.0165	0.02	0.63298
0.0165	0.025	0.43576
Calcite, 212-250, mean particle size		
0.024	0.0031	0.31535
0.024	0.0043	0.41351
0.024	0.013	0.54671
0.024	0.0168	0.38164
0.024	0.022	0.27
Alumina 74-177, mean particle size		
0.015	0.0176	0.56

The results of Table 4.11 clearly indicate that media with high isoelectric point and small particle size range are necessary to achieve more than 6-log removal of phages as predicted by the modeling results of the AF process. It is clear from the results that conventional adsorption media having large particle size such as sand are not capable of

achieving any significant log removal of phages. The results also show that the use of inexpensive (cost-effective) media such as $MgCO_3$ and $CaCO_3$ holds great promise for the commercial application of the technology.

Calcite was chosen as AM for AF as it satisfied the log removal as well as water quality requirements. No post treatment is necessary for water that has been passed through a calcite filter. Different particle size ranges of calcite were tested for log removal at velocities in the range of 0.001cm/sec to 0.049 cm/sec. Experimental results indicated that calcite consistently has α in the range of 0.4-0.5. The mean particle size to be used in AF was increased due to this α value to about 100 microns. Parametric studies to investigate the effect of pH, ionic strength and divalent anion confirmed that calcite with a mean particle size of 100 microns provides for more than 6-log removal. Commercial sources for calcite with desired particle size was identified at price that make the AF technology possible - $0.1/lb was quoted by the Omya company. In addition calcite has been used of years for neutralizing water in the field. The effect of NOM on virus removal by calcite has been studied in detail and deserves a special emphasis (see Chapter 5).

CHAPTER 5

INFLUENCE OF NATURAL ORGANIC MATTER (NOM) ON THE ADSORPTION DYNAMICS OF VIRUSES - EXPERIMENTAL AND THEORETICAL MODELING

5.1 NOM, its Fractions and their Influence on Virus Adsorption

The review presented in Chapter 2 (Section 2.7) showed that a small Natural Organic Matter (NOM) concentration has negligible influence on virus adsorption, but that NOM might be harmful at higher concentrations. However, this conclusion may not be totally valid since the distribution between adsorbed NOM (on AM) and its bulk concentration changes as a function of time during the filtration run. At longer residence times, the surface concentration of NOM might be large enough to decrease the number of adsorption sites available for virus attachment and this will depend on the residence time of NOM adsorption. Information about NOM residence time is not available; however, according to the theory of adsorption, it is expected to be very sensitive to the surface properties of the adsorption medium. Moreover, NOM includes several fractions with distinctly different chemical and adsorption properties.

NOM consists of at least 6 fractions: hydrophobic (base, acid, and neutral (HN)) and hydrophilic (base, acid (HA), and neutral). Currently, there is no universal adsorbent for the simultaneous effective removal of all NOM fractions. Consequently, the application of activated carbon (AC) as the only adsorbent cannot provide a large log removal of NOM because its removal efficiency for at least some of the fractions is poor. A significant increase in log removal of NOM was achieved by the application of dual media (AC and ferric chloride) (Leppard et al., 1986). Unfortunately, published studies

express their findings in terms of the removal of total dissolved organic contaminants (DOC), without reference to the specific fraction of NOM. The physical and chemical processes used in the conventional water treatment train removes about 50% of NOM only. Conventional water treatment processes remove some NOM fractions because such processes are not designed for effective removal of all NOM fractions. At first glance, it seems that the use of a pre-filter for NOM removal may not be capable of entirely eliminating the influence of NOM on virus removal. However, this problem can be solved since it is only necessary to address the effect of NOM fractions that will compete with virus attachment to the surface of the collector.

In this study, it was convenient to classify NOM into only two major fractions: i). Fractions that can be adsorbed by $CaCO_3$, and ii). Fractions that cannot be adsorbed by $CaCO_3$. The fraction that does not adsorb on CaCO3 would not interfere with virus adsorption and the fraction that adsorbs on CaCO3 will have the potential to interfere with virus adsorption. Humic substances (HS) are expected to interfere with virus attachment, since HS contain negative functional groups -- viruses normally possess negative charge.

5.2 Effect of Humic Substances (HS)

In order to gain a better understanding of the chemical properties of HS, a great deal of attention has been devoted to determining their physicochemical properties, including size, charge and structure, especially under conditions relevant to water treatment (Lead et al., 2000a, 2000b; Stevenson, 1994). Nonetheless, no consensus has been reached in the literature with respect to the structure and molecular conformation of HS (Jones and

Bryan, 1998; Schulten et al., 1998). Complexation studies with divalent ions like Ca and Mg often consider HS as a collection of homologous small ligands with a few complexing sites per molecule (Kramer and Duinker, 1984).

The unique properties of HS are due in large part to the fact that HS are polyfunctional (Buffle et al., 1990) and behave as polyelectrolytes (Cleven, 1984; Ephraim et al., 1986). The capacity of HS molecules to aggregate was discussed in early studies (Leppard et al., 1986). Furthermore, due to their small size, HS are at the limit between the domain of small soluble molecules and colloids. For this reason, HS have been modeled as rigid spheres or cylinders (Benedetti et al., 1996; Avena et al., 1999a; Carballeira et al., 1999), permeable Donnan gel phases (Ephraim et al., 1986; Marinsky and Ephraim, 1986), and as branched (Wolterink et al., 1999) or linear (Gosh and Schnitzer, 1980) polyelectrolytes.

More recently, due to the novel applications of nuclear magnetic resonance spectroscopy (NMR), fluorescence correlation spectroscopy (FCS), atomic force microscopy, pyrolysis mass spectrometry and numerical modeling, the representation of HS as predominantly consisting of small and relatively simple near spherical molecules (1-2 nm) able to form reversible aggregates has been accepted (Lead et al., 2000a, 2000b; Schulten et al., 1998; Balnois et al., 1999). Very recently, electrophoretic mobilities and diffusion coefficients of HS were systematically determined over a wide range of pH and ionic strengths using capillary electrophoresis (CE) and FCS, respectively (Hosse and Wilkinson, 2001). The data obtained were converted into information about the size and charge parameters for three HS (International Humic Substances Society (IHSS); these

included: Standard Suwannee River fulvic (FA), Humic (HA) and peat humic acids (PHA) (Hosse and Wilkinson, 2001).

It must be stressed that all HS are both poly-disperse and chemically heterogeneous, i.e., HS solutions are always present as mixtures of a large number of homologous molecules with similar but not identical properties. From average radii, the average space charge densities (per unit HS) for each type of site, ρ_{oi}, can be estimated using molar masses of 991, 1136, and 1264 g mol^{-1} for the FA, HA and PHA, respectively (Hosse and Wilkinson, 2001). For a polyelectrolyte, electrostatic arguments would suggest that the size should decrease with decreasing pH due to a reduction of intramolecular repulsion. For HS, an increased size is observed, especially at pH conditions above the carboxylic pK_a.

These results strongly suggest that HS aggregation takes place, perhaps simultaneously, due to a decreased intermolecular repulsion (Lead et al., 2000a, 2000b; Hosse and Wilkinson, 2001). Furthermore, the size of HS only weakly depends on the electrolyte concentration (Avena et al., 1999b). These observations, in addition to the known branched structure of the HS, are consistent with the interpretation that aggregation processes predominate over electrostatic swelling for the HS.

5.3 Adsorption Dynamics for Virus-HA Mixture in $CaCO_3$ Packed Bed

5.3.1 Regular Regime of Adsorption Dynamics

Normal operation of flow in a packed-bed reactor may be represented by Figure (5.1), which shows the building of a saturated zone of adsorbers near the inlet end of the bed. As more contaminated water is passed through the bed, the saturated zone moves forward

until the breakthrough point is reached. Once this point is reached, the exit concentration of contaminants begins to rise rapidly above accepted limits. If the passage of the fluid is still further continued, the exit concentration continues to rise until it becomes substantially the same as the inlet concentration. At this point, the bed becomes fully saturated. While the concentration at the saturation point is a function of the materials used, the dynamic capacity is also dependent on the operating conditions, such as inlet concentration, fluid flow rate, and bed depth.

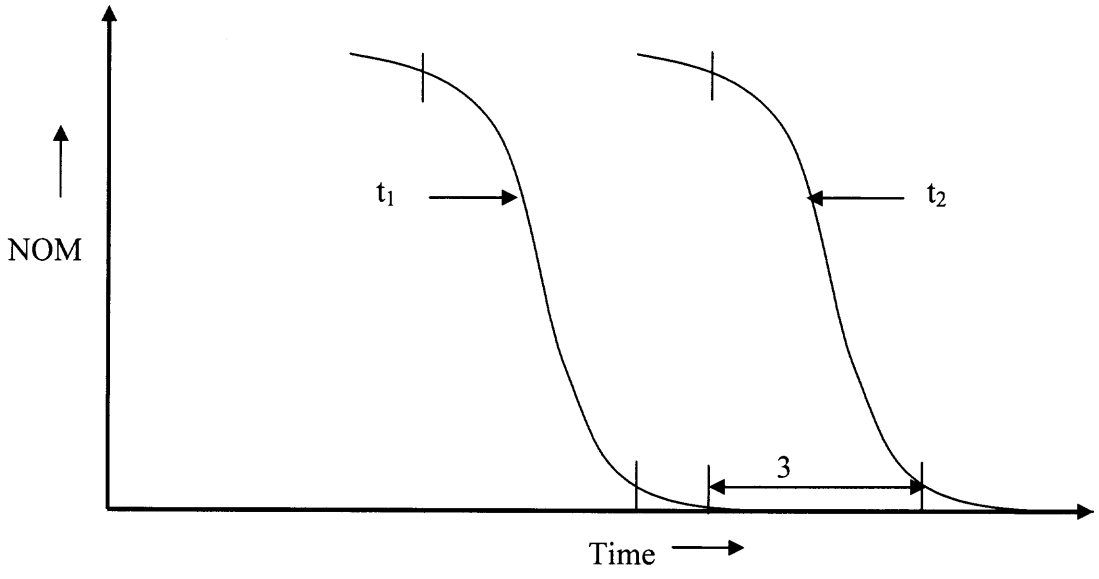

Figure 5.1 Formation and movement of the mass transfer zone (MTZ) through an adsorbent bed.t_1 – MTZ concentration at half-life, t_2 – MTZ concentration at breakthrough. Zone 3 – free zone for t_1, $t_2 > t_1$.

The zone of the bed where the concentration gradient is present is often called the mass transfer zone (MTZ). Dynamic adsorption results are normally expressed in terms of the dynamic capacity or the breakthrough capacity at given inlet concentrations, and flow rate conditions of the bed, together with the bed dimensions. It is important that the adsorber bed be at least as long as the transfer-zone length of the key component to be

adsorbed. Therefore, it is necessary to know the depth of the mass transfer zone, and its movement as a function of time.

Factors that play important roles in dynamic adsorption, and determine the length and shape of the MTZ are:

i) The type of adsorbent.

ii) The particle size of an adsorbent (may depend on maximum allowable pressure drop).

iii) The depth of the adsorbent bed and the velocity.

iv) The concentration of contaminants to be removed.

v) The removal efficiency required.

The following illustration (Figure 5.2) characterizes the so-called regular regime of adsorption dynamics (curve B). Its main features are: a) existence of a completely saturated zone, b) in-variancy of MTZ (MTZ shifts without its deformation), and c) a rather small thickness of MTZ. This latter regime is favorable for wastewater treatment. When MTZ is narrow, its thickness may be very small in comparison with the bed length. This means the breakthrough is negligible up to the moment when MTZ approaches the column backside. In this case, the adsorbent capacity is completely used in the saturated zone, which will almost include the entire volume.

The provision of a regular regime of adsorption dynamics is the main condition required for effective water purification with the use of flow packed bed. The quantitative characterization of the adsorption dynamics is the function of n(x,t), which describes the contaminant bulk concentration within the flow packed bed reactor (FPBR) as a function of time and distance, and whose crude illustration is given in Figure (5.2). The adsorption

dynamics are described with multi-variant theories which yield rather complicated expressions of n(x,t).

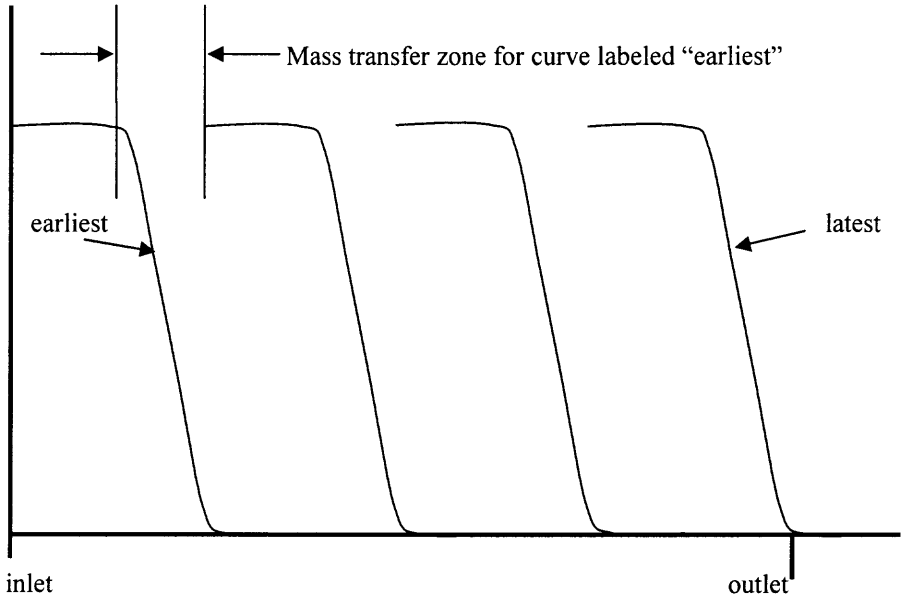

Figure 5.2 A regular regime of adsorption dynamics.

There is an initial step in the adsorption dynamics when the adsorbate accumulation and correspondingly, its concentration, are small, and consequently its desorption may be neglected in comparison with adsorption which simplifies the function n(x,0). With time, the surface concentration increases because of adsorption. Desorption is also a time dependant process, and depends on instantaneous surface concentration. Desorption, in turn, influences the bulk concentration. Therefore, accumulation of adsorbate enhances desorption, and hence bulk concentration changes with time as n(x,t).

With the desorption enhancement, a local quasi-equilibrium is achieved when desorption flux is almost equal to adsorption flux. This means the saturation of the adsorption zone (formation of a dead zone) between the entrance and the adsorption front does not contribute to HA removal.

5.3.2 Free Zone for Virus Adsorption

The weak influence of NOM is caused by large NOM molecule diffusivity compared to the diffusivity of the virus. As diffusivity (D) is inversely proportional to molecule dimension, and since the average NOM molecular dimension is in the order of 1 to 2 nm, this means that the NOM molecule is about 12 to 40 times smaller than the size of MS2 (27 nm).

$$D_n \sim 12\text{-}40\ D_v \tag{5.1}$$

As the NOM diffusivity is larger, the NOM penetration length (the distance to the adsorption front) will be shorter than that of viruses. This means that at a distance from the adsorbent entrance longer than the penetration length of NOM, the adsorbent will be free from NOM, and viruses will be adsorbed in the free zone (Figure 5.3). This mechanism will lead to the saturation of the adsorbent after time, in other words, when the NOM adsorption front approaches the end of FPBR, the free zone available for virus adsorption will become shorter. If this analysis is valid, NOM should not compromise the effectiveness of virus adsorption during the time necessary for NOM adsorption to reach the back/end of the packed bed. Therefore, NOM adsorption determines only the duration of the filter run, but not the efficiency of virus removal. Unfortunately, this favorable scenario is valid only for the case when NOM adsorption is almost irreversible.

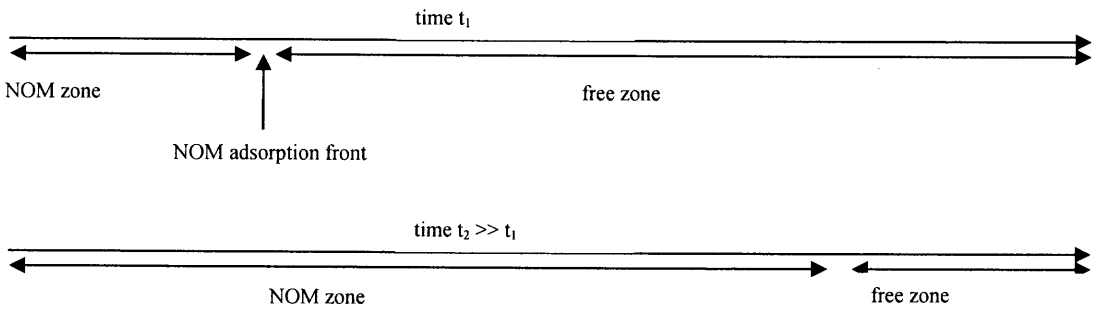

Figure 5.3 Movement of NOM front and its effect on virus removal.

5.4 Modes of NOM Adsorption on $CaCO_3$ Adsorbent

The general picture of NOM-virus competition for the adsorption site is complicated due to the following:

1) The NOM group/fraction, whose adsorption is almost irreversible, determines the duration of the filter run only;
2) The NOM group/fraction, whose adsorption is very weak, does not interfere with virus adsorption;
3) The NOM group/fraction, whose adsorption is reversible and whose equilibrium surface concentration Γ_{eq} is of intermediate value between 1 and 2 (above) may be dangerous for virus adsorption and may compromise its removal efficiency.

The above processes deserve further analysis and modeling.

Due to adsorption reversibility, the bulk concentration of this group/fraction of NOM cannot decrease below its value Ceq, which is the concentration that is in a dynamic equilibrium with NOM surface concentration Γ_{eq}. Hence, from the beginning of the filtration, the back portion of the filter, as well, is subjected to flow with NOM concentration C_{eq}. Consequently, the entire packed bed will attain the NOM surface concentration Γ_{eq}. Let us introduce a critical value Γ_{cr}. When $\Gamma_{eq} < \Gamma_{cr}$, NOM will not suppress virus adsorption.

On the other hand, when $\Gamma_{eq} > \Gamma_{cr,}$ NOM may interfere with virus adsorption and can suppress its removal efficiency. For reversible adsorption, Γ_{eq} is always smaller than that of the surface concentration for irreversible adsorption, at the same bulk concentration. Meanwhile, the latter is smaller than the surface concentration at saturation, and this occurs only at high bulk concentration. Therefore, one concludes that

$\Gamma_{eq,}$ in the case of reversible adsorption, is rather small in comparison with the maximal surface concentration corresponding to the saturation concentration. In turn, this means that there is sufficient concentration of free adsorption sites even if the reversible adsorption of NOM is present.

Perhaps there is a narrow fraction with bulk adsorbability (Γ/n) when reversible adsorption may cause the surface concentration to approach saturation concentration. In addition, it is necessary to define a special residence time. Special analysis is needed to clarify the specific and seldom conditions of reversible adsorption when competition with viruses may occur. This unfavorable situation corresponds to conditions that are rarely found, and accordingly, they may be disregarded. At large NOM concentration, NOM may form aggregates with a dimension of 50-200 nm (Caceci and Billon, 1990), which is comparable to the size of viruses. In this case, the favorable phenomenon of the preferential adsorption near the FPBR entrance disappears. Consequently, in this case the NOM's irreversible adsorption does not provide for a free zone, but competition with viruses for the same adsorption sites.

For HA, aggregation is possible at low pH only. With increasing pH, HA dis-aggregation occurs, i.e., aggregates disappear. This condition is very favorable in the adsorption filtration system since calcite normally results in increasing the pH along the packed bed. Therefore, HA aggregates that may be present near the entrance of packed bed will disappear downstream of FPBR.

5.5 Materials and Methods

Experiments to test the influence of NOM on virus removal and filter run of AF were performed either with deionized water contaminated by HA or with Newark tap water. Humic acid-sodium salt (HA) was purchased from Sigma Aldrich Chemicals. Stock solutions (100 mg/l) were prepared by dissolving this HA in required quantity in deionized water. Solutions (1-10 mg/l) for HA experiments were prepared by diluting this stock in deionized water. Packed beds to test the NOM influence were prepared in the same way as described in Chapter 4 (Section 4.2.3 (A)).

Composite filter experiments were performed in chromatography columns of length 50 cm. To prepare a composite filter, first a virus filter layer was prepared (Section 4.2.3 (A)). The column was kept filled with deionized water. NOM filter layers were formed on the top of virus filter by slowly adding calcite from top of the column. Testing of these packed beds for virus removal efficiency was performed in the same way as described in Chapter 4 (Section 4.2.3 (B)).

5.6 Experimental Evidence of Polymolecular Adsorption of HA and its Mechanism

5.6.1 Effect of NOM on Flow Rates and Observation of HA Polymolecular Layer

Experimental studies were performed to define the effect of NOM on virus' removal efficiency using calcite columns, as described in Chapter 4. Humic acid (HA) was purchased from Sigma and made into solution with different concentrations. During filtration of the HA solution (Humic acid from Sigma in deionized water (1mg/l and 10 mg/l)) through calcite columns (100 microns, and < 75 microns), the velocity sharply

decreased (at constant pressure) during 10-20 hours of continuous filtration, as shown in Figures (5.4) and (5.5). This sharp decrease in flow rates hampered the effort to investigate the long-term NOM influence on virus adsorption/removal.

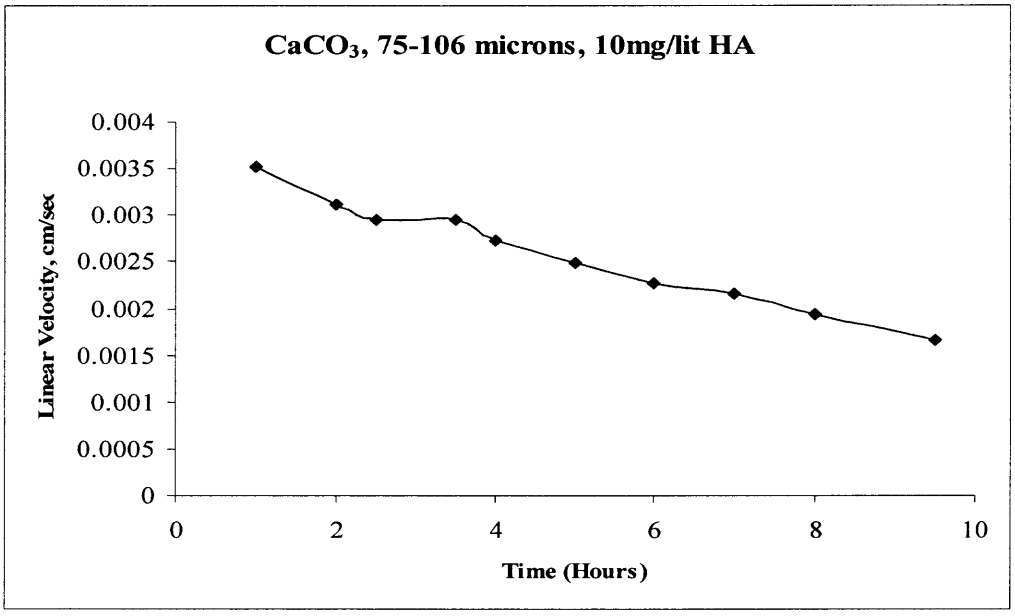

Figure 5.4 Change in linear velocity at ~ constant pressure head of about 80 cm and 10 mg/l HA, for filtration experiments through $CaCO_3$ column in the range of 75-106 microns. About 420 ml of HA-contaminated water was passed in about 9.5 hours.

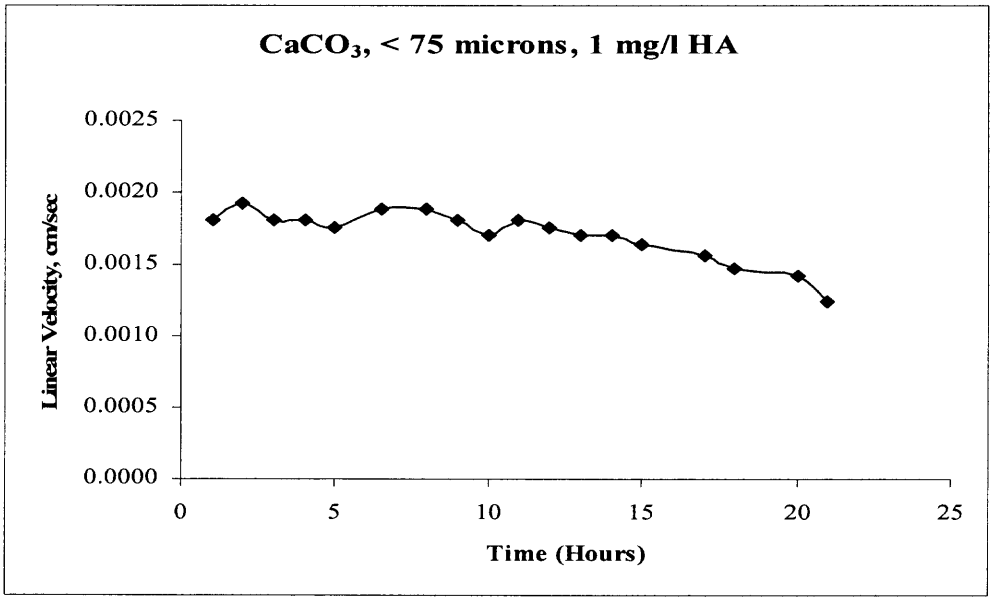

Figure 5.5 Change in linear velocity at ~ constant pressure drop of about 80 cm and 1 mg/l HA for filtration experiments through $CaCO_3$ column in the range of < 75 microns. About 628 ml of HA-contaminated water was passed in about 21 hours.

Visual observations (Figure 5.6) revealed that the reason for rapid increase of packed bed hydrodynamic resistance was due to the formation of a gel-like NOM layer close to the entrance of the packed bed (Figure 5.6). This will be referred as the "poly-layer" or "polymolecular layer" in future discussion. This important discovery proved to be important to understanding the effect of NOM on virus removal using FPBR filled with calcite, and to directing for a revision of the AF designs.

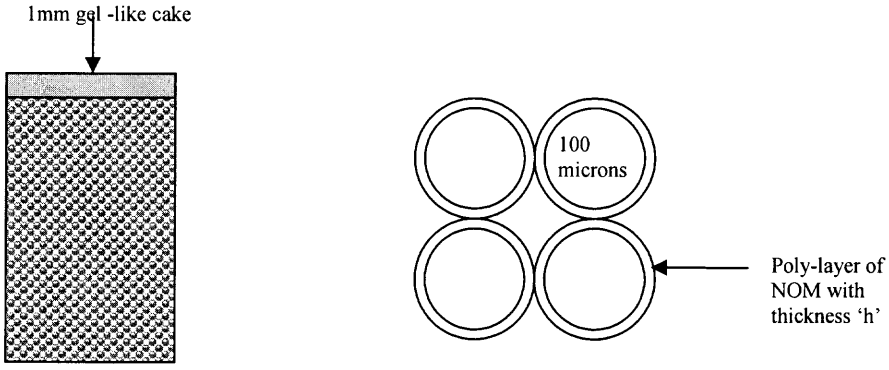

Figure 5.6 Formation of poly-layer of NOM.

5.6.2 Mechanism of Polymolecular NOM Adsorption by $CaCO_3$

No information about polymolecular NOM adsorption was found in the literature. This unusual phenomenon may be caused by $CaCO_3$ dissolution, which generates a permanent stream of Ca^{2+} ions into the bulk. This cation stream and HA anion stream meet at some distance from the adsorbent surface. This interaction results in the neutralization of the HA anion charge with divalent calcium cations, as follows:

$$HA^{(-2M)} + 2mCa^{++} = 2mCaHA \qquad (5.2)$$

where CaHA refers to a calcium humate complex. As a result of this reaction, the electrostatic repulsion which existed between the HA anions disappears. Since CaHA

become neutral, the collision of the newly-formed CaHA with CaHA film leads to their attachment to the surface collector, i.e., CaHA film growth takes place (Figure 5.7).

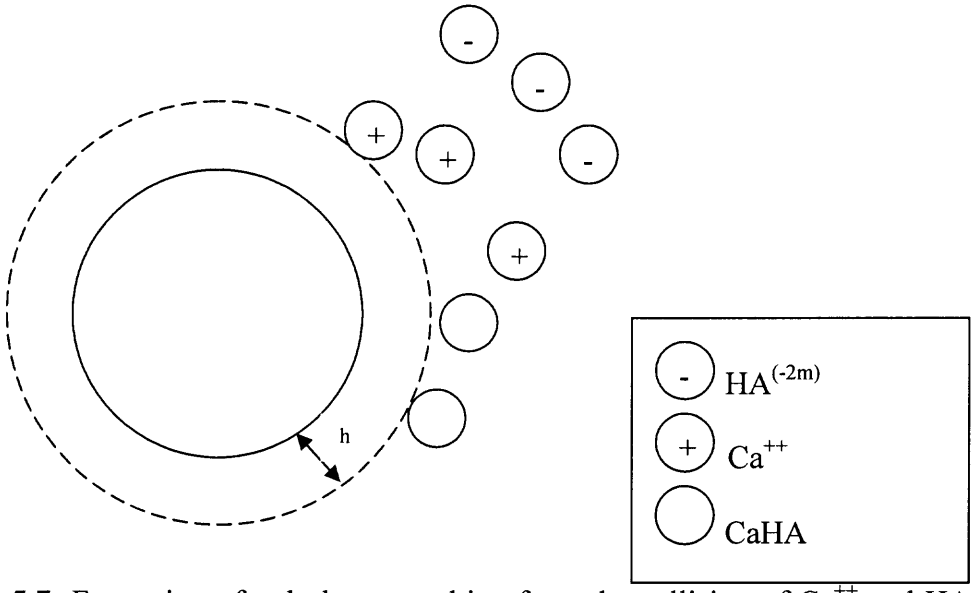

Figure 5.7 Formation of poly-layer resulting from the collision of Ca^{++} and HA anions near upstream of collector. The neutral molecule CaHA forms a deposit downstream to the collector.

The proposed mechanism takes into account research aimed at revealing the electrochemical properties of HA (Section 5.2). It was established that HA undergoes reversible coagulation when the electrostatic repulsion is suppressed by decreasing pH. The neutralization of negative charges of HA anions by Ca^{2+} cations converts the electrostatic repulsion into an attraction, and this causes reversible aggregation. The reversibility indicates that the arising energy of attraction is weak. Accordingly, the disaggregation time is short. This short time of disaggregation determines a small dimension of aggregates at low pH (section 5.2) in the bulk.

Near the calcite collector surface, the condition for the formation of large HA aggregates is more favorable. When the calcium-humate complex approaches the calcite surface due to diffusion, electrostatic attraction is possible when the neutralization of the negative charge of the HA polyanion is not complete. After the neutralization of HA

polyanion, this mechanism does not work. For a single bond between the adsorbed HA molecule and the approaching molecule, the energy of attraction may be small in the bulk. But when a polymer molecule approaches a monolayer, two or more bonds may arise which correspond to double (or larger) energy of attraction as compared to the formation of a single bond. This may increase the residence time of attachment several times because the surface concentration depends exponentially on the energy of attraction. Before the detachment occurs, another molecule may attach and form additional bonds, which may prevent the detachment of the attached molecule.

5.7 Polymolecular Adsorption Suppresses HA Influence on Virus Adsorption

An estimate of the position of the adsorption front when HA forms a monomolecular adsorption layer follows from the equation of conservation for the HA amount. The amount of HA which enters into packed bed is Q(t). This amount forms a monolayer between the front of adsorption and the entrance, i.e., along the distance $x_m(t)$, which is the distance between the entrance and a temporary position of the adsorption front. The adsorbed amount in the moment t is

$$Q_{ad}=x_m(t) * Sh_m \rho_s \tag{5.2}$$

where S is specific surface area of the adsorbent; h_m is the thickness of the saturated monolayer; ρ_s is the HA density in monolayer, i.e., amount of HA in adsorbed state per unit volume. The conservation law is

$$Q_{ad}(t) = Q(t) \tag{5.3}$$

or

$$x_m(t)= Q(t) / S\, h_m \rho_s \tag{5.4}$$

In the case of polymolecular adsorption, the same equation (5.2) is valid with h_p instead of h_m, where h_p is the polymolecular layer thickness. h_p is a function of x and t in distinction from h_m. But an averaged $h^{av}(t)$ value may be introduced.

$$Q_{ad}=x_p(t)\ S\ h^{av}(t)\ \rho_s \tag{5.5}$$

or

$$x_p(t)=Q(t)\ /\ Sh^{av}(t)\rho_s \tag{5.6}$$

Combining equations (5.6) and (5.4) yields

$$x_p(t)\ /\ x_m(t) = h_m\ /\ h^{av}(t)\ \ll 1 \tag{5.7}$$

Q(t) and S cancel each other because the same HA stream and the same packed bed are considered in this case. As $h^{av}(t)$ may exceed h_m by ten, a hundred or more times, the HA zone, i.e., zone occupied by HA where virus adsorption is questionable, may be ten, a hundred or more times smaller due to polymolecular adsorption. Accordingly, the time of existence of the free zone (filter run) may increase ten or a hundred times. However, only the initial portion of this time may be used because the clogging of packed bed occurs rather rapidly with the increasing thickness of the polylayer near the entrance of the packed bed $h(x,t)|_{x=0}$. For instance, in the experiments the clogging of the column took place in about 10 hours (Section 5.7).

However, even during this short time it was sufficient for us to understand how HA influences virus adsorption. The same high log removal from de-ionized water and from HA solutions exceeded 6 for cases where the polylayer was observed (Section 5.7). In other words, the thickness of the adsorption free zone remaining was large in the presence of the polylayer. These results direct us to explore means to minimize processes leading to the significant decrease in flow rates during filtration.

In light of the observations made regarding NOM removal in the packed bed, two conclusions can be made as follows:

1. The polymolecular adsorption prevented the extension of the NOM zone, and the free zone needed for virus attachment preserved for at least 10 hours. Visual observations and measurements confirmed this conclusion. Near the entrance of the HA, a gel-layer was observed with an approximate thickness of 2 mm. A gradual decrease in color was observed below the gel-layer with increasing distance x in the column. At distances longer than 1 cm, the initial color of packed bed preserved (no discoloration was found). This latter clean zone may be identified with the free zone available for virus attachment as discussed above. Therefore, polymolecular adsorption has proven to prevent the influence of that fraction of HA which appears to adsorb irreversibly on calcite packed beds.

2. There was also no noticeable influence on virus adsorption of that fraction of HA which adsorbs reversibly. As was analyzed in Section 5.4, reversible adsorption decreases with decreasing bulk concentration, but this reversible adsorption might be sufficiently large enough to raise the surface concentration of this fraction downstream. If this was the case in the experiments, HA surface concentration would have been sufficiently low to have a significant interference with virus adsorption. This conclusion alleviates concerns about the HA fraction that exhibits reversible adsorption on calcite with respect to virus attachment.

5.8 Experimental Investigation of HA Influence on Virus Adsorption

HA influences virus adsorption in two ways, depending on the type of filter configuration provided: 1) Strong influence which reduces virus removal provided by the AF, and 2) Weak influence on virus removal in which the presence of HA does not have any significant effect on virus removal. These two effects were investigated by performing experiments, as follows:

5.8.1 Suppression of Virus Removal by Strong Contamination of Adsorbent Surface

According to Bixby and O'Brien (1979), the presence of HA and fulvic acids not only interferes with virus adsorption, but also causes their desorption. Nasser et al., (1984) observed that organic matter in water and wastewater interferes with adsorption of viruses by competing for adsorption sites. Pieper et al., (1997) studied the effect of sewage-derived organic matter on PRD1 attenuation in iron oxide-coated quartz sand and gravel aquifer. It was found that PRD1 attenuation was 83% within the first meter in uncontaminated zone, whereas it was only 42% within the first meter of contaminated zone.

Experiments were performed to test the influence of a zone completely contaminated by HA on virus removal. This was done in order to prove that a NOM (HA)-contaminated zone of the column is not effective for virus removal and that a zone free of NOM is necessary to provide for the necessary 6-log removal. Two columns of the same particle size range (75-106 microns) of calcite having a depth of 1 cm were taken. One column was contaminated by passing about 500 ml of 10 mg/l HA solution, while 500 ml of DI water was passed through another column. Virus removal was tested

in these two columns, as shown in Table 5.1. As seen from the results in Table 5.1, the NOM-contaminated zone suppresses virus removal.

Table 5.1 Experimental Results Showing that NOM-Contaminated Zone does not remove viruses

Adsorption media	Contaminant	Linear velocity cm/sec	Volume of MS2 seeded water passed ml	Influent concentration (log_{10} pfu/ml)	Effluent concentration (log_{10} pfu/ml)	Log_{10} removal pfu/ml
75-106 microns $CaCO_3$	500 ml of 10mg/l HA	0.002	42	6.12	6.21	0
75-106 microns $CaCO_3$	500 ml of DI water	0.002	36	5.87	0	5.87†

† - See comment for Table 4.5.

Experiments were also performed to observe the NOM influence on virus removal, when viruses are present in NOM contaminated water. Viruses were seeded in HA-contaminated deionized water and in tap water and the packed beds were tested for virus removal. Results (Table 5.2) show that complete log removal is provided by calcite in the presence of NOM.

Table 5.2 Log removal of viruses in NOM-Contaminated Water

Adsorption media	NOM concentration	Linear velocity cm/sec	Volume of MS2 seeded water passed ml	Influent concentration (log_{10} pfu/ml)	Effluent concentration (log_{10} pfu/ml)	Log_{10} removal† pfu/ml
75-106 microns $CaCO_3$	10 mg/l HA (420 ml)	0.0011	20	7.05	0	7.05
		0.0008	15	6.80	0	6.80
30 microns $CaCO_3$	Tap water (~ 2.0 mg/l)	0.013	40	6.50	0	6.50

† - See comment for Table 4.5.

5.8.2 Experimental Proof of Weak Influence of HA on Virus Removal

To reduce the effect of NOM influence on virus removal and to reduce clogging of AF, a composite filter was proposed. The composite filter tested had either one or two layers of coarse calcite fraction ranging from 212-800 microns on top of a finer fraction (< 106 microns). The coarse fraction served as a NOM filter reducing the loading on virus filter.

Long-term experiments were conducted for these composite filters by contaminating them with 1 mg/l of HA solution. Virus removal was tested for the composite filter after long-term exposure to HA solution. The long-term feeding of the stream with viruses is excessive and very complicated because the long-term NOM accumulation on the adsorbent surface does not depend on the presence of the virus. The larger the HA surface concentration, the weaker is the electrostatic attraction of viruses to the positive surface of calcite because the neutralization of this charge by the negative adsorbed HA will be larger. This means that the virus residence time may decrease with the increasing surface concentration of HA.

The analysis in Section (5.4) showed that the HA fraction with long residence time, and accordingly, with large adsorbability, Γ_N / C_N, may suppress virus adsorption, distinct from the fractions with even longer residence time (almost irreversible adsorption) or with shorter residence time, because in the latter case, the surface concentration is low even at its large bulk concentration. Although a fraction with longer residence time may provide higher surface concentration, this may occur only when its bulk concentration is not too small. The minimal bulk concentration for this most harmful fraction is determined by two conditions. First, it has to correspond to a large surface concentration. Second, as the bulk concentration of this narrow fraction may be small, a

rather long time of filtration is necessary to saturate the surface with this HA fraction. This means that the presence of this fraction in the HA may not be dangerous for a short virus residence time. But longer virus residence time may be limited due to the accumulation of the harmful NOM fraction on the surface. This is the reason, why long-term testing of virus adsorption reversibility was necessary.

Long-term testing of virus removal for columns contaminated by 1mg/l HA solutions (see Section 5.5) was carried out by using a 3-layer composite filter (2 layers of NOM prefilter layer and 1 virus filter) and a 2-layer composite filter (1 layer of NOM prefilter and 1 virus filter) as shown in Figure (5.8). The results of these experiments are presented in Figure (5.9) (3-layer composite filter) and in Figure (5.10) (2- layer composite filter). For both the filters (3-layer and 2-layer composite filter), the testing of virus removal was performed when the linear velocity dropped to about 0.001 cm/sec by seeding MS2 in 1mg/l HA solution.

More than 6-log removal was measured in these experiments (Table 5.3), i.e., long-term feeding of HA does not affect virus residence time noticeably. As viruses were fed after 4 days, the accumulation of the most harmful fraction (if it was present) of HA during 4 days of HA solution filtration did not affect virus adsorption.

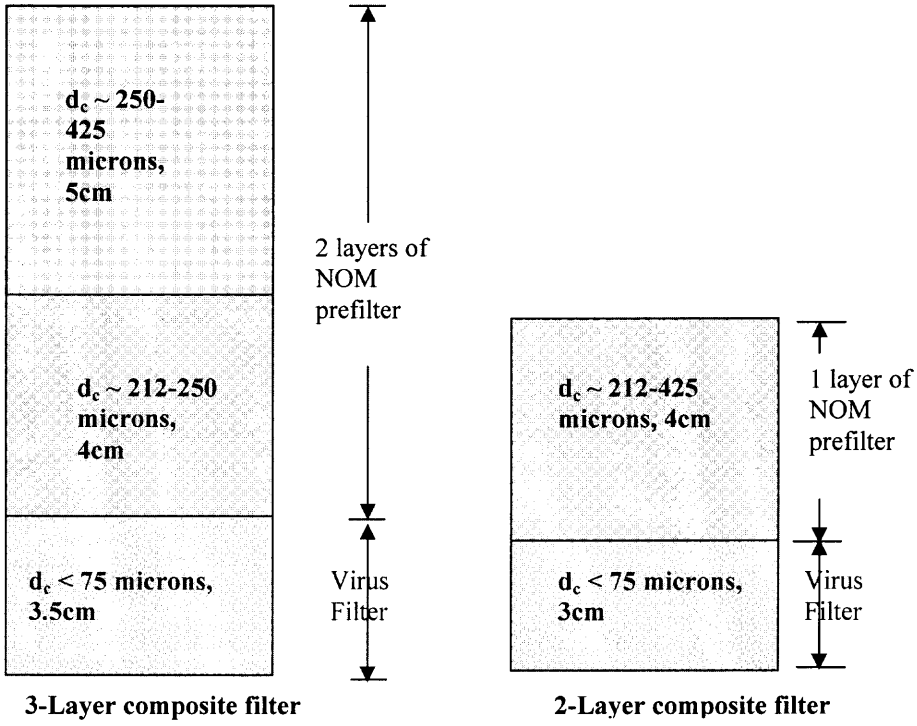

Figure 5.8 Laboratory model of 2 and 3-layer composite filter.

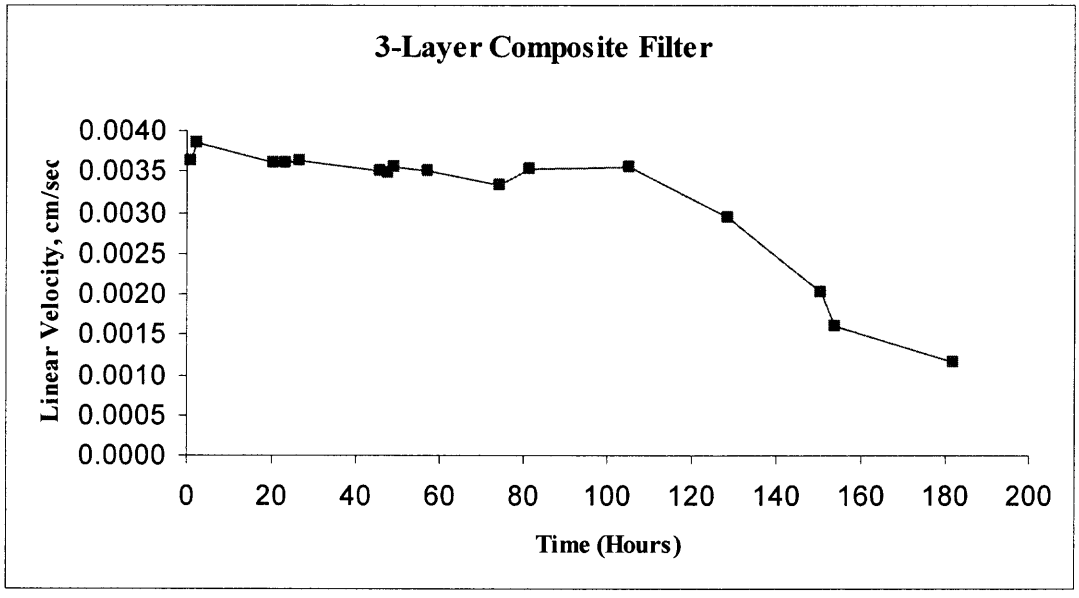

Figure 5.9 3-layer composite filter having first 2 coarse layers as NOM prefilters and 1 fine layer as virus filter, i) 250 - 425 microns with height 5 cm, ii) 212 - 250 microns with height 4 cm and, iii) < 75 microns of 3.5 cm. Total flow through the composite filter was about 10.2 liters in about 181.8 hours.

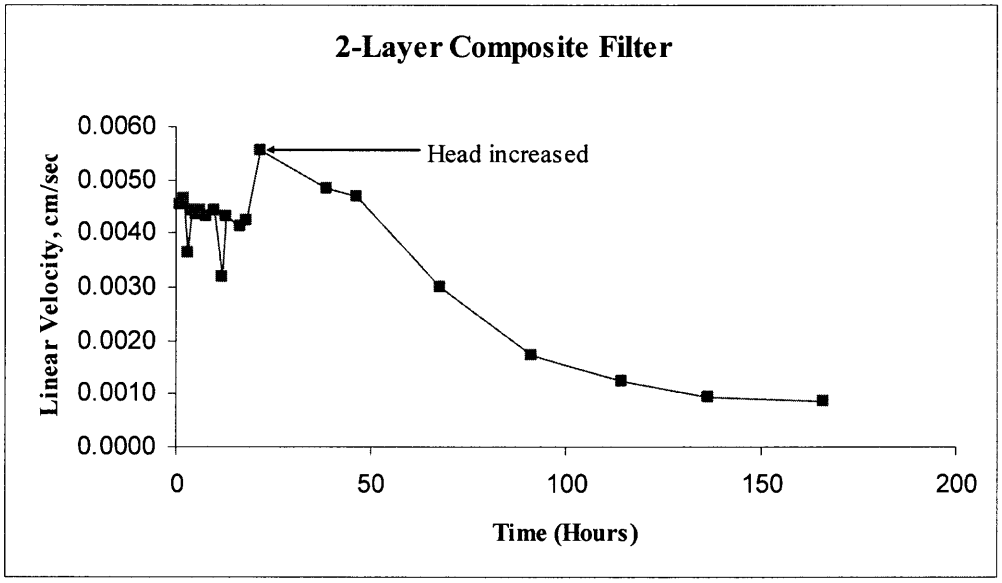

Figure 5.10 2-layer composite filter having one coarse layer of NOM prefilter and one fine layer of virus filter , i) 212 - 425 microns) with height 4 cm, and ii) virus filter layer of < 75 microns of 3.0 cm. Total flow through the composite filter was about 7.0 liters in about 166 hours.

A summary of long-term testing of 3-layer and 2-layer composite filters is presented in Table 5.3.

Table 5.3 Results of virus removal in composite filters for long-term experiments

Adsorption media (Dosed with HA 1 mg/l)	Linear velocity sec/sec	Volume of MS2 seeded water passed ml	Influent concentration (log_{10} pfu/ml)	Effluent concentration (log_{10} pfu/ml)	Log_{10} removal† pfu/ml
3-layer composite filter	0.0014	27	7.02	0	7.02
	0.0014	26	6.92	0	6.92
2-layer composite filter	0.0011	39	6.87	0	6.87
***2-layer composite filter**	0.005	94	5.74	0	5.74

* Presidential Lakes field sample, 2-layer filter having 250-425 microns NOM prefilter of height 4 cm and a virus filter with < 75 microns calcite of height 2.5 cm. **

† - See comment for Table 4.5.

5.9 Conclusions

NOM influence on virus adsorption revealed that NOM competes with viruses for the adsorption sites (Table 5.2), which is in agreement with other studies (Nasser et al., 1984; Pieper et al., 1997). In the presence of NOM, the availability of a free zone provides for more than 6-log removal of viruses (Table 5.3). The competition of NOM for virus adsorption sites can be reduced by adding coarse layer/s of calcite particles (NOM prefilter) to the virus filter, which not only protects the free zone for virus removal, but also reduces virus filter clogging, thus increasing the filter run of the composite filter. Long-term experiments performed with composite filter indicate a weakened influence of NOM as the virus filter provided for more than 6-log removal after the composite filter was contaminated with NOM for more than 6 days.

In Chapter 6, experiments of technological significance are discussed. In these experiments, NOM prefilter and virus filter were separated as two different filter units and connected in series to increase filter run while still providing high log removal of viruses for the entire duration of treatment.

CHAPTER 6

LONG-TERM TESTING OF COMPOSITE NOM PREFILTER / VIRUS FILTER EXPERIMENTAL AND THEORETICAL MODELING

The concept of adsorption filtration (AF) was introduced to overcome the limitations of conventional deep-bed filtration to effectively remove viruses during water treatment, and to place special emphasis on developing a technology to remove viruses from groundwater (GW) sources in New Jersey.

As elaborated in Chapter 5, the presence of NOM in large concentration appears to decrease the filtration rate due to the deposition of a polymolecular layer within the calcite filter, and to compete with virus attachment for the negatively-charged sites on the surface of collector. In order to validate the effectiveness of the AF technology for virus removal and to demonstrate its applicability for GW treatment, experiments were designed to use composite (or hybrid) filter arrangements to treat large quantities of water contaminated with NOM and to test virus removal efficiency under various conditions. Attention was paid to keeping the filter active with respect to virus removal and to ensuring that large amounts of water could be treated before the pressure drop in the composite/hybrid filter increased to twice its initial value.

A two-layer composite/hybrid filter (one NOM prefilter and one virus filter) and a three-layer composite filter (two-NOM prefilters and one virus filter) were tested using Newark (NJ) tap water as a source of NOM. Since Newark tap water (treated surface water) contains residual NOM higher than most GW sources, it was used to perform long-term filtration experiments to test the virus removal efficiency of the composite

filter, as described above. The details of these experiments and the results are discussed in this chapter.

6.1 Virus Filter Model

As shown in Chapter 4, filtration experiments performed at the following operational parameters: bed height (h) ~ 4cm, linear velocity (u) ~0.003 cm/sec and AM particle diameter (d_c) 75-106 microns, achieved log removal of about 6, or even higher (complete log removal). All experiments were based on using calcite as the adsorption medium, and are described in Chapter 4.

Based on these results, it may be assumed that the actual virus log removal might be even much larger, since the level of dosing water with MS2 was limited to 6 logs. If this assumption is valid, it may be possible to increase filtration linear velocity through the AF filter or to increase the adsorbent particle dimension while still maintaining virus log removal of about 6 under the above experimental conditions. This has proven to be possible in the experiments performed with calcite particles in the range of 106-150 microns at h = 10 cm and a linear velocity of about 0.035 cm/sec, i.e., 6-log removal was preserved at this higher velocity.

In earlier experiments, it was noticed that the measured pressure drop exceeded that calculated with the Ergun equation by a factor of 5. This excessive increase in pressure drop was attributed to the presence of fine particles (< 75 microns) in the adsorption medium, and this effected an increase in flow resistance. The presence of finer particles (< 75 microns) within the packed bed was confirmed by optical microscopy examination. Particles < 75 microns were found to be attached to the surface of larger

particles. Due to this mode of aggregation, the remaining smaller particles (fines) could not be effectively removed by dry sieving. As a result, the packed bed was filled with aggregates having smaller particles attached to larger particles. This may explain why the pressure drop of the packed bed exceeded the prediction of the Ergun equation.

Efforts were made to decrease the amount of smaller particles attached to larger particles as described in Chapter 4 (See Section 4.2.3 (A)). Once this problem was corrected, the hydrodynamic resistance of the packed bed used in the experiments decreased by about 4 times, and the agreement with the Ergun equation became reasonable.

The main outcome of removing excessive fines from the adsorption medium was very significant in this research since it allowed to increase the filtration velocity to about 0.03 cm/sec and still achieve more than 6-log removal of viruses (MS2). The ability to achieve high log removal at this high filtration velocity presented an additional base for further improving the design of the AF filter. Therefore, if a NOM pre-filter is used at about 0.1 cm/sec, only 4 AF virus channels will be sufficient. In this case, the velocity through the adsorbent filtration bed/channel of AF will be 0.025 cm/sec. This is a major advantage over the initial estimates where 15 channels, operating at a much smaller velocity of 0.003 cm/sec, were needed to achieve 6-log removal of viruses. Therefore, this new understanding and discovery will significantly simplify the AF technology.

The second improvement in the operational parameters of the AF filter was the possibility of increasing the filtration depth up to 20 cm, compared to the initial 5-cm filtration depth that was assumed in the original AF designs. For 15 channels with a

height h=5cm and channel width of 2 cm, the cross-section of AF and its volumetric velocity will be the same as that for an AF with 4 channels of h~20 cm each.

The third improvement in the AF technology that was accomplished in this study stems from the fact that larger filtration velocity suppresses NOM cake formation. The collision efficiency (η_T) corresponding to diffusion as expressed by equation (2.10) decreases with increasing velocity, where η_T is the portion of contaminant captured in the first layer of the packed bed. This indicates that the clogging rate has to decrease with increasing velocity, and accordingly, with decreasing η_T.

6.2 NOM Filter Modeling

As advanced earlier, the use of a NOM pre-filter is necessary to simplify the AF design, and this should lead to longer filter runs while maintaining the high virus log removal efficiency. A simplified approach to NOM pre-filter modeling will become clear with the use of the well-known notions of slow and rapid filtration, as presented below.

6.2.1 Slow and Rapid Filtration

As per the experimental results and observations, unrestricted growth of multilayer deposits of HA near the entrance of the packed bed causes clogging of the packed bed. Afterwards, the majority of the arriving HA molecules cannot penetrate through the clogged pores at the front surface of the packed bed, and as result, they accumulate upstream. This accumulation causes an increase in the deposit thickness, which does not grow inside the pores but above the entrance of the packed bed upstream (surface filtration). This cake growth causes a pressure accumulation following almost a constant

rate; this restricts the filter run since only twice the increase in the pressure drop is acceptable for this type of filtration process.

Before cake formation, a small portion of the arrived NOM molecules accumulates near the entrance of the packed bed. The majority of NOM molecules penetrate into AM and accumulate along the packed-bed depth with gradually decreasing deposit thickness downstream. This mode of filtration is called deep filtration. The filter capacity is orders of magnitude higher for deep filtration compared to that of surface filtration because the deposit is distributed over the entire depth of the bed. In surface filtration, the deposit accumulation occurs near the entrance of the filter bed, and this mode of accumulation leads to a high pressure drop -- cake thickness is usually of the order of 2 millimeters.

For cake formation, a slow water stream is necessary because the diffusion of macromolecules to packed bed grains (collector particles) takes time. Therefore, the larger the filtration velocity, the smaller will be the portion of macromolecules that may reach the collectors of the first adsorbent layer by diffusion to form deposit/cake. In earlier days, filtration at slow velocity with cake formation was used on rather small sand collectors; in this case, contaminant accumulation took place within the cake (so called slow filtration). Later in the development of filtration processes for water treatment, both the collector (sand) dimensions as well as the velocity were increased.

The above two changes led to a decrease in the contaminant flux in the first few top layers of collectors, and this development was favorable for achieving deep penetration of the contaminant into the packed bed. There is also some cake formation in deep filtration, but this occurs after the accumulation of a large amount of deposit within

the entire depth of the packed bed, which is normally about a meter. This new mode of deep filtration is also called rapid filtration. In rapid filtration, filter capacity is at least 100 times larger than that of slow filtration. However, the filter run (FR) does not increase proportionally because the velocity in rapid filtration is much higher, and accordingly, much more contamination enters the rapid filter per unit time. The depth of a slow filter can be small (cm) because the accumulation occurs mainly within the cake (mm). In contrast, the depth of a rapid filter is of the order of meters because any collector collects only a small portion of contaminants from the stream.

Due to multilayer NOM formation, slow velocity (0.003-0.02 cm/sec), and small collector dimensions (70 to 150 microns), a slow filtration mode was realized in the experiment with cake formation and a shorter filter run (10 hours); this was before the introduction of the NOM pre-filter (Chapter 4). With increasing collector dimension and velocity, the amount of the contaminant portion captured by the first layer of adsorbent decreases. Accordingly, the time for cake formation increases. But the velocity can be increased only to a certain extent, because at larger velocity, a virus breakthrough will occur.

A solution to this dilemma would be to use a 2-layer composite/hybrid filter, with the first top auxiliary layer for NOM accumulation (NOM prefilter) and the second layer for virus capture (virus filter). As per the findings of this study, the virus filter will be based on calcite particles in the range of 106-150 microns and a filtration depth of about 20 cms. Also, a rather long packed bed (l_H) for NOM removal may become necessary to reduce NOM loading on virus filter. Consequently, the NOM prefilter has to be in the

form of a separate filter unit, maybe in the form of a conventional FPB, in distinction from the AF design of the virus filter elaborated in this dissertation.

6.2.2 Estimation of the Operational Parameters of a Practical NOM Prefilter

Since the diameter of the adsorption medium (AM) for NOM (d_H) is chosen to be coarser than that for viruses (d_v), larger pores between larger collectors within the NOM prefilter allows the accumulation of more NOM materials. This mode of NOM filtration will prolong the time necessary for clogging due to the presence of NOM in the influent. Hence, the larger the d_H/d_v ratio, the longer will be the filter run for the composite filter in comparison with a single virus filter. However, there is a restriction up to which this ratio can be increased because the larger the d_H, the smaller is the NOM capture rate within the NOM prefilter, and correspondingly, the larger will be the NOM concentration in the effluent stream, i.e., in the stream entering the virus filter.

The increase in d_H (collector size for HA) in comparison with d_v (collector size for virus) becomes possible as the dimension of the average NOM molecule is much smaller (1-3 nm) than that of virus, (27-100 nm). Accordingly, the diffusivity ratio

$$D_H / D_V = r_V / r_H = \sim 10 \tag{6.1}$$

where r_v and r_H are radiuses of viruses and HA molecules, respectively. According to equation (2.10,) the collision efficiency increases with increasing diffusivity D (or decreasing macromolecule dimension) and decreases with increasing collector diameter, d. Consequently, d_H may be chosen larger than d_v because D_H is much larger than D_v. This is an important conclusion that will facilitate the development of the technology with respect to virus removal in the presence of NOM, and will allow the achievement of a long filter run for virus removal without increasing the pressure drop.

The ratio of the particle dimension according to equation (6.1) has to be compared with the main equation (2.11)

$$\ln\left(\frac{N_c}{N_o}\right) = 6A_s^{1/3}(1-\varepsilon)\frac{l}{d_c}\left(\frac{D}{ud_c}\right)^{2/3}\alpha \tag{6.2}$$

When this equation is specified for viruses and for NOM, D_v and d_v or D_H and d_H have to be substituted into its right-hand side respectively to obtain log removal for virus and for NOM in left hand side, also respectively. The ratio of the left-hand side of these two equations is equal to the ratio of the right-hand side of these equations.

This yields,

$$\frac{d_H}{d_v} = \frac{l}{h}\left(\frac{r_v u_v}{r_H u_H}\right)^{2/5}\left[\frac{\ln_v(n_o/n_c)}{\ln_H(n_o/n_c)}\cdot\frac{d_H}{d_v}\right]^{3/5} \tag{6.3}$$

where $\ln_v$ and $\ln_H$ are the natural log removal for viruses and HA, respectively.

A certain amount of HA removal is necessary in NOM prefilter to prevent the clogging of virus filter, which restricts a desirable increase in the d_H / d_v value, as is seen from equation (6.3). With the increasing HA log removal, the right-hand side of equation (6.3) decreases, i.e., the decrease of d_H / d_v is necessary in the left-hand side of this equation. Nevertheless, d_H / d_v of about 4 is possible even at a rather high log removal of HA (about 2-log removal or 99%) due to the possibility of increasing the length of the NOM prefilter l (50 to 100 cm) as compared to that of the virus filter (20 cm) and because rv / r_H is rather large, namely 10. Taking into account these estimates, the design parameters of the NOM filter have been chosen as follows: i) particles size --- $425<d_H<800$; (d_H ~ 600 microns) ii) filtration depth -- l_H= 45 cm; iii) linear velocity -- u_H~0.1 cm/sec; iv) pressure drop -- ~ 110 cm (~ 0.1bar).

6.3 NOM Prefilter Testing

Long-term testing of the NOM prefilter is necessary to determine two main characteristics, namely: the clogging time and the protection kinetics of the virus filter from NOM contamination. The combination of the above two characteristics defines the overall filter run for high efficiency virus removal.

6.3.1 NOM Prefilter Clogging

The decrease in filtration velocity through the NOM prefilter was measured as a function of time (Figure 6.1).The laboratory setup of the NOM prefilter is shown in Figure (6.2) The operational parameters were chosen in accordance with the results of modeling presented in Section 6.2.2: $l_H \sim 45$ cm, $425<d_H<800$ microns ($d_H \sim 600$ microns); $u_H=0.12$ cm/sec. An essential decrease in velocity occurs after 4 to 5 days, while virus filter clogging (without NOM prefilter protection) occurs in 5 to 10 hours (Figure 5.3).

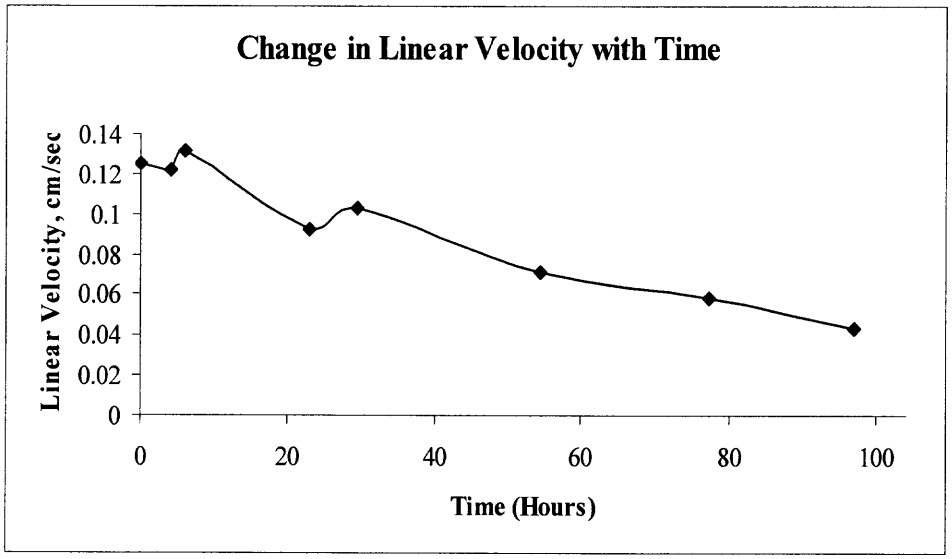

Figure 6.1 Kinetics of NOM prefilter clogging – Calcite particle size ~ 600 microns, column height 45 cm, total amount of water treated was about 121 liters in 97 hours.

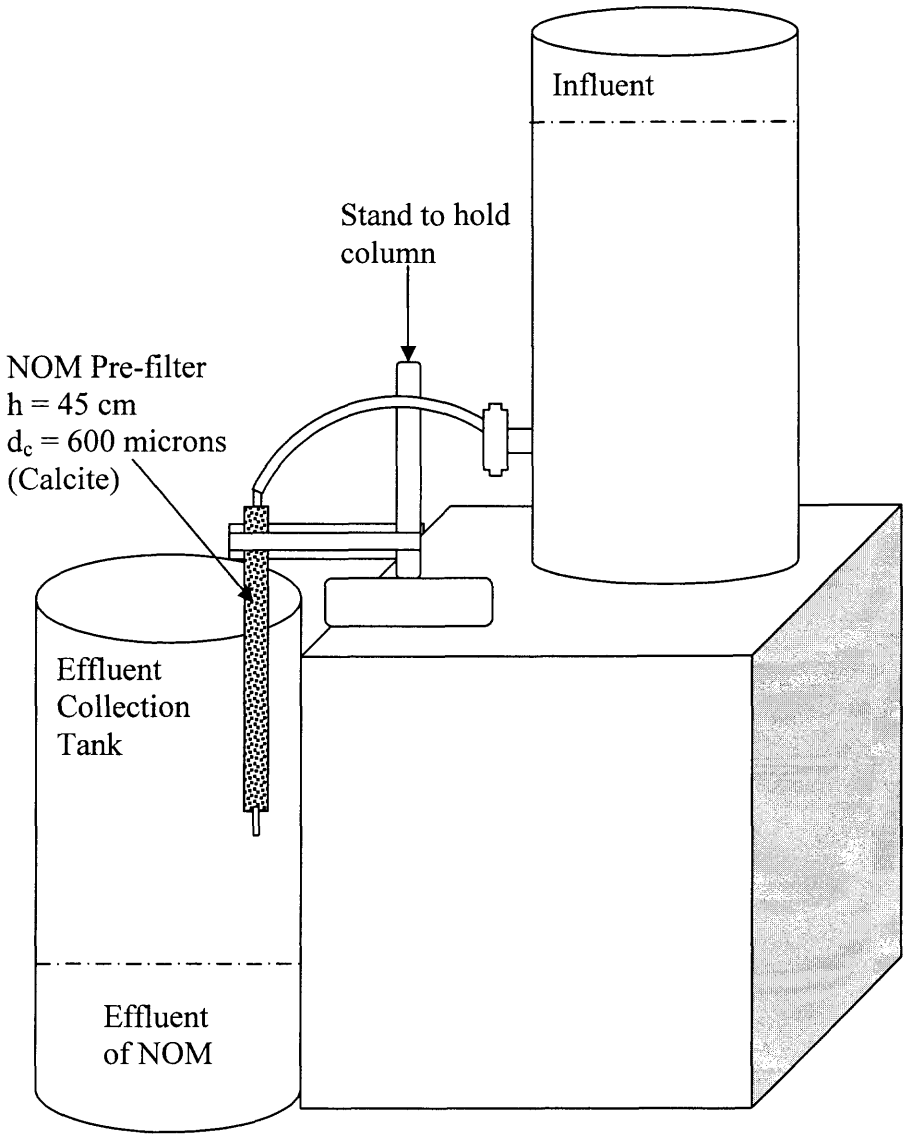

Figure 6.2 Laboratory setup to study the NOM Pre-filter

6.3.2 Retardation of Virus Filter Clogging due to Protection by NOM Prefilter

A simple experimental set-up was constructed as shown in Figure (6.3) to study the effect of the NOM prefilter on the filter run regarding virus removal. The effluent of the NOM prefilter was used as the influent for the virus filter. It was observed that the velocity exceeded 0.1 cm/sec under gravitational flow with the vertical orientation of the packed bed when calcite particle dimensions of about 600 microns were used, even without any

application of pressure drop. The initial velocity was controlled to 0.1 cm/sec by means of applying additional resistance with the aid of a valve. The change in linear velocity due to clogging over a period of time was studied at this constant resistance (pressure drop). After the packed bed resistance increased due to clogging, and the velocity decreased about 30%, the additional resistance of the valve was eliminated. This caused a temporary increase in the velocity. Afterwards, it started to decrease again.

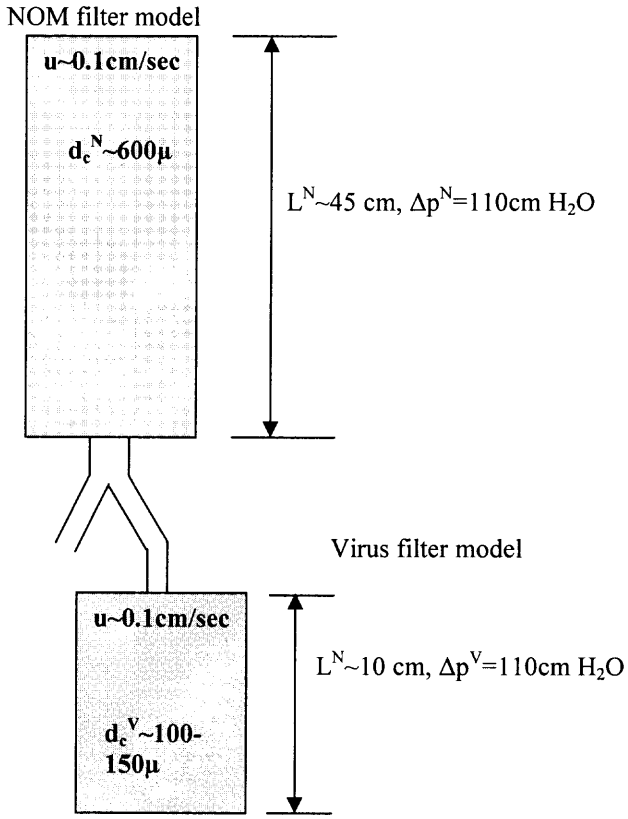

Figure 6.3 Laboratory model of composite NOM prefilter and virus filter

The decrease in the filtration velocity through the virus filter was measured as a function of time (Figure 6.4).

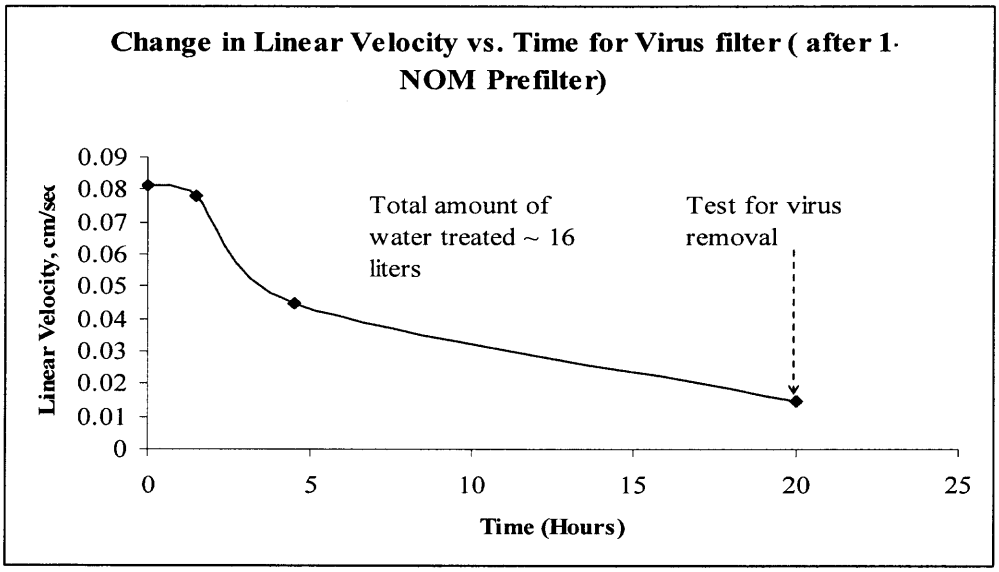

Figure 6.4 Retardation of virus filter clogging due to NOM prefilter.

The time dependence for a decrease in velocity through the virus filter in the absence of the NOM prefilter (Figure 5.3) was compared with the velocity decrease in the virus filter after having a NOM prefilter (Figure 6.3). It was found that the NOM prefilter application extends the filter run of the virus filter. However, the rate of the virus velocity decrease in the virus filter is higher than that for the NOM prefilter (Figure.6.1). Accordingly, the clogging of the virus filter controls the filter run for the composite filter. One concludes that a decrease in the NOM effluent concentration from the NOM prefilter is desirable.

6.3.3 Model of 2-layer NOM Prefilter

Although the desirable increase in NOM log removal may be achieved, either by decreasing d_c or u_H, this does not provide the best solution. Both d_H decrease and u_H decrease cause the collision efficiency to increase, or, in other words, to result in an

enhancement in clogging. In addition, a decrease in u_H means a decrease in filtration throughput, and this would diminish the value of the technology.

A possible improvement in the design is to increase the NOM prefilter length l to about 100 cm, because the effluent concentration decreases rapidly with the increase in length, namely, exponentially according to Equation (2.11). However, two layers of the NOM prefilter (Figure 6.5) may provide even smaller NOM penetration, if the additional layer consists of an adsorbent with dimension $d_{H2} < d_{H1}$. At this smaller d_{H2}, the collision efficiency is higher according to equation (2.10), and correspondingly, log removal is higher according to equation (2.11). The only limitation, which arises with the decreasing d_{H2}, is the accompanied increase in the pressure drop, as was explained in Section (6.3.2).

However, there is a scope of reducing this pressure drop. When $d_{H1} / d_v \sim 4$ and $l_{H1} / d_v \sim 2.5$, the pressure drop for the virus filter exceeds that for the NOM prefilter by about 10 times, according to the Ergun equation. Hence, the second layer of the NOM prefilter can impose a pressure drop equivalent to that of the virus filter, although the velocity $u_{H2} = u_{H1}$ exceeds u_v by about 4 times. With this condition and with the use of the Ergun equation, the operational parameters for the second layer of the NOM prefilter have been estimated to be $200 < d_{H2} < 425$ microns ($d_{H2} \sim 300$ microns); $20 < l_{H2} < 50$cm.

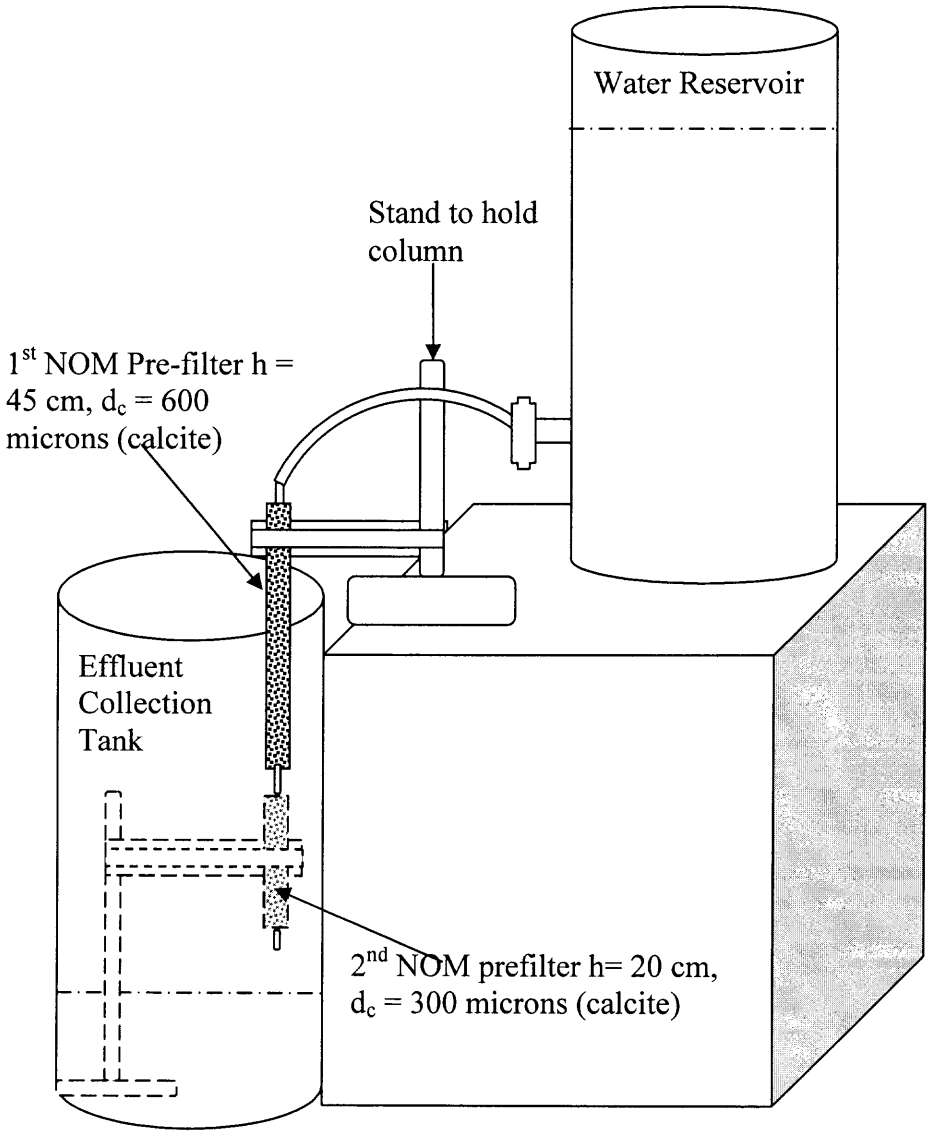

Figure 6.5 Laboratory setup to study two NOM Pre-filters in series.

6.3.4 Clogging of 2-layer NOM Prefilter

Tap water includes many kinds of impurities, which are characterized with different diffusivities and will have different collision efficiencies according to equation (2.10). For better understanding of the advantages of two layers of NOM prefilter, the impurities can be classified into two fractions. The first fraction is characterized by larger collision efficiency, and accordingly, is accumulated within the first layer of the NOM prefilter.

The collision efficiency for the second fraction is smaller, and thus it can penetrate through the first layer. But the collision efficiency of this second fraction increases when it enters the second layer because $d_{H2}<d_{H1}$. Therefore, this second fraction accumulates at least partially within the second layer.

As the particle dimension of the collector of the first layer is large, its clogging is rather slow, as demonstrated in Section (6.3.1). Additionally, this first layer of the NOM prefilter retards the clogging of the second layer because the concentration in the effluent of the first layer is lower than that of its influent.

The initial velocity for this NOM prefilter was also decreased to 0.1 cm/sec by means of the application of additional resistance with the aid of a valve. After the packed bed resistance increased due to clogging and the velocity decreased about 30% (about 2-3 days), the additional resistance of a valve was eliminated. This caused a temporary increase in the velocity. Afterwards, it started to decrease again. The decrease in filtration velocity through the NOM prefilter consisting of two layers is demonstrated in Figure (6.6).

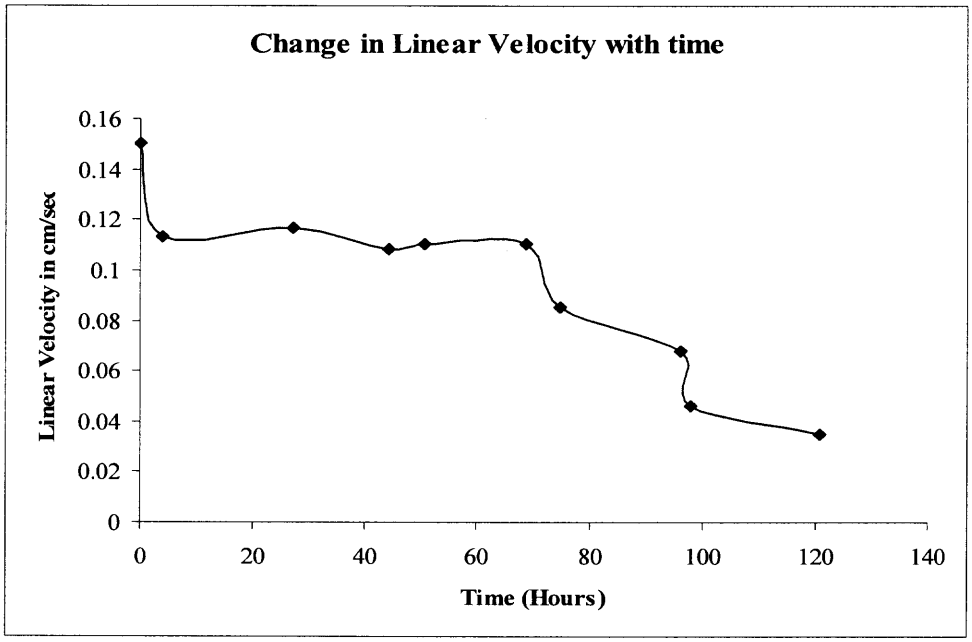

Figure 6.6 Kinetics of velocity decrease for 2-layer NOM prefilter, i) 600 microns with a length of 45 cm length, ii) 300 microns with a length of 20 cm. Total amount of water treated was about 135 liters in 120 hours.

6.3.5 Retardation of Virus Filter Clogging with Protection by 2-layer NOM Prefilter

The decrease in filtration velocity through the virus filter was measured as a function of time (Figure 6.7). The comparison between Figure (6.7) and Figure (6.4) shows that 2 layers of NOM prefilter essentially extend the filter run of the virus filter as compared to the filter run of the virus filter when 1 layer of NOM prefilter one was used. Because the experiment was set up in such a way as to keep the same pressure drop for both the NOM prefilter and the virus filter (about 110 cm), initially it was an excessive pressure drop for the virus filter, and an additional hydrodynamic resistance was introduced by a valve to adjust the initial velocity to about 0.03cm/sec. During the first day, the velocity through the virus filter decreased from 0.03 to 0.02 cm/sec. This was counterbalanced by a decrease in the resistance caused by the valve, which enabled us to establish the velocity

at about 0.03cm/sec in spite of the increased resistance in the virus filter. This procedure was repeated every day until the virus filter was operating without any resistance from the valve under a hydrostatic head of 110 cm.

It is important to note that the velocity through the virus filter decreases more rapidly than that through the NOM prefilter because the velocity through the NOM prefilter decreased from 0.15 to 0.11cm/sec during 4 days.

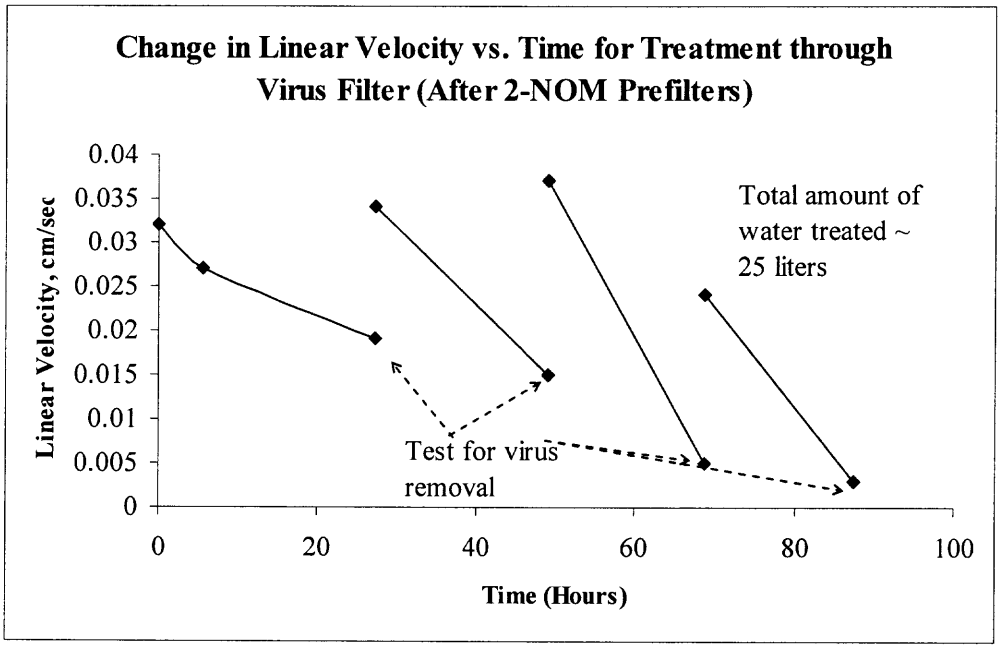

Figure 6.7 Kinetics of virus filter clogging retarded due to protection by two layers of NOM prefilter. The discontinuity in the Figure is due to adjusting the flow rate of the influent by manipulating the control valve, i.e., the same column was used in the experiment.

6.4 Long-term Testing of Virus Removal by Composite Filter Model

The essential suppression of virus filter clogging due to the application of two layers of NOM prefilter created the possibility of long-term testing of virus removal. The same experimental set-up shown in Figure 6.6 was used to perform virus removal efficiency.

Long-term continuous feeding of a tap water stream dosed with a high virus load is very complicated and excessive. This is not necessary since the long-term accumulation of NOM on adsorbent surface does not depend on virus presence -- viruses occupy a very small portion of the adsorption surface area in distinction from NOM. Consequently, there is no interference between preliminary adsorbed viruses and the adsorption of additional virus portions. Therefore, it is sufficient to dose the effluent of the NOM prefilter with viruses to provide high phage titer (of about 10^6 pfu/ml) in order to determine the efficiency of the virus filter. The volume of liquid can then be filtered through the virus filter at a velocity of about 0.03 cm/sec to check for virus removal efficiency.

Each day the influent for the virus filter was prepared by using ~10 liters of the last portion of NOM prefilter effluent. Every day the NOM surface concentration within the virus filter increased. This may have complicated the adsorption of the next portion of viruses. Two scenarios are possible: The clogging is more rapid than the decrease in log removal due to NOM accumulation. The decrease in virus log removal is more rapid than the decrease in velocity due to clogging. In the experiment, the first scenario was observed. Testing of virus removal was performed by seeding MS2 in the effluent water from NOM prefilter/s. Table 6.1 shows the results of log removal of viruses obtained during long-term testing for this composite filter.

Table 6.1 Virus Removal by Composite Filter after Long-term Contamination with NOM

	Volume of water treated liters	Time of testing after NOM contamination (hours)	Linear velocity, cm/sec	Volume of MS2 seeded water treated ml	Initial log concentration (log_{10} pfu/ml)	Final log concentration (log_{10} pfu/ml)	Log_{10} removal† pfu/ml
Virus Filter (After 1 NOM prefilter)							
	15.7	28	0.026	272	5.93	0	5.93†
Virus Filter (After 2 NOM prefilters)							
	10	27	0.029	214	5.93	0	5.93†
	17	49	0.027	198	6.25	0	6.25†
	22.8	69	0.022	154	6.66	0	6.66†
	25.3	87	0.018	110	6.73	0	6.73†

†- See comment for Table 4.5.

6.5 Conclusions

Modeling to determine the optimal operational parameters for the NOM prefilter has been accomplished on a theoretical basis. The reliability of this modeling effort has been confirmed by measuring the efficiency of virus removal in the presence of the NOM pre-filter. Since the average NOM molecule is about 10 times smaller than that of viruses, the diffusivity of NOM is 10 times larger than that of viruses. Therefore, the diffusional transport of NOM to calcite collector surface can be provided by particles of larger dimension (of about 600 microns) and at higher linear velocity (of about 0.1 cm/sec). The use of larger collector dimension and larger velocity suppresses cake formation because the pores are wider and the deposit formed stops growing after a critical thickness is

achieved. At the higher liquid velocity, the increased viscous stress destroys the deposit and detaches NOM in the form of larger fragments.

The experimental results confirm the semi-quantitative predictions. The velocity through the NOM prefilter decreased by a factor of 2 of its initial value after about 120 hours, while for the virus filter, the same velocity decrease was observed in about 10 hours when it was not protected by the NOM prefilter. This new design has significantly prolonged the virus filter run, i.e., with the use of the NOM prefilter.

The experiments also confirmed that the NOM prefilter provides protection for the virus filter against clogging, even at rather high filtration velocity (about 0.03 cm/sec). Although this protection is not complete, the results now show that a filter run of about 100 hours for the virus filter can be achieved. Virus log removal of about 6 was preserved during about 100 hours in spite of the accumulation of impurities during this period. The stable and high log removal of about 6 for viruses and the prevention of virus filter clogging during about 100 hours at a high operational linear velocity of about 0.1 cm/sec provide for a sufficient scientific base for AF technology, and for considering it to enhance virus removal in drinking water treatment.

CHAPTER 7

CONCLUSIONS AND FUTURE WORK

The annual societal cost of waterborne gastrointestinal illnesses in the United States has been estimated to be over 22 billion dollars. A recent report by the Academy of Microbiology indicates that our surface and drinking waters are no longer microbiologically safe (Ford and Colwell, 1996). According to this report, there has been a rise in waterborne diseases worldwide. These outbreaks caused an estimated 17,464 persons to become ill in 1991-1992 (Lukasik et al. 1999).

Groundwater sources have also become unsafe, especially those that are under the influence of surface water. It was generally believed that viruses are inactivated in the groundwater environment (aquifer) in a matter of days. However, recent studies (Schulze-Makuch et al. 2003a) have revealed that viruses might be capable of surviving for much longer periods of time in the natural subsurface than previously thought. Technologies available to effectively remove viruses from water include nanofiltration, reverse osmosis and disinfection. However, these technologies are expensive and have many limitations, including the need to use high pressures and, for some disinfection technologies, the production of disinfection byproducts (DBPs). Therefore, new approaches and further understanding of virus removal in water treatment are necessary.

Many studies have examined the possibility of modifying particulate filtration media (adsorbents) to improve virus removal efficiency during water treatment. Among the many candidate adsorbents proposed for virus removal, the best results have been achieved with metal oxides. The theory of colloidal interactions indicates that irreversible

adsorption of a negatively-charged virus onto a positively-charged metal oxide having high isoelectric points would be favorable for use in water treatment. In addition, the theory of filtration predicts that filtration media with the above surface properties in a flow packed bed (FPB) should enhance virus removal efficiency if small particle dimension is used. In spite of these known advantages, technologies for virus adsorption technology have not advanced over the past 20 years. The industry has mainly focused on the use of membrane technologies, namely reverse osmosis.

Two fundamental technological difficulties have hampered the development of the conventional FPB filtration process for effective virus removal. First, in order to provide rapid virus transport to an adsorbent surface, filtration media with a particle size of 100 microns or less are required. However, the pressure drop in the conventional FPB adsorber would increase very rapidly with decreasing adsorbent particle dimension, and would become unacceptably high if particles with < 100 microns are used. Second, there is an additional difficulty caused by competition for adsorption sites between negatively-charged viruses and humic acid (HA) anions because both species are adsorbed onto positively-charged sites of metal-oxide filtration media, mainly by electrostatic attraction. Occupancy of the adsorbent surface by HA anions may be very high, and accordingly, the number of vacant adsorption sites available for virus attachment may not be sufficient for efficient removal of viruses during water treatment.

Therefore, any successful technology for virus removal must consider: i) selecting an adsorbent with optimal surface chemistry for virus adsorption/attachment, ii) using small particle dimension filtration media without the need to use high driving pressures, and iii) overcoming problems arising from competition with HA and other ions in water,

including pH. The adsorption filtration (AF) technology explored in this study provides solutions for the above demands, and advances the understanding of virus attachment in FBP filtration.

The two main tasks of this study were to overcome the above difficulties and to develop adsorption filtration technology for enhanced virus removal during water treatment. Special emphasis was placed on groundwater sources in the State of New Jersey. The following are the main conclusions of this research:

1. Selection of calcite ($CaCO_3$) and its advantages as virus absorbent

While there is data in the literature indicating that virus removal decreases with decreasing pH, below 5, this shortcoming is eliminated when calcite is used as the adsorbent. In addition, the special filtration experiments performed with Na_2SO_4 concentration about 0.05 M/*l* demonstrated that virus log removal of about 6 could be achieved, i.e., the presence of SO_4^{2-} does not cause a decrease in virus removal efficiency.

The above result, namely, overcoming interference from divalent anions such as sulfate and phosphate, is an essential requirement for effective virus removal. In addition, no decrease in virus log removal occurred at high salt concentrations in the case of calcite, while such a decrease was documented for metal oxide-coated sand media. The decrease in attraction energy with increasing salt concentration may be harmful; however, this does not occur in the case of calcite. Since calcite is rather cheap, namely 7 - 10 cents per pound, the AF technology can thus be seriously considered as a cost-effective technology for virus removal, and for other applications in water treatment.

2. Experimental verification of the virus removal theory

The selection of an optimal combination of operational process parameters for slow filtration with the FPB configuration (d_c ,h, *l*, and u) for virus removal is impossible without considering the main equation (2.11) which predicts log removal dependence on such parameters. Although equation (2.11) has been tested (Elimelech and O'Melia 1990; Penrod et al. 1996) for virus filtration, investigations regarding the dependency of virus removal efficiency on velocity and collector dimension are not sufficient. With the use of calcite as the filter medium (pH_{iso}=8.2) with particle size ranges between 75 and 150 microns, the dependency of virus removal on $d_c^{-5/3}$ and $u^{-2/3}$ were confirmed in the experiments. The attachment efficiency factor α was found to be 0.4 for calcite, and this is almost the same as for metal oxide-coated sand. The above findings established the experimental base for modeling and optimizing the AF technology.

3. Weak influence of Natural Organic Matter (NOM) on virus removal and its mechanism

Log removal higher than 6 for MS-2 was achieved for 1 mg/*l* and 10 mg/*l* of HA in deionized water using the calcite FPB column experiments. Further, no decrease in MS-2 removal efficiency was detected when tap water was used – log removal remained > 6. In the filtration studies, the experimental value of α~0.4 remained the same both in the presence and in the absence of HA. This weak influence of HA was analyzed and found to be due to the larger diffusivity of the HA molecule compared to that of the virus. This means that HA are removed by calcite at a shorter filtration distance in the FBP compared to that of viruses. The analysis showed that the adsorbable fraction of HA

occupies the topmost portion of the FPB length, and this leaves an HA-free zone sufficient to achieve > 6 log removal of viruses.

4. Discovery of the polylayer mode of NOM adsorption and its effect in preventing the rapid shrinkage of the clean zone available for virus adsorption/attachment

The observed decrease in hydrodynamic velocity (or increase in hydrodynamic resistance) with HA accumulation was found to be due to the formation of a polylayer HA zone near the entrance of the FPB. This observation is consistent with the visual and microscopic examinations of the polylayer HA zone. When larger amounts of HA are introduced in the FPB, the thickness of the polylayer increases. This retards the rate of the movement of the HA adsorption front, and consequently, retards the shrinkage of the clean zone needed for virus removal.

5. Calcite is an optimal adsorbent for the NOM prefilter when calcite adsorbent is used in the virus filter

While the removal of all NOM fractions is a very complex task, removing the fraction that can be adsorbed by calcite (and interferes with virus removal) is a much easier task. To minimize the effect of the competitive adsorption of NOM on virus removal efficiency, and to remove this NOM fraction a special calcite prefilter was proposed to be placed upstream of the virus filter. No matter how large or small NOM adsorbability by calcite is, the virus filter will be protected. If the NOM adsorbability is small, the use of additional protection may not be necessary. But if it is large, this NOM fraction needs to be removed to prevent its penetration into the virus filter.

6. Protection of the virus filter from the harmful influence of NOM adsorption and development of NOM/virus composite filter

In addition to providing reliable removal of the harmful fraction of NOM that may be adsorbed in the virus filter, NOM transport to the adsorbent surface needs to be much

more rapid than that of the virus. This is possible since NOM molecular dimension is 10 to 15 times smaller than that of viruses, and accordingly, NOM diffusivity exceeds that of viruses by 10 to 20 times. This fact creates an opportunity to use calcite particles 3 to 4 times larger in the NOM prefilter compared to the calcite particle size used in the virus filter. If 600-micron calcite is used in the NOM prefilter, the pressure drop necessary to provide velocity of 0.1 cm/sec is about 0.1 bar. Therefore, the NOM prefilter may be designed using a simple FPB, and this would not complicate the design of the AF filter.

7. The NOM prefilter can protect the virus filter from clogging during 100 to 150 hours of filter run

Since the NOM diffusivity is about 15 times larger than that of the virus, the diffusional transport of NOM to the calcite surface can be adequately achieved using larger calcite particles (about 600 microns) and higher velocities (about 0.1 cm/sec). The simultaneous use of larger collector dimension and larger velocity suppresses polylayer cake formation in the NOM filter, and this prevents pressure build-up during filtration. The experimental studies have confirmed this semi-quantitative, theoretical prediction. The velocity through the NOM prefilter decreased to half the initial rate after about 100 hours. The experiments thus confirmed that the use of the NOM prefilter provides the virus filter with the sufficient protection necessary for long filter runs, in the order of at least 100 hours.

8. The NOM prefilter prevents harmful influence of NOM on virus adsorption during about 100 filtration hours

Virus log removal of about 6 does not decrease during about 100 hours when the NOM prefilter is placed before the virus filter. This stable and high log removal of 6 for viruses and the prevention of virus filter clogging during about 100 filtration hours at a high

phase velocity of about 0.1 cm/sec constitute a rigorous base for the development of the AF technology for virus removal in water treatment.

9. Cardinal revision of the entire hydrodynamic process configuration of flow packed bed (FPB) adsorber is necessary for efficient virus removal without increasing the pressure drop

The need for using small adsorbent particle dimension to remove viruses from water is universal. However, the fundamental difficulty regarding this is that although small adsorbent particle size is needed for high log removal, the head loss caused by using such small particles (100 microns) makes it difficult to employ the technology in large-scale applications. This controversy cannot be eliminated with the improvement of adsorbent properties because the universal law of convective diffusion transport controls the entire process rate. The single possibility of avoiding this dilemma is by cardinal revision of the entire hydrodynamic process configuration of the FPB adsorber. This constituted the basis for the adsorption filtration design developed during this study.

10. AF design combines adsorber with modified hydrodynamic process configuration of membrane technology, and provides an acceptably low operating pressure

A significant increase in hydrodynamic conductivity (HC) can be achieved by incorporating into the FPB body two arrays of transport channels; this constitutes the transition to the AF hydraulic process configuration. One array of channels (feeding channels) is connected to the upstream influent, and the second array of channels (receiving channels) is connected to the downstream effluent. Feeding and receiving channels alternate along the AF front area. During treatment, water filtrates through the adsorption media (AM) from a feeding channel to the nearest receiving channel and flows out along it. In the AF design, the filtration area is increased and the filtration depth

is decreased, and this design provides a volumetric velocity equivalent to that of conventional FPBs (sand filters) with the same footprint and pressure drop. In the AF filtration, the pressure drop decreases due to a decrease in both the filtration velocity and the filtration depth.

11. The composite filter consisting of FPB for NOM removal and of AF for virus removal is the basis for the new technology which will provide virus log removal of about 6 and filter runs in excess of 100 hours

Virus removal is a complex problem that cannot be solved without the use of the principles of physico-chemical hydrodynamics and colloid transport. Examination of the literature indicates that other research groups have disregarded this scientific approach. In this research, the theory of colloid transport and mathematical modeling have been included in every step during the development of the new concept of adsorption filtration, and for understanding virus removal processes in water treatment. Efforts have been expended to advance the concept of adsorption filtration and to advance its development as a practical technology for virus removal, with initial emphasis on groundwater treatment in New Jersey.

Future Research

The concept of AF was tested and validated in this study. The next step would be the investigation of backwashing of the composite NOM/virus filter. Long-term investigation of the microbiological growth inside the adsorbent and its suppression by disinfection is also required. It would be also useful to study the removal of different viruses and microorganisms in the AF. Subsequently, pilot scale studies can be performed at water treatment plants to gain an insight regarding the implementability and cost issues for the AF technology to be ready for use in small and large-scale water treatment systems.

REFERENCES

Ackermann, H., "ICTVdB - Picture Gallery" Retrieved in October (2003). From the World Wide Web, "http://www.ncbi.nlm.nih.gov/ICTVdb/Images/Ackerman/Phages/Leviviri/089-29.htm".

Adamczyk, Z., Dabros T., Czarnecki, J., van de Ven, T.G.M. "Particle transfer to solid surfaces" Adv. Colloid Interface Sci., (1983), 19 183-252.

Adams, M. H., *Bacteriophages*, (1959), Interscience Publishers, Inc.

Ahammed, M. M., Chaudhuri, M. "Sand-based filtration / adsorption media" J.Water SRT-Aqua, (1996), 45, 67-71.

Ahmad, R., Amirtharajah A., Al-Shawwa A., Huck P.M. "Effects of backwashing on biological filters" J. AWWA, (1998), 90, 62-73.

American Water Works Association, *Water Quality & Treatment Handbook*, Fifth Edition, (Letterman, R. D., Ed), (1999), McGraw-Hill.

Atherholt, T., Feerst, E., Hovendon, B., Kwak, J., Rosen, J. D. "Evaluation of indicators of fecal contamination in groundwater" J. AWWA, (2003), 95, 119-131.

Atherton, J.G., Bell, S.S. "Adsorption of viruses on magnetic particles-I. Adsorption of MS2 bacteriophage and the effect of cations, clay and polyelectrolyte" Water Res., (1983a), 8, 943-948.

Atherton, J.G., Bell, S.S. "Adsorption of viruses on magnetic particles-II. Degradation of MS2 bacteriophage by adsorption to magnetite" Water Res., (1983b), 8, 949-953.

Avena, M. J., Koopal, L. K., van Riemsdijk, W. H. "Proton binding to humic acids: Electrostatic and Intrinsic Interactions" J. Colloid Interface Sci., (1999a), 217, 37-48.

Avena, M. J., Vermeer, A. W. P., Koopal, L. K. "Volume and structure of humic acids studied by viscometry: pH and electrolyte concentration effects" Colloids Surf. A., (1999b), 151, 213-224.

Bales, R.C., Hinkle, S.R. "Bacteriophage adsorption during transport through porous media: chemical perturbations and reversibility" Environ. Sci. Technol., (1991), 25, 2088-2095.

Bales, R.C., Li S., Maguire, K.M., Yahya, M.T., Gerba, C.P., Harvey, R.W. "Virus and bacteria transport in a sandy aquifer, Cape Cod, MA". Ground Water, (1995), 33, 653-661.

Balnois, E., Wilkinson, K. J., Lead, J. R., Buffle, J. "Atomic force microscopy of humic substances: Effects of pH and ionic strength" Environ. Sci. Technol., (1999), 33, 3911-3917.

Bellamy, W. D., Silverman, G. P., Hendricks, D. W., Logsdon, G. S. "Removing Giardia cysts with slow sand filtration" J. AWWA, (1985), 77, 52-60.

Benedetti, M. F., van Riemsdijk, W. H., Koopal, L. K. "Humic substances considered as a heterogeneous Donnan Gel Phase" Environ. Sci. Technol., (1996), 30, 1805-1813.

Berner, E. K. Berner, R. A. *The Global Water Cycle*, Prentice-Hall, (1987) pp. 72, Englewood Cliffs, N.J.

Billen, G., Servais, P., Fontigny, A. "Growth and mortality in bacterial population dynamics of aquatic environments" Archiv fur Hydrobiologie, (1998), 31, 173-183.

Bird, R. B., Stewart, W. E.; Lightfoot, E. N. *Transport Phenomena*, John Wiley & Sons: (1960), New York.

Birge, E.A. *Bacterial and Bacteriophage Genetics*, Springer, (1981) New York.

Bixby, R.L., O'Brien, D.J. "Influence of fulvic acid on bacteriophage adsorption and complexation in soil" Appl. Environ. Microbiol., (1979), 38, 840–845.

Blackburn, B. G., Craun, G. F., Yoder, J. S., Hill, V., Calderon, R. L., Chen, N., Lee, S. H., Deborah A. Levy, D. A., Beach, M. J. "Surveillance for Waterborne-Disease Outbreaks Associated with Drinking Water --- United States, 2001—2002". (2004), 53 (SS08) 23-45.
Retrieved on May 5th, 2005, From the World Wide Web, http://www.cdc.gov/mmwr/preview/mmwrhtml/ss5308a4.htm.

Blanc, R., Nasser, A. "Effect of effluent quality and temperature on persistence of viruses in soil" Water Sci. Technol., (1996), 33, 237-242.

Bowen, B. D., Epstein, M. "Fine particle deposition in smooth parallel-plate channels" J. Colloid Interface Sci., (1979), 72, 81-97.

Bowman, R. S., Li, Z., Roy, S. J., Burt, T., Johnson, T. L., Johnson, R. L. "Pilot test of a surfactant modified zeolite permeable barrier for ground water remediation" in *Physical and Chemical Remediation of Contaminated Aquifers*, (Smith, J. A., Burns, S., Eds), Kluwer Academic Publishers, (2001), Dordrecht, The Netherlands, pp. 161-185.

Bowman, R. S., Sullivan, E. J., Li, Z. "Uptake of cations, anions, and nonpolar organic molecules by surfactant-modified clinoptilolite-rich tuff" in *Natural Zeolites for the Third Millennium*, (Colella, C., Mumpton, F. A., Eds), De Frede Editore, (2000), Naples, Italy, pp. 287-297.

Brown, T. S., Malina, J. F., Jr., Moore, B. D. "Virus removal by diatomaceous earth filtration, part 1" J. Am. Water Works Assoc. (1974a), 66, 98-102.

Brown, T. S., Malina, J. F., Jr., Moore, B. D. "Virus removal by diatomaceous earth filtration, part 2" J. Am. Water Works Assoc. (1974b), 66, 735-738.

Buffle, J., Altmann, R. S., Filella, M., Tessier, A. "Complexation by natural heterogeneous compounds. II. Site occupation distribution functions, a normalized description of metal complexation" Geochim. Cosmochim. Acta, (1990), 54, 1535-1553.

Caceci, M. S., Billon, A., "Evidence for large organic scatters (50-200 nm diameter) in humic acid samples" Org. Geochem., (1990), 15, 335-350.

Cadena, F., Bowman, R. S. "Treatment of waters contaminated with BTX and heavy metals using tailored zeolites" Proceedings of the 4th Annual WERC Technology Development Conference, (1994), 297-310.

Carballeira, J. L., Antelo, J. M., Rey, F., Arce, F. "Modeling the effects of ionic strength on ionization parameters for a soil fulvic acid at low concentrations" Anal. Chim. Acta., (1999), 401, 243-249.

Chang, A. C., Page, A. L. "Soil deposition of trace metals during groundwater recharge using surface spreading" in *Artificial Recharge of Groundwater*, (Asano, T., Ed) Butterworth, (1985), Boston, MA, pp 610.

Cleven, R. F. M. J., "Heavy metal / polyacid interaction: an electrochemical study of the binding of Cd(II), Pb(II) and Zn(II) to polycarboxylic and humic acids" Ph.D., Thesis, (1984), Wageningen University, The Netherlands.

Cookson, J. T. "Adsorption of viruses on activated carbon: Adsorption of *Escherichia coli* bacteriophage T4 on activated carbon as a diffusion-limited process" Environ. Sci. Technol., (1967), 1,157-160.

Cooney, D.O. *Adsorption Design for Wastewater Treatment*, CRC Press LLC, (1999).

Crittenden, J. C., Trussell, R. R., Hand, D. W., Howe, K. J., Tchobanoglous, G. *Water Treatment: Principles and Design*, Second Edition, (2005), John Wiley and Sons, Inc. Hoboken, New Jersey.

Dahneke, B. "Diffusional deposition of particles: Short communication." J. Colloid Interface Sci., (1974), 48, 520-522.

Debartolomeis, J., Cabelli, V. J. "Evaluation of an *Escherichia coli* host strain for enumeration of F male-specific bacteriophages" Appl. Environ. Microbiol. (1991), 57, 1301-1305.

Derjaguin, B. V., Landau, L.D. "Theory of the stability of strongly charged lyophobic sols and of the adhesion of strongly charged particles in solutions of electrolytes" Acta Physicochim. URSS, (1941), 14, 733-62.

Elimelech, M., Gregory J., Williams, R. A., *Particle Deposition and Aggregation: Measurement, Modeling and Simulation,* Butterworth-Heinemann, (1995), Oxford.

Elimelech, M., O'Melia C.R., "Kinetics of deposition of colloidal particles in porous media" Environ. Sci. Technol., (1990), 24, 1528-36.

Ephraim, J. H., Alegret, S., Mathuthu, A., Bicking, M., Malcom, R. L., Marinsky, J. A. "A unified physicochemical description of the protonation and metal ion complexation equilibria of natural organic acids (humic and fulvic acids). 2. Influence of polyelectrolyte properties and functional group heterogeneity on the protonation equilibria of fulvic acid" Environ. Sci. Technol., (1986), 204, 354-366.

Farrah, S. R., Bitton, G. "Methods (other than microporous filters) for concentration of viruses from water" in *Methods in Environmental Virology*, (Gerba, C. P., and Goyal, S. M., Eds.), Marcel Dekker, Inc., (1982), New York.

Farrah, S. R., Gerba, C. P., Wallis, C., Melnick, J. L. "Concentration of viruses from large volumes of tap water using pleated membrane filters" Appl. Environ. Microbiol., (1976), 31, 221-226.

Farrah, S. R., Girard, M. A., Toranzos, G. A., Preston, D. R. "Adsorption of viruses to diatomaceous earth modified by in situ precipitation of metallic salts" Z. Gesamte Hyg., (1988), 34, 520-521.

Farrah, S. R., Preston, D. R. "Adsorption of viruses to sand modified by in situ precipitation of metallic salts" Second International Symposium on Contamination of the Environment by Viruses and Methods of Control, (1989) Vienna, September 5-7.

Farrah, S. R., Preston D. R. "Concentration of viruses from water by using cellulose filters modified by in situ precipitation of ferric and aluminum hydroxides" (1985), 50,1502-1504.

Farrah, S. R., Preston D. R., Toranzos G. A., Girard M., Erdos G. A., Vasuhdivan V. "Use of modified diatomaceous earth for removal and recovery of viruses in water" (1991), 57, 2502-2506.

Faust, S.D., Aly, O.M. *Adsorption Processes for Water Treatment*, Butterworths, (1987) Boston.

Faust, S.D., Aly, O. M. *Chemistry of Natural Waters*, Ann Arbor Science, (1981) Ann Arbor, MI, pp. 1-58.

Federal Register, National Primary Drinking Water Regulations; Filtration, Disinfection; Turbidity, Giardia lamblia, Viruses, Legionella, and Heterotrophic Bacteria; Final Rule. June 29, 1989: Vol. 54, 124, pp. 27486-27541.

Federal Register, National Primary Drinking Water Regulations: Interim Enhanced Surface Water Treatment; Final Rule. December 16, 1998: Vol. 63, 241, pp. 69478-69521.

Federal Register, National Primary Drinking Water Regulations: Ground Water Rule; Proposed Rules. May 10, 2000: Vol. 65, no. 91, pp. 30194-30274.

Federal Register, National Primary Drinking Water Regulations: Long Term 1 Enhanced Surface Water Treatment Rule; Final Rule. January 14, 2002: Vol. 67, 9, pp. 1812-1844.

Ford, T. E., Colwell, R. R. "A Global Decline in Microbiological Safety of Water: A Call for Action" Report: The American Academy of Microbiology, (1996), 1-40. Retrieved on May 1st, 2005. From the World Wide Web, http://www.asm.org/ASM/files/CCPAGECONTENT/docfilename/0000003773/waterquality1995[1].pdf

Friedlander, S. K. "Theory of aerosol filtration" Ind. Eng. Chem. (1958), 50, 1161-1164.

Fulton, G. P. *Diatomaceous Earth Filtration for Safe Drinking Water*, (2000), ASCE Press, Reston, Virginia.

Gagliardo, P.F., Adham, S. S., Trussell, R. R., Olivieri, A. W., Najm, I. N., Richardson, T. G. "Membranes: An alternative to disinfection", Disinfecting Wastewater for Discharge & Reuse, Proceedings (1996), Portland. Oregon.

Gavaskar, A.R., Gupta, N., Sass, B.M., Janosy, R.J., O'Sullivan D. *Permeable Barriers for Groundwater Remediation*, (1998), Battelle Press, Columbus, Ohio.

Gosh, K., Schnitzer, M. "Macromolecular structures of humic substances" Soil Science, (1980), 129, 266-276.

Gregory, J. "Approximate expressions for retarded van der Waals interaction" J. Colloid Interface Sci., (1981), 83, 138-145.

Gregory, J. "The calculation of Hamaker constants" Adv. Colloid Interface Sci., (1970), 2, 396-417.

Gregory, J. Wishart, A. "Deposition of latex particles on alumina fibers" J. Colloids Surf., (1980), 1, 313-334.

Gupta, A., Chaudhuri, M. "Enteric virus removal/inactivation by coal-based media" Water Res., (1995) 29, 511-516.

Happel, J. "Viscous flow in multiparticle systems: slow motion of fluids relative to beds of spherical particles" AIChE J., (1958), 4,197-201.

Havelaar, A.H., Pot-Hogeboom, W.M., Furuse, K., Pot, R., Hormann, M. P. "F-specific RNA bacteriophages and sensitive host strains in faeces and wastewater of human and animal origin" J. Appl. Bacteriol., (1990), 69, 30-37.

Helmer, R. D., Finch, G. R. "Use of MS2 coliphage as a surrogate for enteric viruses in surface waters disinfected with ozone" Ozone Science & Engineering (1993), 15, 279-293.

Hoff, J. C., Akin, E. W. "Removal of viruses from raw waters by treatment processes" in *Viral Pollution of the Environment*, (Berg, G., Ed.), (1983) CRC Press, Inc., Boca Raton, Fla. pp. 53-75.

Hogness, T. R., Johnson, W. C. *Qualitative Analysis and Chemical Equilibrium*, (1954), Holt, Rinehart & Winston, Inc., New York. p. 563.

Hogg, R., Healy, T. W., Fuerstenau, D. W. "Mutual coagulation of colloidal dispersions" Trans. Faraday Soc., (1966), 62, 1638-1651.

Hosse, M., Wilkinson, K. J. "Determination of electrophoretic mobilities and hydrodynamic radii of three humic substances as a function of pH and ionic strength" Environ. Sci. Technol., (2001), 35, 4301-4306.

Hozalski, R.M. Bouwer, E.J. "Deposition and retention of bacteria in backwashed filters" J. AWWA, (1998), 90, 71-85.

Hull, M., Kitchener, J. A. "Interaction of spherical colloidal particles with planer surfaces" Trans. Faraday Soc. (1969), 65, 3093-3104.

IAWPRC study group on health related water microbiology, "Bacteriophages as model viruses in water quality control" Water Rese., (1991), 25, 529-545.

Jacangelo, J. G., Adham, S. S., Laine, J. M. "Mechanism of Cryptosporidium, Giardia, and MS2 virus removal by MF and UF. J. AWWA, (1995), 87, 107-121.

Jones, M. N., Bryan, N. D. "Colloidal properties of humic substances" Adv. Colloid Interface Sci., (1998), 78, 1-48.

Keswick, B.H., Gerba, C.P. "Viruses in groundwater" Environ. Sci. Technol., (1980), 14, 1290-97.

Keswick, B.H., Wang, D.S., Gerba, C.P. "The use of microorganisms as ground-water tracers: a review. Ground Water" (1982), 20, 142-149.

Kramer, C. J. M., Duinker, J. C., (Eds) *Complexation of Trace Elements in Natural Water*, (1984), Nijhoff.

Landry, E.F., Vaughn, J.M., Thomas, M.Z., Beckwith, C.A. "Adsorption of enteroviruses to soil cores and their subsequent elution by artificial rainwater" Appl. Environ. Microbiol., (1979), 38, 680-687.

Lead, J. R., Wilkinson, K. J., Balnois, E., Cutak, B. J., Larive, C. K., Assemi, S., Beckett, R. "Diffusion coefficients and polydispersities of the Suwannee river fulvic acid: Comparison of fluorescence correlation spectroscopy, pulsed-field gradient nuclear magnetic resonance, and flow field-flow fractionation" Environ. Sci. Technol., (2000 b), 34, 3508 – 3513.

Lead, J. R., Wilkinson, K. J., Starchev, K., Canonica, S., Buffle, J. "Determination of diffusion coefficients of humic substances by fluorescence correlation spectroscopy: Role of solution conditions" Environ. Sci. Technol., (2000 a), 34, 1365-1369.

Leppard, G. G., Buffle, J., Baudat, R. "A description of the aggregation properties of aquatic pedogenic fulvic acids: Combining physico-chemical data and microscopical observations" Water Res., (1986), 185-196.

Levich, V. G. *Physicochemical Hydrodynamics*, (1962), Prentice Hall, Englewood Cliffs, NJ.

Li, Z., and Bowman, R. S. "Sorption of perchloroethylene by surfactant-modified zeolite as controlled by surfactant loading" Environ. Sci. Technol., (1998), 32, 2278-2282.

Litton, G. M. and Olson, T. M. "Colloid deposition rates on silica bed media and artifacts related to collector surface preparation methods" Environ. Sci. Technol., (1993), 27, 185-193.

Littleton Electric Light & Water Departments, Littleton Water Department Drinking Water Treatment Plant: Simplified Schematic Diagram Retrieved on May 2nd, 2005. From the World Wide Web, http://www.lelwd.com/lwd/wtreatment.html.

Loveland, J. P., Ryan, J. N., Amy, G. L., and Harvey, R. W. "The reversibility of virus attachment to mineral surfaces" Colloids and Surfaces, (1996), 107, 205-221.

Lukasik, J., Cheng Y., Lu, F., Tamplin, M., Farrah, S. R. "Removal of microorganisms from water by columns containing sand coated with ferric and aluminum hydroxides" Wat. Res., (1999), 33, 769-777.

Lukasik, J., Farrah, S. R., Shah, D. O., Kang P. K., Koopman B. L., "Novel Methods and Apparatus for Improved Filtration of Submicron Particles" European Patent Office, Patent number WO0013764, (2000).

Madigan, M.T., Martinko, J.M., Parker, J. *Brock Biology of Microorganisms*, (2000), Ninth Edition, Prentice Hall Inc., Englewood Cliffs, NJ.

Maier, R. M., Pepper, I.L., Gerba, C.P. *Environmental Microbiology*, (2000), Academic Press, San Diego, CA.

Marinsky, J. A., Ephraim, J. H. "A unified physicochemical description of the protonation and metal ion complexation equilibria of natural organic acids (humic and fulvic acids). 1. Analysis of the influence of polyelectrolyte properties on protonation equilibria in ionic media: fundamental concepts" Environ. Sci. Technol., (1986), 20, 349-354.

Marvin, D. A., Hoffman-Berling, H. "A fibrous DNA phage (fd) and a spherical RNA phage (fr) specific for male strains of E.coli. Part II. Physical characteristics" Z. Naturforsch., (1963), 186, 884-93.

Metcalf and Eddy Inc. *Wastewater Engineering: Treatment, Disposal, and Reuse*, Revised by Tchobanoglous G., Burton, F. L., Stensel, D. H. (1991), McGraw-Hill, New York.

Moeglich, K. "U.S. patent 4,048,028" September (1977).

Mossel, D. A. A. "Marker (index and indicator) organisms in food and drinking water. Semantics, ecology, taxonomy and enumeration" Antonie van Leeuwenhoek, 48, (1982), 609-11.

Murray, J. P., Parks, G. A., in *Particulates in Water. Characterization, Fate, Effects and Removal*, (Kavanaugh, M. C., and Leckie, J. O., Eds.), ACS Advances in Chemistry Series 189. American Chemical Society, (1980), Washington D.C., pp 97-103.

Nasser, A. M., Adin, A., Fattal, B. "Adsorption of Poliovirus 1 and F^+ bacteriophages onto sand" Wat. Sci. Tech., (1993), 27, 331-338.

Nasser, A.M., Dizer, H., Lopez, J.M. "Elimination of viruses after secondary and tertiary sewage treatment and by sand filtration" Monog. Virol., (1984), 15, 163-170.

Nasser, A. M., Hall, R. M., Dunham, C., Sobsey, D. M. "Comparative reduction of Hepatitis A virus, model enteric viruses, bacteriophage MS2 and indicator bacteria from primary sewage in unsaturated loamy sand soil columns" Environ. Quality and Ecosystem Stability. ISEEQS Pub. (Luria, M., Steinberger, Y., and Spanier, E., Eds.), (1989), pp. 505-516.

New Jersey Department of Environment Protection "Bureau of Safe Drinking Water: Safe Drinking Water Act Regulations (N. J. A. C. 7:10), November 04, 2004. Retrieved on May 3rd, 2005. From the World Wide Web, http://www.state.nj.us/dep/watersupply/sdwarule.pdf.

Nir, S., "Van der Waals interactions between surfaces of biological interest" Prog. Surf. Sci,. (1976), 8, 1-58.

Noonan, M.J., McNabb, J. F. "Movement of Bacteriphages in groundwater in New Zealand" Ann Mtg. Am. Soc. Microbiol, (1979), 221.

O'Melia, C. R. in *Aquatic Chemical Kinetics*, (Stumm, W., Ed.) Wiley-Interscience, (1990), New York.

O'Melia, C. R. In *Aquatic Surface Chemistry*, (Stumm, W., Ed.) Wiley-Interscience, (1987), New York,

Overby, L. R., Barlow, G. H., Doi, R. H., Jacob, M., Spiegelman, S. "Comparison of two serologically distinct ribonucleic acid bacteriophages. I. Properties of the viral particles" J. Bact., (1966), 91, 442-48.

Oza, P.P., Chaudhuri, M. "Removal of viruses from water by sorption onto coal" Water Res., (1975), 9, 707-712.

Oza, P.P., Chaudhuri, M., "Virus-coal sorption interaction" J. Environ. Eng. Div. Am. Soc. Civil Eng., (1976), 102, 1255-1262.

Payment, P., Fortin, S., Trudel, M. "Ferric chloride floculation for nonflocculating beef extract preparations" Appl. Environ. Microbiol., (1984), 47, 591-592.

Penrod, S. L., Olson, T. M., Grant, S. B. "Deposition kinetics of two viruses in packed beds of quartz granular media" Langmuir, (1996), 12, 5576-5587.

Persson, M. "Surface and colloid chemistry in ceramic casting operations" in *Surface and Colloid Chemistry in Advanced Ceramics Processing. Surfactant Science Series*, (Pugh, R. J., BergstroÈm, L., Eds.), (1994), Vol. 51, Marcell Dekker, New York,

Pieper, A. P., Ryan, J. N., Harvey, R.W., Amy, G. L., Illangasekare, T.H., Metge, D.W. "Transport and recovery of bacteriophage PRD1 in a sand and gravel aquifer: effect of sewage-derived organic matter" Environ. Sci. Technol., (1997), 31, 1163-1170.

Powell, T., Brion, G.M., Jagtoyen, M., and Derbyshire, F. "Investigating the effect of carbon shape on virus adsorption" Environ. Sci. Technol., (2000), 34, 2779-2783.

Redman, J. A., Grant, S. B., Olson, T. M., Adkins, J. M., Jackson, J. L., Castillo, M. S., Yanko, W. A. "Physicochemical mechanisms responsible for the filtration and mobilization of a filamentous bacteriophage in quartz sand" Water Res., (1999), 33, 43-52.

Ruckenstein, E., Prieve, D. C. J. "Rate of deposition of Brownian particles under the Influence of London and double-layer forces" Chem. Soc., Faraday Trans.2, (1973), 69, 1522-1536.

Ryan, J. N., Elimelech, M. "Colloid mobilization and transport in groundwater" Colloids and Surfaces, (1996), 107, 1-56.

Ryan, J. N., Elimelech, M., Ard, R.A., Harvey, R.W., Johnson, P. R. "Bacteriophage PRD1 and silica colloid transport and recovery in an iron oxide-coated sand aquifer" Environ. Sci. Technol., (1999), 33, 63-73.

Roberts, J. "Chemistry of Paper Formation and Additives" Module 2: Chemistry of Paper & Papermaking Materials, Dept of Paper Science, UMIST.
Retrieved on May'1st, 2005. From the World Wide Web,
http://www2.umist.ac.uk/paper/msc/dept_page/CM02_unit14.pdf.

Sabin, A. B. "Experiments on the purification and concentration of the virus of poliomyelitis" J. Exp. Med., (1931), 56, 307-317.

Schiffenbauer, M., Stotzky. G. "Adsorption of coliphages TI and T7 to host and non-host microbes and to clay minerals" Curr. Microbiol., (1982) 43, 590-596.

Schijven J. F., Hassanizadeh S. M. "Removal of viruses by soil passage: overview of modeling, processes, and parameters" Crit. Rev. Env. Sci. Technol., (2000), 30, 49-127.

Schijven, J. F., Hoogenboezem, W., Hassanizadeh, S. M., Peters, J. H. "Modeling removal of bacteriophages MS2 and PRD1 by dune infiltration at Castricum, The Netherlands" Water Resource Res., (1999), 35, 1101-1111.

Schuler, P. F., Ghosh, M. M., Boutros, S. N. "Comparing the Removal of Giardia and Cryptosporidium using slow sand and diatomaceous earth filtration" in "Proceedings AWWA Annual Conference", (1988), Denver, Colorado, June 19-23.

Schulten, H. R., Leinweber, P., Schnitzer, M. "Analytical pyrolysis and computer Modeling of humic and soil particles" in *Environmental Particles: Structure and Surface Reactions of Soil Particles*, Vol. 4, IUPAC Analytical and Physical Chemistry Series, (Huang, P. M., Senesi, N., and Buffle, J., Eds), (1998), Wiley, Chichester, Chapter 8, pp. 281-324.

Schulze-Makuch, D., Bowman, R. S., Pillai, S. D., Guan, H. "Field evaluation of the effectiveness of surfactant modified zeolite and iron-oxide-coated sand for removing viruses and bacteria from ground water" Ground water monitoring and remediation, (2003a), 23, 68-75.

Schulze-Makuch, D., Guan, H., Pillai, S.D. "Effects of pH and geological medium on bacteriophage MS2 transport in a model aquifer" Geomicrobiology Journal, (2003b), 20, 73-84.

Scott, T. M., Sabo, R. C., Lukasik, J., Boice, C., Shaw, K., Barroso-Giachetti, L., El-Shall, H., Farrah, S. R., Park, C., Moudgil, B., Koopman, B. "Performance and cost-effectiveness of ferric and aluminum hydrous metal oxide coating on filter media to enhance virus removal" Kona, (2002), 20, 159-164.

Seeley, N. D., Primrose, S. B. "Concentration of bacteriophages from natural waters" J. Appl. Bacteriol., (1979) 46, 103-116.

Servais, P., Billen, G., Bouillot, P. "Biological colonization of granular activated carbon filters in drinking-water treatment" J. of Environ. Engineering, (1994), 120, 888-899.

Sobsey, M. D. "Inactivation of health related microorganisms in water by disinfection processes" Water Sci. Technol., (1989), 21, 179-95.

Sobsey, M. D., Gerba, C. P., Wallis, C., Melnick, J. L "Concentration of enteroviruses from large volumes of turbid estuarine water" Can. J. Microbiol. (1977), 23, 770-778.

Spielman, L.A., Friedlander, S.K. "Role of the electrical double layer in particle deposition by convective diffusion" J. Colloid Interface Sci., (1974), 46, 22-31.

Stanley, W. M. "The precipitation of purified concentrated influenza virus on calcium phosphate" Science, (1945), 101, 332-333.

Stannard, L. M. "Virus ultra-structure"
Retrieved in October (2003). From the World Wide Web, "http://web.uct.ac.za/depts/mmi/stannard/linda.html".

States, S., Scheuring, M., Rulison, E., Evans, R., Buzza, E., Movahed, B., Gigliotti, T., Casson, L. "Membrane filtration as post-treatment" J. AWWA., (2000), 92, 59-68.

Sterritt, R. M., Lester, J. N. *Microbiology for Environmental and Public Health Engineers*, E. & F. N. Spon, (1988).

Steven, M.L., Stotzky, G. "Adsorption of reovirus to clay minerals: Effects of cation-exchange capacity, cation saturation, and surface area" Appl. Environ. Microbiol., (1983), 46, 673-682.

Steven, M.L., Stotzky, G. "Infectivity of reovirus adsorbed to homoionic and mixed-cation clays" Water Res., (1984) 19, 227-234.

Stevenson, F. J., *Humus Chemistry: Genesis, composition, reactions*, Second Edition, (1994), John Wiley and Sons, New York.

Taylor, D.H. "Interpretation of the adsorption of viruses by clays from their electrokinetic properties" in *Chemistry in Water Reuse*, (Edited by Cooper, U.J.), (1981), Ann Arbor Sciences, Ann Arbor, Michigan, 595-612.

Taylor, D. H., Bosmann, H. B. "The electrokinetic propereties of Reovirus type 3: electrophoretic mobility and zeta potential in dilute electrolytes" J. Colloid Interface Sci., (1981), 83, 153-162

Tien, C., *Granular Filtration of Aerosols and Hydrosols*, Butterworth, (1989), Stoneham, MA.

Tobiason, J. E. "Chemical effects on the deposition of non-Brownian particles" Colloids Surf., 1989, 39, 53-75.

Toranzos, G. A., G. W. Erdos, and S. R. Farrah. "Virus adsorption to microporous filters modified by in situ precipitation of metallic salts" Water Sci. Technol., (1986), 18,141-148.

USEPA- United States Environmental Protection Agency, "Secondary Drinking Water Regulations: Guidance for Nuisance Chemicals" EPA 810/K-92-001, July 1992. Retrieved on April 10th, 2005. From the World Wide Web, http://www.epa.gov/safewater/consumer/2ndstandards.html.

USFDA- U.S. Food & Drug Administration, Foodborne Pathogenic Microorganisms and Natural Toxins Handbook. Center for Food Safety & Applied Nutrition, Retrieved in October (2003), From the World Wide Web, http://www.cfsan.fda.gov/~mow/chap31.html, October (2003).

United Water, Inc. "Well Water Treatment Schematic" Retrieved on May, 2nd , 2005. From the World Wide Web, http://www.unitedwater.com/wtrtrtmt.htm#wellwater.

Vaughn, J. M., Landry, E. F. "Viruses in soils and groundwaters" in *Viral Pollution of the Environment*, (Berg G., Ed.), , CRC Press., (1983), Boca Raton, Fla., pp. 163-210.

Verwey, E. J. W., and Overbeek, J. Th. G. *Theory of the stability of lyophobic colloids*, Elsevier, (1948), Amsterdam.

Vilagines, P., Sarette, B., Vilagines, R. "Preformed magnesium hydroxide precipitate for second-step concentration of enterovirus from drinking and surface waters" Can. J. Microbiol., (1982), 28, 783-787.

Wagner, E. K., Hewlett, M. J. *Basic Virology*, Blackwell Science, Inc., (1999).

Wallis, C., Melnick, J. L. "Concentration of viruses on aluminum and calcium salts" Am. J. Epidemiol., (1967), 85, 459-468.5.

Wallis, C., Melnick, J. L. "U.S. patent 3,816,304" June 1974.

Walter, R., Durkop, J., Friedman, B., Dobberkau, H. J. "Interactions between biotic and abiotic factors and viruses in a water system" Water Sci. Technol. (1985), 17, 139-151.

Wang, Z. Ph.D. Dissertation; Johns Hopkins University, (1985).

Weber-Shirk, M.L., Dick, R.I. "Biological mechanisms in slow sand filters" J. AWWA, (1997), 89(2), 72-83.

Wiese, G. R., Healy, T. W. "Effect of particle size on colloid stability" Trans. Faraday Soc., (1970), 66, 490-500.

Wolterink, J. K., Leermakers, F. A. M., Fleer, G. J., Koopal, L. K., Zhulina, E. B., Borisov, O. V. "Screening in solutions of star-branched polyelectrolytes" Macromolecules, (1999), 32, 2365-2377.

World Health Organization (WHO), "Guidelines for drinking water quality, Vol. 1. Recommendations, (1984), Geneva, Switzerland.

Yahya, M. T., Galsomies, L., Gerba, C. P., and Bales, R. C. "Survival of bacteriophages MS2 and PRD1 in groundwater" Water Sci. Technol., (1993), 27, 409-412.

Yao, K.M., Habibian, M.T., and O'Melia, C.R. "Water and waste water filtration. Concepts and applications" Environ. Sci. Technol., (1971), 1105-1112.

Yao, K. M. Ph.D. Dissertation; University of North Carolina at Chapel Hill, (1968).

Yates, M. V., Gerba, C. P., Kelly L. M. "Virus persistence in groundwater" Appl. Environ. Microbiol., (1985), 58, 1609-16.

Yates, M. V., Yates, S. R., Wagner, J., and Gerba, C. P. "Modeling virus survival and transport in the subsurface" J. Contam. Hydrol., (1987), 1, 329-345.

You, Y., Vance, G. F., Sparks, D. L., Zhuang, J., Jin, Y. "Sorption of MS2 bacteriophage to layered double hydroxides: Effects of reaction time, pH, and competing anions" J. Environ. Qual., (2003), 32, 2046-2053.

Zhaung, J., Jin Y. "Virus retention and transport through Al-oxide coated sand columns: effects of ionic strength and composition" J. Contam. Hydrol., (2003), 60, 193-209.